DOCTORAL THESIS

High Performance Bio-based Composites

Mechanical and Environmental Durability

Newsha Doroudgarian

Polymeric Composite Materials

This thesis is the result of a collaboration between Luleå University of Technology and Universitat Politècnica de Catalunya that aims toward a double degree.

UNIVERSITAT POLITÈCNICA DE CATALUNYA

LULEÅ UNIVERSITY OF TECHNOLOGY

High Performance Bio-based Composites

Mechanical and Environmental Durability

Newsha Doroudgarian
Composite Centre Sweden
March 2016

UNIVERSITAT POLITÈCNICA
DE CATALUNYA

Printed by Luleå University of Technology, Graphic Production 2016

ISSN 1402-1544
ISBN 978-91-7583-541-9 (print)
ISBN 978-91-7583-542-6 (pdf)

Luleå 2016

www.ltu.se

To my parents, Malihe & Fereydoun. ♥

Abstract

The presented work is a part of the ongoing effort on the development of high performance bio-based composites with enhanced durability, under static and dynamic mechanical loading including the exposure to elevated humidity. The impact of relative humidity on the performance of cellulosic fibers (natural and regenerated), bio-based resins and their composites was studied. The material performance was rated against the data for glass fiber epoxy, as the reference. The comparison of water absorption results for unreinforced resins and for composites showed that the cellulosic reinforcement is primarily responsible for the transport and uptake of moisture in the composites. The effect of chemical treatment on the cellulosic fibers, as a protection against moisture, was evaluated. However, the treatment did not improve the moisture resistance in composites significantly. Quasi-static tensile tests revealed that some of the bio-based resins and their composites performed very well and comparable to the composites of synthetic epoxy, even at high humidity. However, any structural material is supposed to hold mechanical loads over a long service time and most often in harsh environmental conditions. Hence, tension-tension fatigue tests were performed on the fiber bundles as well as on the composites. The fibers of choice as the reinforcement for further mechanical testing were regenerated cellulose fibers (RCF), mainly owing to the stable geometry and properties. Due to the high nonlinearity of RCF, the fatigue tests were limited in number and the focus was on analyzing the mechanisms underlying the fatigue behavior rather than on constructing S-N curves. Strain evolution of the bio-based composites during the dynamic fatigue was very similar to that observed in the static fatigue (creep). It confirmed the strong influence of viscoelastic and viscoplastic phenomena on the overall performance of the material under the rapid loading conditions in fatigue. Since the durability of composites greatly depends on the material's ability to stand the internal damages (e.g. debonding, microcracking, delaminations), the interfacial properties in the bio-based composites were addressed. To investigate the fracture toughness of bio-based composites, the double cantilever beam (DCB) tests were carried out, under static and dynamic loading. Moreover, the DCB results were utilized as a measure of the fiber chemical treatment's efficiency to improve the adhesion between RCF and the resin. The nonlinearity of RCF strongly influenced the results obtained from DCB tests, which complicated the analysis regarding the effectiveness of the fiber surface treatment. Nevertheless, this study brings forward the issues that have to be dealt with, in order to characterize and predict the performance of these composite materials with highly nonlinear reinforcing fibers. Overall, the results presented in this thesis give an insight into the behavior of bio-based composites, at various environments and under different types of mechanical loading. Based on these findings, the potential use of these materials in structural applications can be assessed.

Preface

This thesis was accomplished within the framework of DocMASE joint European doctoral program, at Luleå University of Technology in Sweden, collaborating with Technical University of Catalonia in Spain.

I would like to gratefully thank a couple of people and organizations that provided me with different types of support, encouragement and security along this journey:

My supervisor at Luleå University of Technology, Prof. Roberts Joffe, for sharing his know-how and expertise as well as for the smart B-plans;

Prof. Marc Anglada, my co-supervisor at Technical University of Catalonia for the warm welcome into his group and the continuous support;

the group of Polymeric Composite Materials at LTU, for educating me and more importantly for supporting me;

SWEREA Sicomp and DocMASE program for financing and coordinating;

my caring and supportive colleagues in the division of Materials Science at LTU and in CIEFMA at UPC. Tack för de mysiga fikastunderna and gracias por todas las risas;

my loving family, especially my adorable parents and my lifelong buddy, my brother, who have stood by me no matter what;

and, of course my friends, who trusted me, listened to me, inspired me, and with whom I shared lots of happy moments, and sometimes sad ones.

You helped me to be my better self, thank you.

18 March 2016 / ۲۸ اسفند ۱۳۹۴

List of appended papers

Paper A

Pupure L, Doroudgarian N, Joffe R. Moisture uptake and resulting mechanical response of biobased composites. I. Constituents. Polymer Composites. 2014; 35(6):1150-9.

Paper B

Doroudgarian N, Pupure L, Joffe R. Moisture uptake and resulting mechanical response of bio-based composites. II. Composites. Polymer Composites. 2015; 36(8):1510-9.

Paper C

Doroudgarian N, Anglada M, Joffe R. Bio-based composites under fatigue loading: review on characterization and performance. Composites Science and Technology. *To be submitted*.

Paper D

Doroudgarian N, Anglada M, Joffe R. Fatigue on regenerated cellulose fiber bundles and composites. Industrial Crops and Products. *Submitted* 2015.

Paper E

Doroudgarian N, Hajlane A, Anglada M, Joffe R. Interlaminar fracture toughness of composites with nonlinear cellulose reinforcement. Composites Part A. *Submitted* 2016.

Table of contents

1 Introduction

The environmental concerns have been largely promoting the use of bio-based materials in the industries as the "green" alternatives to the petroleum based counterparts. The overall focus of the current project is on the development of bio-based composites for structural applications. In this respect, the long term behavior of the composite becomes a concern. Composite structures in high demanding applications, such as automotive or aerospace, are required to undergo a variety of static and dynamic loads during their service life. These structures often experience exposure to harsh environmental conditions, like elevated humidity or temperature. Hence, in this study, as an initial step toward this development, the performance of bio-based composites and their constituents was characterized, with respect to the moisture impact as well as under static and dynamic loads. Figure 1 demonstrates an example of the projects on use of the fully bio-based composites in designing of the vehicles.

Figure 1. Prototype vehicle, "verte". Lower part of the body frame made of fully bio-based composites [M. Perraudin, BioMobile.ch].

1.1 Natural fibers

Carbon dioxide neutrality of natural fibers and their renewable and biodegradable nature provide great potentials to encourage their wider usage as reinforcement in the polymer composites [1]. The term "natural fibers" can be applied to any type of potential reinforcement for polymers with high aspect ratio that is found in the nature. The sources of fibers may be plants (e.g. wood, flax, hemp, sisal, etc.), animals (e.g. wool, silk) or minerals (e.g. asbestos, basalt).

However, the fibers derived from plants are the main focus of this thesis. Plant fibers, based on their origin, can also be classified in different categories. The two main sub-

divisions within plant fibers can be made by separating the fibers obtained from the various species of wood and the fibers extracted from different parts of the plants (so-called "non-wood" fibers). Figure 2 presents the classification of plant fibers which gives an idea how wide the range of wood and non-wood fibers is. It is to be noted that natural fibers of interest in this study are of non-wood fibers with high cellulose content.

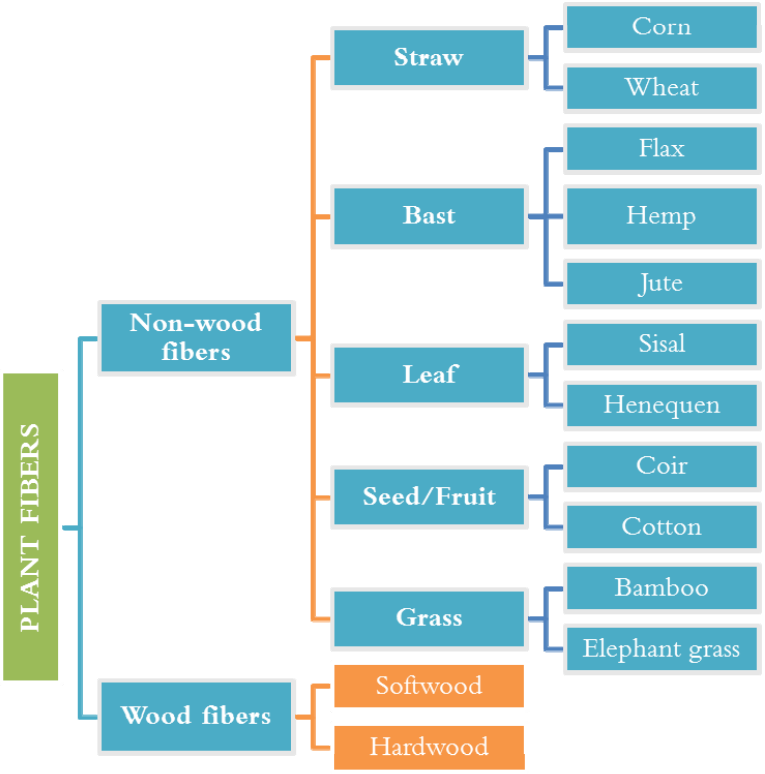

Figure 2. Classification of plant fibers, adapted from [2].

Another standpoint for the intensifying interest on the use of natural cellulosic fibers as reinforcement is their mechanical performance combined with light weight. Natural fibers, containing high amount of cellulose, offer high stiffness and descent mechanical strength compared to synthetic glass fibers. Moreover, the low density of these fibers results in their high specific mechanical properties.

In order to obtain composites with high stiffness and strength, fibers should be long and well oriented, to ensure the highest reinforcing efficiency. This requires a rather comprehensive pre-processing of natural fibers, including the extraction of fibers from the plant and separation into the single fibers. Depending on the extent of the pre-processing, technical fibers (bundled fibers for textile applications) or elementary fibers

(reinforcing fibers for composites) are obtained. The full separation of natural fibers into elementary fibers is difficult to achieve and requires severe mechanical treatments of the fibers, which might introduce damages and degrade the properties of the reinforcement. The amount of mechanical processing of the fibers in the separation step highly depends on how they were initially extracted from the plants. Typically, to facilitate the separation of the fiber from the stem, they are retted and then mechanically separated. However, the retting process is often not efficient enough. Therefore, the fibers should go through a harsh mechanical processing before they can be used. More recently, a more efficient extraction process, combining retting with a bacterial treatment, has been employed (e.g. flax produced by Finflax in Finland) [3]. The bacterial treatment removes the residues of the plant more effectively and requires a less mechanical treatment afterwards to separate the fibers. This results in less damaged elementary natural fibers and with higher mechanical properties. These fibers are further assembled in various types of reinforcement, such as mats, rovings, yarns, and other textile-like products (e.g. weaves, non-crimp fabrics). It should be noted that each extra processing step adds to the cost of the fibers. It also reduces the environmental friendliness aspect of these materials since they often undergo chemical treatments, in order to protect the natural fibers from moisture and to improve the compatibility with polymers.

Apart from the damage and defects introduced by pre-processing, natural fibers possess inherently irregular and somewhat unpredictable properties. These variations depend on the type of the plant which natural fibers are derived from, the region of harvest and the annual weather conditions during the growth. The variety influences not only the geometry of the fibers (diameter and length) (see Figure 3) but also the chemical composition, and consequently variability of the mechanical properties.

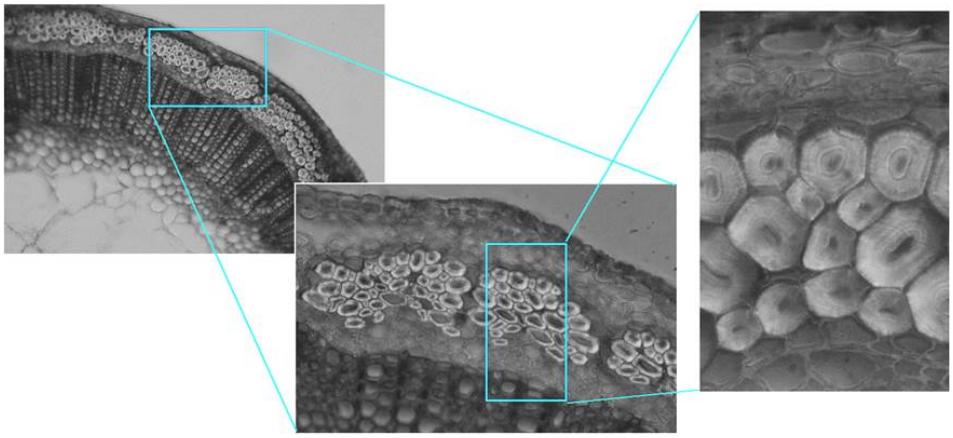

Figure 3. Hierarchical structure of the flax stems (micrographs with x10, x40 and x100 magnifications from left to right) [4].

Many of the issues associated with the variability of plant based natural fibers are resolved if cellulose is extracted from these plants and manmade cellulose fibers are produced.

1.2 Regenerated cellulose fibers

Research on plant cellulose in the early 1850s led to an accidental discovery of a substance from which the first successful textile fiber was manufactured. During 1940s and 1950s the technology development resulted in producing of strong rayon yarns which caused their massive use in automobile tires. The world production of viscose rayon continued to rise until 1970s but steadily the production of synthetic fibers (e.g. nylon, polyester) took over the market since the conversion of oil based polymers to fibers began to offer cheaper products [5]. Figure 4 represents the manmade cellulose bundles stitched together in form of a non-crimp fabric, consisting of continuous fibers with controlled diameter.

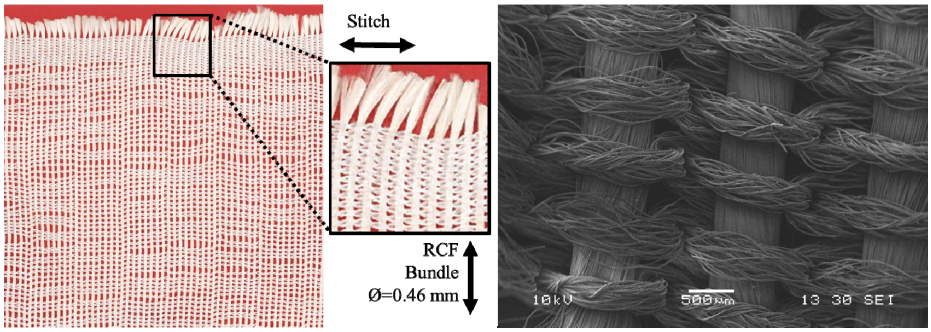

Figure 4. Regenerated cellulose fiber bundles stitched together in a non-crimp fabric.

The variety of type in cellulose fibers and fibers from different manufacturers or dates can alter the physical properties, like density, moisture absorption, etc. Typical fiber fineness of RCF would be 0.1-0.5 tex (10-20 μm in diameter) and most of the fibers are less than 50% crystalline [6].

The following summarizes some of the major production routes of RCF [5]:

Cellulose nitrate

This was the very first artificial fiber process and proved to be a simple but slow operation. This process suffered another strong drawback. It was impossible to scale it up in a safe manner since cellulose nitrate fibers were very flammable.

Direct dissolution in cuprammonium hydroxide: cupro

Cotton cellulose and copper salts were the original components of the process which were both costly and hence hindered a large scale manufacture.

Dissolution via cellulose xanthate: viscose

The route is the conversion of short fiber cellulose into a spinnable solution (dope). This is followed by stretching longer filaments while controlling the physical properties, such as length, denier and cross sectional shape. Since over a hundred years, viscose (or rayon) has been the most used among all artificial fibers [7].

Direct dissolution in amine oxide: lyocell

According to this route, cellulose is directly dissolved utilizing amine-oxide solvent as a base.

1.3 Bio-based polymers

Along with the use of natural fibers as reinforcement, the polymers synthesized from natural raw materials are also gaining popularity [1]. Some of these polymers are well known and their use is widely accepted (such as starch, lignin, polylactic acid PLA, furan resins, Super Sap epoxy) while the others are still under development and the knowledge about them is limited. Often, these polymers are called "bio-based". Although, it does not necessarily mean that a bio-based polymer is completely derived from plants, it can be a mixture of synthetic and bio-based polymers. Like in the case of synthetic polymers, bio-based ones are classified as thermoplastics or thermosets. It should also be noted that some of these materials are biodegradable.

This thesis is partly dealing with the use and characterization of bio-based thermoset resins. The raw material for bio-based thermosets may be extracted from a number of plants and animals in a form of oil or other liquids. For instance, some of these resins are oils derived from soybean, fish, corn, linseed, cashew nut shell, etc. Examples of commercially available thermoset resins are listed in Table 1 [8].

1.4 Natural fiber reinforced polymers

Research is going on to increase the potential of the eco-friendly, inexpensive natural fibers to be involved in polymers. The goal is to develop these materials with enhanced mechanical properties, hardly affected by ageing and with a wider range of applications [9]. Examples of natural fiber composites are listed in Table 2, in two categories of thermoplastic and thermosetting polymer matrices. Despite the fact that the thermal instability of fibers restricts the choice of appropriate matrix materials, both thermoplastics and thermosets are being used. Polypropylene is the most popular thermoplastic matrix, specially combined with flax fibers [10]. Likewise, thermoset polymers such as epoxies, vinylesters, and polyesters are being used. Table 3 summarizes flexural and tensile properties of a variety of natural fiber based composites.

Table 1. Examples of commercially available bio-based thermoset polymers [8].

Manufacturer	Trade name	Raw materials	Applications
DSM	Palapreg ECO P 55-01	Unsaturated polyester (55% bio-based)	SMC/BMC
Bioresin	Bioresin	Castor oil	Automotive, marine
Reichhold	ENVIROLITE	Unsaturated polyester, Soya oil (25% bio-based)	SMC/BMC, pultrusion
TransFurans Chemicals bvba	BioRez furfuryl resin	Furfuryl alcohol based resins from biomass	Varied
Cognis	Tribest	Acrylate functional resin system derived from soya oil	_
Ashland	ENVIREZ 1807	Unsaturated polyester, soybean oil (18% bio-based)	Tractor panels
Amroy Europe Oy	EpoBioX	Natural phenols distilled from forest industry waste stream, e.g. epoxidized pine oil waste (50-90% bio-based)	Kayaks, boats, tent poles, glues, electrical cars
JVS-Polymers Ltd.	LAIT-X/POLLIT	Lactic-acid based	Composites, impregnated products, coatings, biomedical applications

1.5 Environmental durability

Recent research efforts show a growing attention towards the degradation resistance of synthetic and natural fiber composites. However, the degradation of natural composites is a more serious matter. It is verified that the biodegradation of a composite starts with degradation of its constituents as well as their interfacial bonding (Table 4). The composites in outdoor applications are susceptible to different modes of degradation where moisture plays an important role among them. Moisture absorption deteriorates the fiber matrix interface, causes microcracking and eases microbial attacks.

It is believed that the water absorption and desorption in composites follow a Fickian behavior, i.e. linear in the beginning and slowing down by approaching the saturation level. Fickian behavior is caused by the water concentration gradient from one area to

another. However, at elevated temperature, the diffusion behavior starts to differ and the saturation time becomes significantly shorter. This can be explained by the state of water molecules within the composite. The diffusion coefficient, the ability of permeability of solvent molecules among the polymer segments, also increases by temperature and by cracks or voids present on the material surface or in the bulk [14].

Table 2. Examples of thermoplastic and thermoset matrices for natural fiber reinforced composites [11,12].

	Polymer matrix								
	Thermoplastic					**Thermoset**			
Fiber	PP	PE	PA66	PS	PVC	Epoxy	PET	Vinylester	Phenolic
Cellulose[a]	X	X	X	X		X			
Flax	X	X				X			
Jute	X	X				X	X	X	X
Sisal	X	X			X	X	X		
Kenaf	X					X			X
Ramie	X								
Hemp						X	X	X	X
Bagasse	X								X
Bamboo	X					X	X		
Pineapple		X					X		X
Wood flour/fiber	X	X			X		X		
Wool							X		

[a]Includes cotton.

Table 3. Mechanical properties of different thermoplastic short fiber natural composites [13].

Property	**Composite**						
	PP/ glass	PP/ flax	PP/ jute	PP/ wood	HDPE/ RH[a]	MBY[b]/ sisal	PP/ hemp
Fiber content (wt%)	30	30	30	30	65	15	30
Flexural strength (MPa)	88.1	44.3	52.4	60.0	33.5	–	58.9
Flexural modulus (GPa)	4.70	4.21	–	–	2.90	2.75	3.80
Tensile strength (MPa)	57.4	26.0	34.1	35.0	13.5	16.8	32.9
Tensile modulus (GPa)	3.20	1.74	–	–	2.39	2.20	2.60

[a]Rice husk

[b]MaterBi-Y (commercially available bio-based polymer)

One common approach to improve the moisture resistance in natural fibers is to perform a chemical treatment to modify the fiber surface. The same chemical surface treatment that is used to improve the moisture resistance can be also used to improve the bond of hydrophilic natural fibers with hydrophobic thermoset resins. All this leads to an enhanced wettability of the fibers by the matrix and increased mechanical properties [15,16].

Table 4. Cell wall polymers responsible for properties of lignocellulosic fibers, adapted from [14].

Component	Property
Crystalline cellulose	Strength
Hemicellulose	Thermal degradation, biological degradation, moisture absorption, flammability[a]
Lignin	UV degradation, char formation[a]

[a]Properties contributing to fire degradation.

1.6 Interfacial properties

One of the factors determining a polymer composite's mechanical performance is the interfacial adhesion between the fibers and the polymer matrix. Natural fibers contain hydroxyl (OH) groups therefore are hydrophilic in nature. There is a poor interfacial adhesion between polar and hydrophilic fibers with non-polar and hydrophobic matrices. Mixing these materials becomes difficult when the fibers wetting by the matrix is poor. This may result in non-impregnated reinforcement and high porosity, leading to a low mechanical performance. Chemical treatment can clean the fiber surface, chemically modify it (so it becomes more reactive), increase its roughness and stop the moisture absorption. Right chemical treatment improves the fiber quality, increases the fiber yield and fiber's hydrophobicity and reduces swelling [17]. However, if the chemicals are too aggressive, it might lead to changes of the molecular structure of fibers and the degradation of fiber properties [18]. Chemical surface modification can alter surface tension and polarity of the fibers. Coupling agents improve the stress transfer at the interface between the fiber and matrix. Chemically modified surfaces with improved interfacial bonding decrease the moisture absorption. Chemical surface treatments such as silane treatment, mercerization and acetylation, have achieved improved fiber strength and fiber matrix adhesion in natural fiber reinforced composites [16]. Table 5 summarizes the influence of different fiber treatments on interfacial shear strength (IFSS) for thermoplastics reinforced by flax fibers.

Table 5. IFSS for thermoplastics reinforced with treated and non-treated flax fibers [19].

Flax fiber type	Matrix	Fiber treatment	IFSS, MPa	Test method
Green	PP	_	6.33	SFF[a]
		Acetylation	11.61	SFF
		Stearic acid	9.49	SFF
		_	7.21	Micro-debond
		MAPP	7.20	Micro-debond
Dew retted	PP	_	12.75	SFF
		Acetylation	13.05	SFF
		Stearic acid	13.36	SFF
		Transcrystalline layer	23.05	SFF
	HDPE	_	17.3	Pullout
		_	18.0	Pullout
	LDPE	_	5.6	Pullout
	PP/MAPP	_	17.8	Pullout
Duralin™	PP	_	7.45	Micro-debond
		Hot cleaned	6.63	Micro-debond
		MAPP	7.17	Micro-debond
	HDPE	_	16.2	Pullout
	LDPE	_	7.1	Pullout

[a]Single fiber fragmentation

1.7 Mechanical durability

Composite materials for load carrying applications are required to be designed for long term service under static and dynamic loading. Therefore, the knowledge about the developing damage mechanisms and failure scenarios are crucial. In general, polymers and their composites exhibit a time dependent behavior (viscoelasticity, viscoplasticity). Furthermore, unlike metals, composite materials have anisotropic properties which strongly depend on the composites constituents (fiber, matrix and their interface). Despite the large amount of research efforts on the mechanical behavior of composites, the mechanisms of failure during creep and fatigue are not sufficiently understood [20].

Additionally, the mechanical properties of natural fiber composites, owing to their organic nature and high moisture absorption, have a higher rate of degradation than the synthetic fiber composites. Therefore, it is of great importance to identify the degradation mechanisms under the lifetime of natural fiber reinforced composites.

1.8 Nonlinearity

Most polymers exhibit a nonlinear mechanical behavior and the composites based on these materials perform in a similar manner. Synthetic fibers (like glass, carbon) are stiff, linear elastic and fairly brittle materials. Accordingly, the unidirectional polymer composites reinforced with continuous synthetic fibers, show a linear elastic response when loaded along the fiber direction. This indicates that the behavior of the composites is mainly governed by the fibers. However, the stress-strain curve for short fiber composites as well as multidirectional and off-axis laminates reinforced with continuous fibers might be rather nonlinear. Such a behavior may not be only defined by the properties of the matrix material (showing strong viscoelastic and viscoplastic phenomena) but also by the development of microdamages (e.g. debondings, matrix microcracks, fiber breaks) within the composite. In case of the natural fiber composites, the situation is much more complicated because not only the polymer matrix and microdamages are sources for nonlinearity but also the fibers themselves may exhibit an inherently nonlinear behavior (viscoelastic and viscoplastic). This might be due to the complex hierarchical structure of the natural fibers.

In Figure 5, the stress-strain curve and the loading-unloading sequence for RCF bundles are shown. The drastic slope change in the stress-strain curve and the evolution of hysteresis loops display the nonlinearity of these fibers. Besides, the humidity exposure has shown a magnifying effect on this nonlinearity in the material [21].

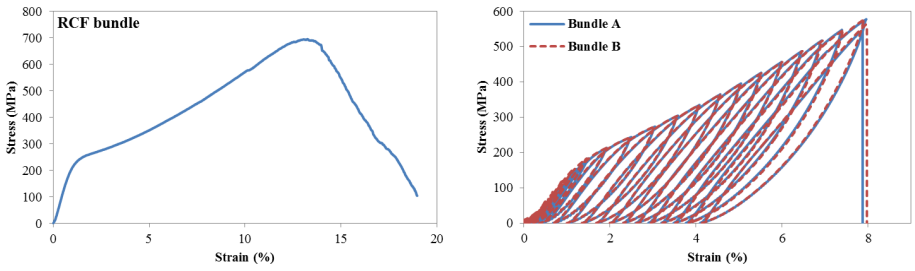

Figure 5. Typical stress-strain curve (left) and loading-unloading sequence (right) for RCF bundle.

Such a nonlinear response to mechanical and environmental loadings complicates the characterization and consequently the modeling process of the bio-based composites. In order to predict the behavior of these materials by models, numerous factors such as nonlinearity and microdamage as well as the environmental effects have to be accounted for. Thus, a comprehensive understanding of the time dependent behavior of these materials (e.g. creep, fatigue) is required, to possibly modify and adapt the models developed for synthetic composites to the bio-based ones.

2 Current work

As it is evident from the discussion above, the bio-based composites may and should become the materials of tomorrow for load bearing structures. However, it is also clear that before this happens many key issues related to the durability of these materials should be addressed and significant improvements are to achieve. The work carried out within this PhD project was directed towards this ultimate goal.

Although the common objective was the overall durability of bio-based composites, the results presented here can be divided into two main parts:

- The effect of moisture on mechanical properties of the bio-based materials, under static loading conditions;
- The study of mechanisms defining the performance of cellulosic fibers and their composites in fatigue.

The first two papers presented in the thesis (**Paper A** and **Paper B**) dealt with the characterization of mechanical properties of the bio-based constituents and their composites. The primary focus was on the evaluation of moisture influence on the behavior of these materials. Bio-based thermoset resins (Tribest, EpoBioX, Palapreg, Envirez SA and Envirez SB) reinforced with cellulosic fibers (flax and regenerated cellulose) were studied. The constituents (fiber and resin) as well as the composites were conditioned at different relative humidity levels, in order to obtain different moisture contents in the material. The typical epoxy resin (Araldite LY556) and E-glass fibers (GF) reinforced bio-based thermosets were used as the reference materials against which bio-based materials were ranked. The chemical treatment (alkali and silane) of fibers was evaluated with respect to the protection against moisture. The main result of **Paper A** and **Paper B** was demonstrating the good performance of bio-based resins and their composites at elevated humidity in comparison with the synthetic counterpart (epoxy). Furthermore, it was confirmed that the moisture uptake in bio-based composites is primarily due to the cellulosic reinforcement. Unfortunately, fiber treatment did not result in any significant improvement in terms of moisture uptake. In general, the results gathered in the two first papers were planned as the reference data for the designing of the structural bio-based composites since such data are often difficult to obtain from the literature.

Paper C was a review paper on characterization of the long term performance of bio-based composites and was intended as a transition stage to turn from studying the environmental durability of bio-based composites towards their mechanical durability. The main purpose of this study was to evaluate the existing conventional methods in analyzing the fatigue performance of polymer composites and their applicability to the bio-based materials. The search in the literature results confirmed that the durability

data for bio-based composites are not so readily available and there are no many comprehensive studies on this subject, particularly for RCF based composites. Hence, the information presented in **Paper C** should help to identify the issues that need to be addressed in the future investigations, for understanding the factors affecting the mechanical durability of natural fiber composites. One of the statements made in this paper was that the conventional approach to analyze fatigue data (construction of S-N diagrams) might not be optimal for natural fiber composites due to their complex structure and variability of properties. The argument behind that would be the hierarchical structure of natural fibers leading to a nonlinear behavior of the reinforcement and subsequently the composite. This phenomenon was proposed to be responsible for the different behavior of these materials in fatigue compared to the synthetic fibers. The further research procedure was designed based on the material screening in **Paper A** and **Paper B** as well as the literature search in **Paper C**.

Paper D is an investigation on the potential use of RCF and their composites in structural applications, by identifying the performance of these materials under fatigue loading conditions. The results obtained in **Paper D** uncovered a rather unusual behavior by these materials under cyclic loading. This was due to the highly nonlinear nature of the reinforcement which also strongly influenced the performance of the composites. Therefore, instead of following the conventional approach to generate S-N diagrams, the main attention in this investigation was on the failure mechanisms and the evolution of mechanical properties during fatigue of RCF bundles and their composites. Moreover, a stiffening effect under fatigue was observed, at large numbers of cycles. This was probably due to the plasticity which ceased with time under loading. The strain evolution during fatigue of these materials strongly resembled that of creep experiments. This time dependent behavior of RCF based materials under fatigue should be further studied and verified in connection with creep experiments. This finding might be used in the future for accelerated testing. Furthermore, based on the behavior exhibited by RCF, the damage sequence observed in the brittle matrix composites (like ceramics) was proposed for RCF composites. It was also speculated that the internal structure of the fibers and composites altered during fatigue loading, which considerably affected their performance. However, these hypotheses have to be validated by proper characterization methods.

Since the failure of structures in fatigue usually occurs due to the propagation of existing defects or cracks and because there are known compatibility issues between the polymers and cellulosic fibers, the last paper in this thesis was dedicated to the characterization of fracture toughness in the natural fiber composites. **Paper E** was on the evaluation of interlaminar properties in composites reinforced with chemically modified as well as with non-treated RCF. The characterization of fracture toughness was carried out by means of double cantilevered beam (DCB) tests in static and cyclic loading. The measured values of fracture toughness for RCF composites were

significantly higher than those typically reported for synthetic fiber reinforced polymers. This high fracture toughness was probably not achieved only due to the good compatibility between the fiber and matrix but also due to the highly nonlinear behavior of reinforcement, resulting in high energy dissipation. Moreover, due to the presence of strong viscoelastic and viscoplastic phenomena it was not possible to make a certain judgment on the effect of fiber treatment on the fiber matrix adhesion. Although, analyzing the images of DCB fracture surfaces by scanning electron microscopy indicated an improvement in the interfacial adhesion. The main outputs of **Paper E** were the applicability assessment of DCB tests to characterize fracture toughness of RCF based materials as well as the identification of energy dissipation mechanisms in these composites. However, a correct estimation of fracture toughness for such materials requires a combination of testing with comprehensive nonlinear analysis of the experimental results (e.g. numerical simulation by FEM).

Knowledge on the mechanical performance of these bio-based materials and on the evaluation technics adapted for characterizing these materials is valuable to the researchers in both academia and industry. The results presented in this thesis give useful input data required for the designing of bio-based composites, regarding the effects of moisture as well as the nonlinear behavior. There is still some considerable work to be done in order to present ready-to-use structural cellulosic fiber composites with enhanced durability to the industries. Even though, this study allows making a substantial step forward along the development of high performance bio-based composites, the new generation of sustainable and environmentally friendlier composite materials.

3 Author contributions

The author participated in the planning of the work and performed a significant part of the experiments. She was also involved in the discussions as well as in the interpretation of results and contributed to the writing of the papers.

- **Paper A.** The author participated in the planning of the experimental work, analysis of the results and writing of the paper.
- **Paper B.** The author was responsible for the general planning and coordinating the efforts on this paper, performed a major share of the experimental work, processing and analyzing of the results as well as writing.
- **Paper C.** The author was in charge of the planning and writing of the paper, carried out most of the literature search as well as the analysis, interpretation and summary of the literature data.
- **Paper D.** The author was responsible for the planning of the experimental program, carrying out all the experiments (including most of the manufacturing), participating in the analysis and interpretation of results as well as writing of the paper.
- **Paper E.** The author contributed to the overall coordination and writing of the paper and carried out a major part of the manufacturing and testing.

4 References

[1] P. Wambua, J. Ivens, and I. Verpoest, *Composites Sci. Technol.*, **63**, 1259-1264 (2003).

[2] J. Biagiotti, D. Puglia, and J.M. Kenny, *Journal of Natural Fibers*, **1**, 37-68 (2004).

[3] J. Andersons, and R. Joffe, *Composites: Part A,* **42,** 1229–1235 (2011).

[4] R. Joffe, and J. Andersons, Mechanical characterization and properties of cellulose fibers, Editors: K. Oksman, A.P. Mathew, A. Bismarck, O. Rojas, and M. Sain, Handbook of green materials: Biobased composite materials, their processing properties and industrial applications, *World Scientific Publishing Co. Pte. Ltd.*, **2**, 7-23 (2014).

[5] C. Woodings, A brief history of regenerated cellulosic fibers, Editor: C. Woodings, Regenerated cellulose fibers, *Woodhead Publishing Limited*, **1**, 1-21 (2001).

[6] J.W.S. Hearle, Physical structure and fibre properties, Editor: C. Woodings, Regenerated cellulose fibers, *Woodhead Publishing Limited*, **8**, 37-61 (2001).

[7] A.G. Wilkes, The viscose process, Editor: C. Woodings, Regenerated cellulose fibers, *Woodhead Publishing Limited*, **3**, 37-61 (2001).

[8] L. Laine and L. Rozite, State of the art: Eco-efficient materials, *ANACOMPO Project Report* (2010).

[9] M. Misra, S.S. Ahankari, and A.K. Mohanty, Creep and fatigue of natural fibre composites, Editor: N.E. Zafeiropoulos, Interface engineering of natural fibre composites for maximum performance, *Woodhead Publishing Limited*, **11**, 289-340 (2011).

[10] K. Van de Velde, and P. Kiekens, *Polymer Testing*, **20**, 885-893 (2001).

[11] D. Puglia, J. Biagiotti, and J.M. Kenny, *Journal of Natural Fibers*, **1**, 23–65 (2004).

[12] A.S. Blicblau, R.S.P. Coutts, and A. Sims, *Journal of Materials Science Letters*, **16**, 1417–1419 (1997).

[13] R. Joffe, J. Andersons, Mechanical performance of thermoplastic matrix natural-fibre composites, Editor: K.L. Pickering, Properties and performance of natural-fibre composites, *Woodhead Publishing Limited*, **13**, 402-459 (2008).

[14] Z.N. Azwa, B.F. Yousif, A.C. Manalo, and W. Karunasena, *Mater Des*, **47**, 424-442 (2013).

[15] S. Kalia, B.S. Kaith, and I. Kaur, *Polymer Engineering & Science*, **49**, 1253-1272 (2009).

[16] A.K. Mohanty, M. Misra, L.T. Drzal, S.E. Selke, B.R. Harte, and G. Hinrichsen, Natural fibers, biopolymers, and biocomposites: An introduction, Editors: A.K. Mohanty, M. Misra, and L.T. Drzal, Natural fibers, biopolymers and biocomposites, *Taylor and Francis Group LLC*, **1**, 1-35 (2005).

[17] Kalia S., Kaith B.S., and Kaur I., Pretreatments of natural fibers and their application as reinforcing material in polymer composites-a review, *Polymer Engineering and Science,* **49**, 1253-1272 (2009).
[18] A. Hajlane, H. Kaddami, and R. Joffe, A green route for modification of regenerated cellulose fibres by cellulose nano-crystals, *Submitted to Cellulose* (2016).
[19] R. Joffe, J. Andersons, and L. Wallström, *Composites Part A: Applied Science and Manufacturing*, **34**, 603-612 (2003).
[20] J. Gassan, *Compos Part A: Appl Sci Manuf*, **33**, 369-374 (2002).
[21] N. Doroudgarian, L. Pupure, and R. Joffe, *Polymer Composites,* **36**, 1510-1519 (2015).

Paper A

Moisture uptake and resulting mechanical response of bio-based composites. I. Constituents

Liva Pupure[1], Newsha Doroudgarian[1], Roberts Joffe[1,2]

[1]Division of Materials Science, Luleå University of Technology, S-97187 Luleå, SWEDEN
[2]Group of Materials Science, Swerea SICOMP, S-94126 Piteå, SWEDEN

Reformatted paper published in:
POLYMER COMPOSITES, Volume 35, Issue 6

PAPER A

Moisture uptake and resulting mechanical response of bio-based composites. I. Constituents

Liva Pupure[1], Newsha Doroudgarian[1], Roberts Joffe[1,2]

[1]Division of Materials Science, Luleå University of Technology, S-97187 Luleå, SWEDEN
[2]Group of Materials Science, Swerea SICOMP, S-94126 Piteå, SWEDEN

Abstract. The mechanical properties of the bio-based fiber and resins have been characterized and moisture influence on the behavior of these materials has been studied. Commercially available bio-based thermoset resins (Tribest, EpoBioX, Palapreg, Envirez SA and Envirez SB) and regenerated cellulose fibers (Cordenka) have been conditioned at different relative humidity (as received, dried, 41%, 70% and 90%) in order to obtain materials with different moisture content. The following properties of polymers were measured: tensile, flexural (3P-bending), impact strength (unnotched Charpy) and fracture toughness (compact tension). The results of characterization of bio-based thermosets were compared against the data for epoxy Araldite LY556, which is used as reference resin. Regenerated cellulose fiber bundles (with and without twist, extracted from fabric) as well as single fibers separated from these bundles were tested in tension. In general, bio-based resins performed well. Moreover, EpoBioX showed better properties than synthetic epoxy.

Introduction

The growing need to reduce the use of oil dependent materials and limited Earth resources stimulate the use of renewable and recyclable materials. Therefore, during the recent years there has been a significant progress in the area of bio-based materials [1]. For example, there has been significant development in bio-based composites for packaging (non-structural) [2] and automotive [3-6] applications. However, sensitivity to moisture [7-11] is one of the main reasons why industry withholds the use of these materials for applications where long term load carrying capabilities are required. Even in synthetic matrix (e.g. epoxy, polypropylene) natural fiber composites, the large uptake of moisture is observed since in this case mostly reinforcement is responsible for water transport inside the material. The material developers are well aware of these issues and there are certain ways to overcome them, for example by chemical treatment of the reinforcement which reduces moisture uptake [12-13] or by protecting the composite surface (and exposed fibers) from environment by application of gel coating [14] (or miscellaneous paints) on the final product.

Lately, the bast natural fibers, such as flax and hemp, have been frequently studied [15-17] due to their good mechanical properties. Even though, their mechanical

performance is often comparable to that of glass fibers, there is one major disadvantage: the large variability of properties of natural fibers depending on conditions of growth and harvest, geographical location, processing etc. Some studies [18-19] showed diameter variability not only from fiber to fiber but also along the length of the filament [20-21]. Even position in the stem where fiber is extracted from is important, as demonstrated on the flax fibers in [18]. Apart from the inherent variation of properties, there are other difficulties associated with the use of natural fibers in composites. For instance, limited fiber length makes it more difficult to control the fiber alignment and orientation. However, another type of reinforcement with natural origin has caught attention of materials researchers developing bio-based composites – regenerated cellulose fibers (RCF). These fibers are manmade fibers produced out of natural polymer directly, contrary to the fibers with fossil origin. RCF are continuous fibers with well controlled geometry (see Figure 1) and properties. Thus, they can be aligned and assembled into various types of fabrics. Recent studies [22-25] have shown that these fibers are well suited for use as reinforcement in polymer composites. However, due to their natural origin they are still very sensitive to the moisture and this issue has to be addressed, in order to be able to develop high performance composites based on RCF.

Latterly, a number of bio-based thermosetting resins became available which promoted development of entirely bio-based high performance composites for structural applications. Properties of the polymers derived from soybean oil and protein fillers have been reported in [26], a critical overview of bio-based thermosets is presented in [27]. However, information available in the literature regarding these polymers is still very limited, especially regarding their performance at elevated humidity.

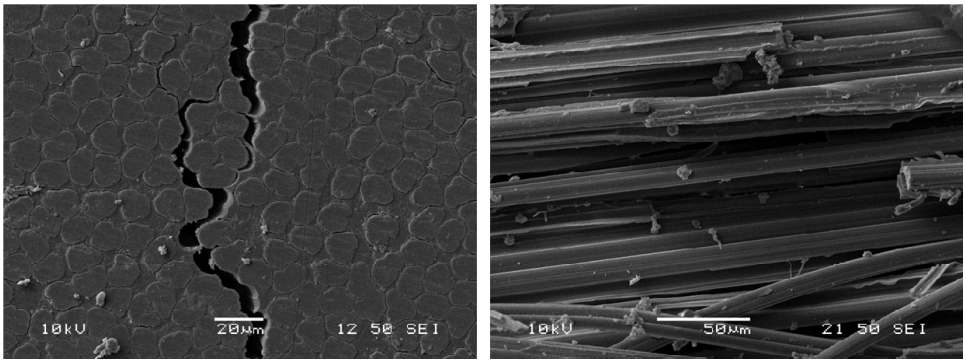

Figure 1. Scanning electron microscopy image of RCF/EpoBioX composite: cross section of the fibers seen from the specimen edge (left) and side view of the fibers seen from the fracture surface of specimen (right).

The main objective of this work is to characterize the mechanical properties of constituents for bio-based composites and to study the influence of moisture on their performance. Five different bio-based thermoset polymers were subjected to tensile, flexural, impact and fracture toughness tests. RCF were tested in simple tension and cyclic loading-unloading experiments. Single fibers as well as bundles were characterized. Moisture uptake of all materials at several humidity levels was studied and its influence was evaluated by testing resins and fibers with different moisture contents. The polymer performance was compared against reference material, Araldite LY556 epoxy resin.

Materials and manufacturing

RESINS

Five bio-based resins, commercially available, were used – Tribest, EpoBioX, Palapreg, Envirez SA and Envirez SB. Tribest (*Cognis GmbH*, Germany) is acrylated, epoxidized soyoil based resin. As a curing agent for Tribest 2.25% peroxide Benox L40LV (*Syrgis Performance Initiators AB*, Sweden) was used. EpoBioX (*Amroy*, Finland) is epoxidized pine oil based resin. As a curing agent for EpoBioX Amroy Ca35Tg hardener was used (mixing ratio 100:27). EpoBioX and Tribest are approximately 75% bio-based, whereas Palapreg (*DSM*, Switzerland) is 55% bio-based. Envirez SA and Envirez SB (*Ashland*, USA) are unsaturated polyester soybean oil based resins. Envirez SB resin is derived from Envirez SA. Both resins are 18% bio-based. It should be noted that EpoBioX is not commercially available anymore. However, SUPER SAP resin produced by Entropy Resins (CA, USA) is of similar origin and properties. These resins were chosen during the preliminary screening of commercially available materials within ANACOMPO project as the potential candidates for structural bio-based composites.

Synthetic epoxy Araldite LY 556 (*Huntsman*, USA) was used as a reference resin in this study (further in the text this resin is referred as Epoxy). Polymer plates were manufactured by use of resin transfer molding. A mold consisting of two stiff steel halves, which was used to manufacture flat polymer plates (225 mm x 325 mm) with even thickness (2mm and 4mm). The resin was infused at room temperature and at low flow speed. The mold was placed vertically (slightly tilted) so that it was filled from the bottom up, to avoid air entrapment. Tribest was cured for 16h and LY 556 for 4h at 80°C. EpoBioX, Palapreg and Envirez were left for curing overnight at room temperature. For some resins the mold was put in the furnace for post curing. Temperature history of post curing depends on the resin type – LY 556 was kept for 4h at 140°C, EpoBioX for 2h and Palapreg for 4h at 80°C and Envirez for 2h at 70°C.

REGENERATED CELLULOSE FIBERS

RCF produced by a special variant of the viscose process "Cordenka 700 Super 3" (*Cordenka GmbH*, Germany) were used in this work. The main characteristics of these fibers are available from the manufacturer [28] and reported in [24]. Three types of fiber bundles were studied, with twist (Z100: 100 twists per meter), without twist and bundles extracted from unidirectional stitched fabric produced by Engtex (custom made for ANACOMPO project). It should be noted that during manufacturing of fabrics, the bundles were slightly twisted.

Experiments

SPECIMEN PREPARATION AND CONDITIONING

Polymer plates were cut into rectangular shaped specimens and their edges were grinded and polished with sandpaper of different grades (up to 1200 grit). The approximate dimensions of specimens are summarized in Table 1. It should be noted that even though, there is a standard listed for each test, some of these standards were used only as guidelines. In some cases, it was not possible to use the exact dimensions of specimens according to standards due to the limited amount of available material. However, this did not cause problems for using obtained results to rank studied materials with respect to their properties.

Table 1. Summary of specimen dimensions used for different tests.

Experiment	Width, mm	Thickness, mm	Length[a], mm	Standard
Tensile test (NC)[b]	13	4	150 (100)	ASTM D 638-95 [29][c]
Tensile test (conditioned)	10	2	165 (100)	ASTM D 638-95 [29][c]
Three-point bending test	10	4	80 (64)	ASTM D 790M-93 [30]
Impact test (Charpy)	10	4	80 (43)	ISO 179:1993 [31][c]
Fracture toughness test	8	4	40 (32)	ASTM D 5045-95 [32]

[a]In parentheses, working zone (gauge length or support span) of specimen is given.

[b]Dimensions (mm) of non-conditioned specimens without strain gages for EpoBioX, Tribest and Epoxy were: 10x2x165 (100), whereas for other resins: 10x4x110 (60).

[c]Standard is used only as a guideline for test (sample geometry slightly differs from the standard).

Specimens were divided in two groups – conditioned and not conditioned (NC). For NC specimens no conditioning was done and they were tested as received (at room environment: relative humidity (RH) 24%, room temperature (RT) ≈23°C). The conditioned specimens were stored in an environment with controlled humidity until the moisture content in materials reached equilibrium. Prior to conditioning, specimens were kept in the oven at 50°C and their mass was constantly monitored to confirm the samples were dried (mass of specimens did not change anymore after that point). Afterwards, specimens were divided in three groups and placed in desiccators with different RH levels: 41%, 70% and 90%. RCF bundles were conditioned at 41% and 70% RH. The fixed level of relative humidity was achieved by using of a saturated solution of different salts. The weight of polymer samples as well as fibers was regularly measured, to ensure that moisture content reached the saturation level and also to observe the kinetics of moisture sorption. Conditioning at 41% and 70% was done on rectangular samples with approximate dimensions of 4x10x20 mm. Due to very small mass gain, moisture uptake at RH=41% was not possible to measure with acceptable accuracy.

Diffusion according to Fick's law is assumed and apparent diffusion coefficient, D_a, for the material in case of one-dimension is given by [33]:

$$\frac{4C_s}{b\sqrt{\pi}}\sqrt{D_a} = \frac{C_2 - C_1}{\sqrt{t_2} - \sqrt{t_1}} \tag{1}$$

where C_s is the mass gain at saturation level, b thickness of the sample and $\frac{C_2 - C_1}{\sqrt{t_2} - \sqrt{t_1}}$ is the slope of initial moisture uptake curve (moisture gain C versus square root of time). It should be noted that the edges of conditioned samples were not sealed. Therefore, one-dimensional diffusion through the surfaces of samples was not ensured and in order to obtain the actual diffusion coefficient, the correction factor, k, should be used [33]:

$$k = \left(1 + \frac{b}{l} + \frac{b}{w}\right)^{-2} \tag{2}$$

where w is the width of sample and l the length. The true one-dimensional diffusion coefficient, D, is then calculated as:

$$D = k \cdot D_a \tag{3}$$

TENSILE TEST

Quasi-static tensile tests of polymers were performed in the displacement controlled mode at 2mm/min (≈2%/min) on an electromechanical tensile machine Instron 3366 equipped with a 10 kN load cell and pneumatic grips. Standard Instron extensometers 2630-111 and 2620-601 (50mm or 25mm base depending on sample length) were used

to measure the longitudinal strain, whereas transverse strain was measured by strain gages. Tensile elastic modulus E and Poisson's ratio ν was calculated from the stress-strain and transverse-axial strain curves, respectively, by a linear fit of experimental data points in the axial strain region 0.05-0.2%. It was observed that the samples with strain gages failed at lower stress levels than samples without strain gages. Most probably, small defects which act as stress concentrators were introduced on the surface of polymer specimens during the installation of strain gages. Therefore, max stress σ_{max} and strain at max stress $\varepsilon_{\sigma max}$ were obtained from the experiments on samples without strain gages. It should be noted that for materials which do not exhibit any yielding, the strain at max stress corresponds to the strain at failure.

Single fiber tensile tests were performed according to the ASTM D 3379-75 standard [34]. Single filaments were manually separated from the bundles and their ends were glued onto a paper frame. Even though, the fibers have somewhat irregular "heart-like" shape (see Figure 1), the calculation of fiber cross section area was done assuming circular cross section for the filament with an average diameter of 12.5 μm. The diameter was measured under an optical microscope from the side view of the fiber. The limited number of measurements (≈25) showed that the diameter did not change significantly (±0.1 μm) from fiber to fiber. Single fiber specimens with gauge length of 50 mm were prepared. Tension tests were carried out on an electromechanical tensile machine Instron 4411 equipped with a 5N load cell and pneumatic grips. During mounting, the specimens were handled only by the paper frame. After clamping of the ends of paper frame by the grips of test machine, the frame sides were carefully cut in the middle. The tests were displacement controlled with the loading rate of 5 mm/min (which corresponded to 10 %/min). Two types of single fiber specimens were tested: fibers extracted from twisted bundles (7 fibers) and fibers separated from bundles with no twist (7 fibers). These fibers were not conditioned. They were stored and tested at room ambient temperature and relative humidity (RT≈23°C, RH≈24%). Since direct strain measurement was not possible to perform during these tests, the displacement of the crosshead of the tensile machine was used to calculate strain. In order to obtain the true strain for fiber, machine's compliance was calculated and taken into account (as described in the standard [34]). Elastic modulus for single fibers was measured in a similar manner as for polymer specimens but within a different strain region of 0.3-0.7%. Fiber bundle tensile tests (gauge length of bundles 100 mm) were also performed on Instron 4411 in the displacement controlled mode with loading rate 10mm/min (≈10%/min). Machine was equipped with mechanical grips and a 500N load cell. Every bundle was fitted with end tabs, flat pieces of wood were glued at each bundle end (Araldite 2011 two component epoxy adhesive was used). The fiber bundle, with and without twist, and bundles extracted from fabric were tested. Fiber bundles were conditioned and tested at four different humidity levels – dry (kept in the oven at 50°C for 9 days), NC (humidity in the room RH≈24%), RH=41% and RH=70%. Similarly,

as in the case of single fiber tensile tests, in order to obtain the true strain in bundle, machine's compliance was calculated and taken into account. Due to the accumulation of residual strains and the resulting shift of stress-strain curves towards higher strains in the consecutive loading steps, the elastic modulus for RCF bundles was calculated by a linear fit for the curve within a stress region of 20-90MPa, instead of the pre-defined strain interval. All the mechanical tests were performed at least on three samples.

THREE POINT BENDING TEST

Bending tests of polymer samples were done according to ASTM D 790M-93 standard [30]. These tests were performed on Instron 4411 equipped with a 500N load cell and a standard Instron three-point bending fixture. Rate of the crosshead motion was calculated [30] for each specimen individually, based on their dimensions, in order to achieve the same strain rate (2%/min) for all of them. From three point bending tests, flexural modulus E_B was measured in the strain region 0.05-0.2% (calculated by a linear fit of stress-strain curve). Max flexural stress σ_B and strain at max flexural stress ε_B were also obtained.

IMPACT TEST

Charpy impact tests on unnotched specimens were performed, following guidelines of ISO 179:1993 standard [31]. The energy of pendulum at impact was W=14.7J, mass of the hammer m=2.035kg and the length of pendulum l=380mm. Impact tests were performed for NC samples and samples conditioned at RH=90%. Charpy impact strength of unnotched specimen a_{cU} is calculated according to:

$$a_{cU} = \frac{W_a}{bw} \tag{4}$$

where, W_a is the energy, absorbed by the test specimen during failure.

FRACTURE TOUGHNESS TEST

Fracture toughness tests were performed according to ASTM D 5045-95 standard [32] on Instron 4411 by use of compact tension samples. Tests were done in the displacement controlled mode with a crosshead speed of 10mm/min. The stress intensity factor, K_{IC}, was calculated from:

$$K_{IC} = \frac{P}{bw^{1/2}} f\left(\frac{a}{w}\right) \tag{5}$$

where P is the load at failure, a length of the crack and $f\left(\frac{a}{w}\right)$ is an empirical function dependent on the ratio of pre-crack length and specimen width, a/w (see [32]).

LOADING-UNLOADING TENSILE TEST OF FIBER BUNDLES

To investigate how the material was behaving after application of high stress levels, loading-unloading experiments on fiber bundles were carried out. One cycle of this test consisted of increasing load to a certain level and unloading to 0.1N level (this was considered to be the completely unloaded state). With each cycling step, the load increment increased by 5N. Loading-unloading tests were performed in the displacement controlled mode at 5mm/min (which corresponded to 10%/min) on Instron 3366 equipped with a 500N load cell and mechanic grips. Tests were performed on twisted (gauge length of bundles 50 mm) RCF bundles (the same specimen lay-out as in bundle tensile tests).

Results and discussions

MOISTURE UPTAKE

The moisture uptake data for resins at RH=70% and RH=90% are presented in Figure 2. The corresponding results for RCF at RH=41% and RH=70% are shown in Figure 3. The diffusion coefficients calculated from the results at RH=90% according to Equations 1-3 are presented in Table 2. Out of all polymers, EpoBioX showed the slowest moisture uptake. However, the saturation level for EpoBioX was approximately the same as for Epoxy, Envirez SA and Envirez SB (see Table 2). Tribest and Palapreg absorbed moisture much faster than other studied resins, according to Figure 2. It should be noted that some dark spots appeared on Tribest samples conditioned at RH=90% and EpoBioX resin changed color. Due to smaller size of the samples used at RH=70%, the obtained data were less stable than for RH=90%. RCF showed a very significant moisture uptake – the saturation levels (mass gain) were 6.4% and 10.4% for RCF conditioned at RH=41% and RH=70%, respectively. This is approximately 7.2 times higher than for the worst performing resins, Tribest and Palapreg.

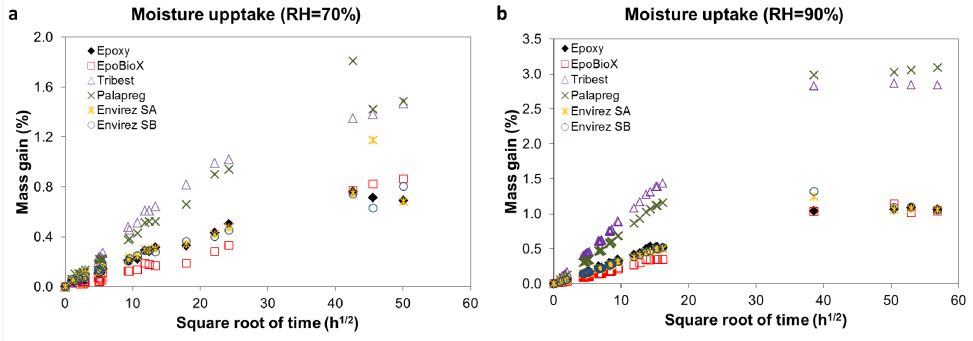

Figure 2. Moisture uptake for resins at: a) RH=70% and b) RH=90%.

Table 2. Diffusion coefficients for resins at RH=90%.

Resin	Epoxy	EpoBioX	Tribest	Palapreg	Envirez SA	Envirez SB
D_a, m^2/s	$1.1\cdot10^{-12}$	$4.7\cdot10^{-13}$	$1.1\cdot10^{-12}$	$5.4\cdot10^{-13}$	$8.4\cdot10^{-13}$	$8.0\cdot10^{-13}$
C_s, %	1.06	1.06	2.85	3.04	1.11	1.14
K	0.451	0.445	0.449	0.467	0.461	0.460
D, m^2/s	$4.8\cdot10^{-13}$	$2.1\cdot10^{-13}$	$4.7\cdot10^{-13}$	$2.5\cdot10^{-13}$	$3.9\cdot10^{-13}$	$3.7\cdot10^{-13}$

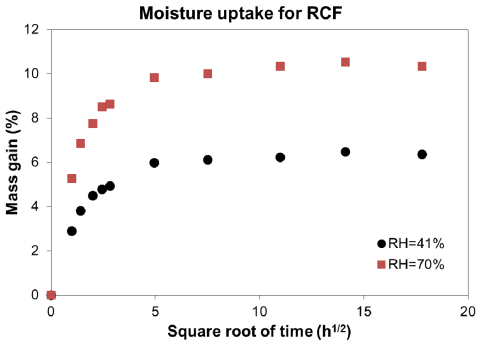

Figure 3. Moisture uptake for RCF.

MECHANICAL CHARACTERIZATION

Resins. The average mechanical properties of bio-based resins are presented in Table 3. The value of standard deviation is shown in parentheses. The shear modulus presented in Table 3 was calculated using the formula used for isotropic materials:

$$G = \frac{E}{2(1+\nu)} \tag{6}$$

where E is the elastic modulus and ν is Poisson's ratio.

Elastic modulus and maximum stress from tensile and bending tests in normalized form are presented in Figure 4. Normalization was done with respect to the properties of Epoxy resin, thus obtaining the standard deviation in normalized form.

Stress-strain and transverse-axial strain curves from tensile tests for NC resins are presented in Figure 5. The results from three point bending tests are shown in Figure 6. For a better visualization, only one representative curve for each resin is shown and transverse strain axis is inverted in Figure 5b. It also should be noted that stress-strain and transverse-axial strain curves for Epoxy, Palapreg, Envirez SA and Envirez SB are overlapping, therefore they cannot be distinguished from each other.

Table 3. Mechanical properties of bio-based resins.

Material property	LY 556	EpoBioX	Tribest	Palapreg	Envirez SA	Envirez SB
E, GPa	3.2 (0.3)	3.6 (0.1)	0.7 (0.0)	3.5 (0.1)	3.4 (0.1)	3.4 (0.1)
ν	0.37 (0.03)	0.37 (0.01)	0.35 (0.02)	0.37 (0.00)	0.37 (0.01)	0.37 (0.00)
G, GPa	1.17	1.31	0.26	1.28	1.24	1.24
σ_{max}, MPa	84.4 (1.4)	56.8 (1.4)	14.1 (0.5)	50.7 (1.9)	39.4 (1.1)	49.0 (10.7)
$\varepsilon_{\sigma max}$, %	5.3 (0.3)	1.8 (0.1)	4.3 (0.8)	1.7 (0.1)	1.2 (0.1)	1.7 (0.5)
E_B, GPa	3.1 (0.0)	3.2 (0.0)	0.6 (0.0)	3.2 (0.0)	3.0 (0.1)	3.0 (0.1)
σ_B, MPa	135.5 (1.5)	125.9 (0.7)	22.4 (0.5)	108.8 (14.4)	54.5 (2.6)	100.4 (10.6)
ε_B, %	6.67 (0.17)	5.57 (0.05)	8.01 (0.31)	4.74 (1.17)	1.88 (0.10)	4.51 (1.09)
a_{tU}, KJ/m^2	42.7 (27.1)	30.2 (10.6)	23.2 (10.3)	16.1 (2.6)	10.1 (1.3)	15.5 (4.9)
a_{tU}, KJ/m^2 (RH=90%)	18.5 (6.3)	16.1 (3.2)	18.9 (12.7)	3.6 (1.1)	3.3 (1.1)	5.9 (1.3)
K_{IC}, MPa·m$^{1/2}$, compact tension	0.31 (0.05)	0.87 (0.10)	0.37 (0.04)	0.17 (0.02)	0.32 (0.06)	0.43 (0.04)

Most of the studied bio-based resins, except Tribest, had comparable properties to synthetic Epoxy resin. Moreover, bio-based resins, except Tribest, had stiffness higher than Epoxy. Even though, EpoBioX had the highest fraction of bio-based material (75%), it performed better (higher stiffness and strength) than other bio-based resins with lower fraction of natural material. However, Epoxy had a significantly higher strength than other polymers.

All curves showed a linear behavior with respect to transverse-axial strain curves (see Figure 5b). However, Tribest and Epoxy showed high nonlinearity after reaching 2% strain and other resins showed some nonlinearity with respect to the stress-strain behavior (see Figure 5a).

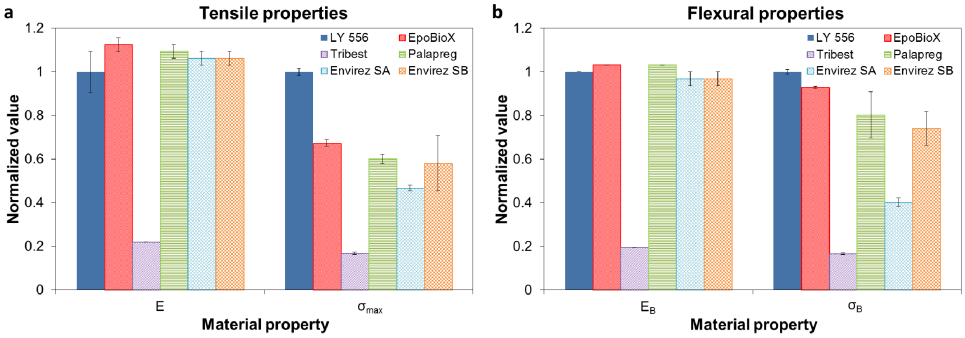

Figure 4. Normalized elastic modulus and max stress from: a) tensile test and b) bending test.

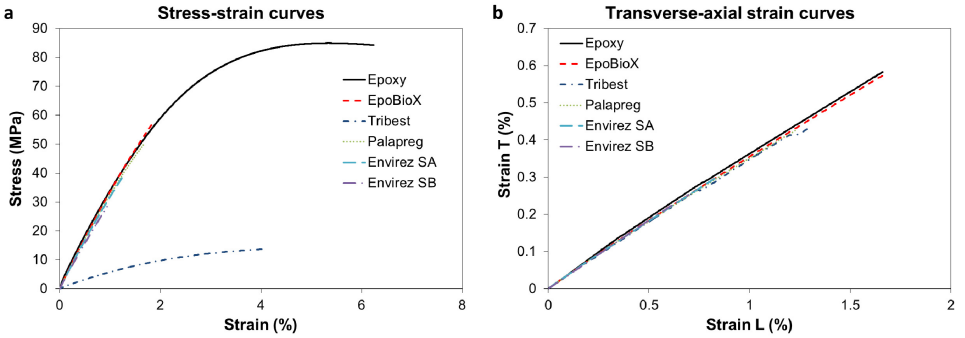

Figure 5. a) Stress-strain curves and b) transverse-axial strain curves for resins.

Impact strength was significantly affected by moisture. The highest decrease (by 78%) was observed for Palapreg while Tribest was the least affected (reduction by 19%). The impact strength of Epoxy and EpoBiox decreased respectively by 57% and 47%, whereas Envirez SA and Envirez SB showed a decrease of impact strength by 67% and 62%, correspondingly.

Flexural stress-strain curves (Figure 6) for resins showed a similar trend to that observed in tensile test. Tribest curve was significantly lower than all other curves, which were overlapping. The influence of moisture on Epoxy, EpoBioX and Tribest could be seen from stress-strain (samples without strain gages) and transverse-axial strain curves (samples with strain gages) presented in Figures 7-9 and the average values shown in Table 4.

The results showed very small moisture influence on the mechanical properties for Epoxy and EpoBioX. It could be seen that the scatter for synthetic Epoxy was much larger than for EpoBioX – stress-strain curves in Figure 8 are overlapping and separate

curves cannot be distinguished. Curves for Epoxy in Figure 7 are presenting a higher scatter than EpoBioX.

Tribest resin was affected the most out of all polymers: after the increase of RH by ≈17% (from room environment to RH=41%) the elastic modulus and Poisson´s ratio showed a decrease by 28% and 19%, respectively. But when the relative humidity was further increased by 29% (from RH=41% to RH=70%), the corresponding changes of elastic properties were 16% and 10%. The total changes of elastic modulus and Poisson´s ratio with the increase of moisture by ≈46% (from room environment to RH=70%) were 39% and 28%, respectively.

Table 4. Moisture influence on mechanical properties of resins.

Material	RH level, %	Elastic modulus, GPa	Poisson's ratio	Max stress, MPa	Strain at max stress, %
Epoxy	NC	3.20 (0.32)	0.37 (0.03)	84.4 (1.4)	5.33 (0.32)
	41	3.06 (0.07)	0.32 (0.04)	78.6 (7.9)	4.23 (1.53)
	70	3.17 (0.47)	0.34 (0.01)	57.7 (20.6)	2.38 (1.25)
EpoBioX	NC	3.64 (0.13)	0.37 (0.01)	56.8 (1.4)	1.82 (0.05)
	41	3.44 (0.06)	0.35 (0.01)	60.7 (3.1)	2.01 (0.22)
	70	3.58 (0.19)	0.35 (0.01)	55.3 (4.5)	1.83 (0.22)
Tribest	NC	0.69 (0.03)	0.36 (0.02)	14.1 (0.5)	4.33 (0.75)
	41	0.50 (0.01)	0.29 (0.06)	10.2 (2.1)	2.60 (1.07)
	70	0.42 (0.03)	0.26 (0.01)	9.1 (0.6)	2.91 (0.44)

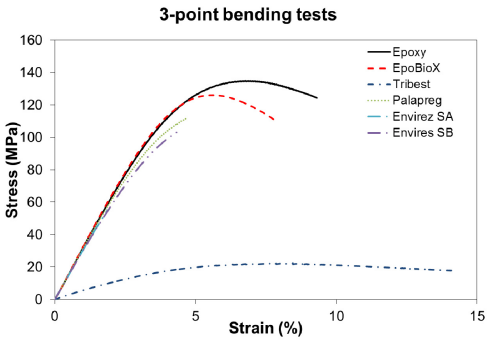

Figure 6. Stress-strain curves for resins from three point bending.

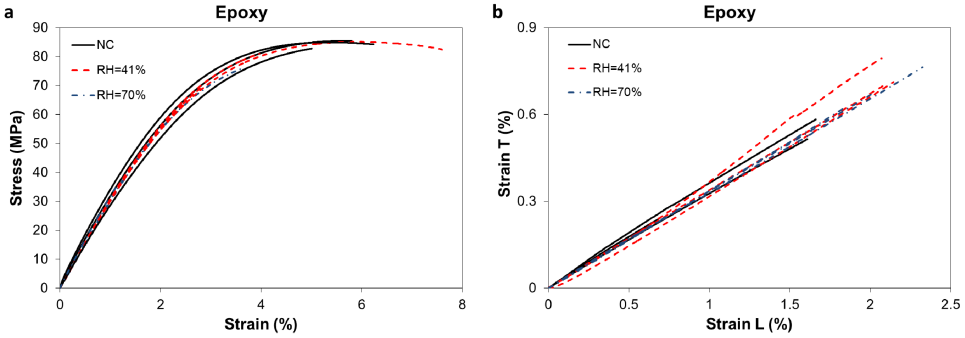

Figure 7. a) Stress-strain curves and b) transverse-axial strain curves for Epoxy.

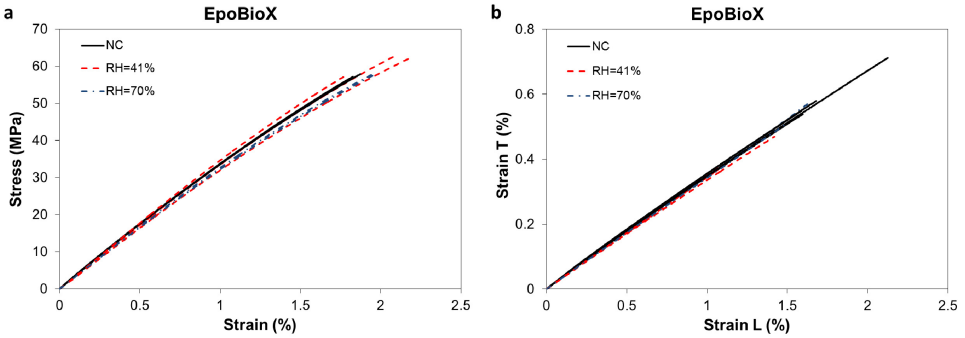

Figure 8. a) Stress-strain curves and b) transverse-axial strain curves for EpoBioX.

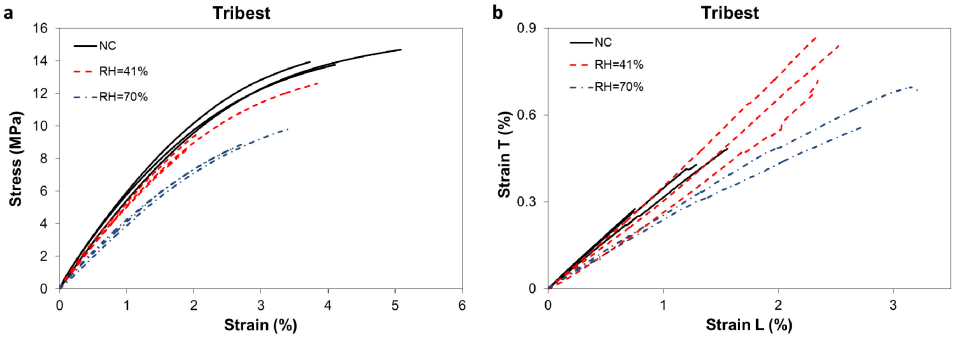

Figure 9. a) Stress-strain curves and b) transverse-axial strain curves for Tribest.

Regenerated cellulose fiber. The stress-strain curves from single fiber tensile tests of all types of fiber are shown in Figure 10 and the average values are given in Table 5. The curves in the graph are overlapping and there is no visible difference between the fibers extracted from bundles, with and without twist, and bundles from the fabric. The

average values presented in Table 5 show the small differences between fibers extracted from bundles. However, this difference was rather insignificant, especially considering the experimental scatter. Thus, it could be neglected for all practical purposes. This led to the conclusion that the mechanical performance of fibers was affected neither by the twisting process nor by the assembly into fabrics (the additional processing step did not cause any significant fiber damage).

Table 5. Mechanical properties of RCF single fibers.

Fiber type	Elastic modulus, GPa	Max stress, MPa	Strain at max stress, %
Extracted from twisted bundle	22.5 (1.5)	762.7 (106.3)	8.21 (1.77)
Extracted from bundle without twist	24.2 (1.9)	674.7 (75.7)	6.51 (1.48)
Extracted from fabric	21.3 (3.3)	767.2 (90.5)	9.26 (0.92)

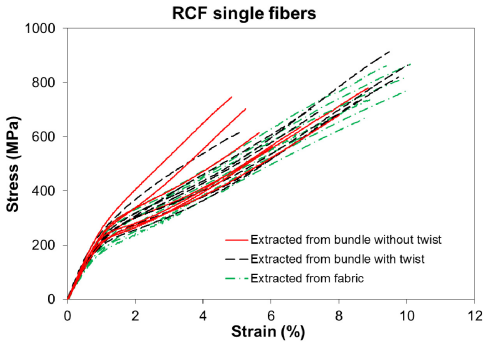

Figure 10. Stress-strain curves from single fiber tensile tests.

A more comprehensive analysis of strength distribution with use of a statistical approach for single fibers can be found in [25]. Stress-strain curves for different types of RCF bundle tests are presented in Figure 11a and characteristic values are presented in Table 6. As it is shown in Figure 11a, there is some difference between bundles with and without twist. The stress-strain curve for bundles with twist was slightly shifted to the right on strain axis. This means that stress in the bundle with twist is lower at the same strain as in bundle with no twist (which of course should indicate that the apparent stiffness of bundles with no twist is higher). It should also be noted that the bundles with twist failed rather catastrophically and their stress-strain curves were very similar to those of single fiber curves, whereas the bundles without twist failed progressively, and it was a more typical behavior of conventional fibers used in

composites (e.g. glass fibers). This means that untwisted bundle consists of fibers that are acting individually rather than all together as one filament, which is the case in twisted bundles where filaments are acting together due to the high friction within the bundle caused by tight twisting.

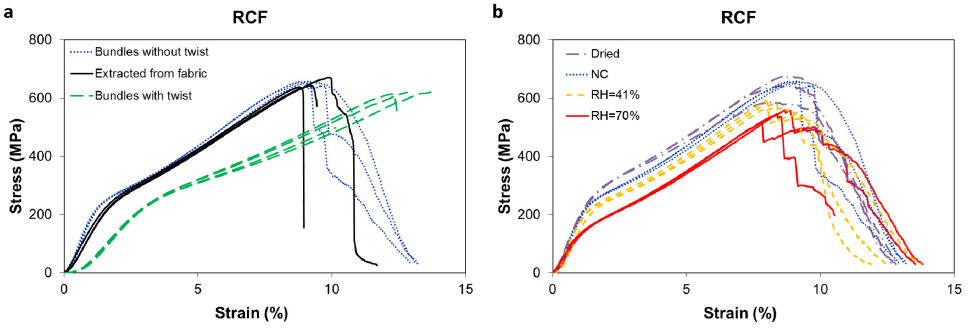

Figure 11. Stress-strain curves for RCF bundles a) with twist, without and extracted from fabric and b) at different RH levels.

Table 6. Mechanical properties of RCF bundles.

Bundle type	Elastic modulus, GPa	Max stress, MPa	Strain at max stress, %
Twisted	9.7 (0.4)	622.4 (8.0)	12.50 (1.26)
No twist	22.6 (0.9)	654.4 (3.7)	8.92 (0.16)
Extracted from fabric	15.8 (0.9)	650.3 (17.8)	9.25 (0.54)

As expected, the strength of untwisted bundles was lower than that of single fibers (by approximately 15%). Twisted bundles showed slightly lower strength. However, the strain at failure and stiffness of bundles without twist were rather close to those of single fibers. It was also evident that stiffness of twisted bundles was much lower (by ≈57%) than that of the bundles without twist (and single fibers), whereas strain at failure was considerably higher (by ≈29%). Bundles extracted from fabric showed similar strength and strain at max stress. However, stiffness of the bundles extracted from fabric was lower by 30% than fiber bundles without twist. These differences could most likely be attributed to the different mechanisms of deformation of the bundles with and without twist. In case of the bundles without twist fibers were well aligned with respect to the loading direction and they were subjected to the axial load right from the start of the tensile test. Whereas, the twisted bundles were somewhat misaligned due to the twist and bundles were at first rotating and during this rotation were aligning with the loading direction. This speculation was supported with the fact that stress-strain curves

for both types of bundles were parallel at high strains (fibers were fully aligned). Additional rotation and alignment was accounted for additional displacement (and strain) which was observed for twisted bundles.

The influence of moisture on mechanical behavior of RCF bundles without twist is shown in Figure 12b and mechanical properties are presented in Table 7. It can be seen that with the increase of moisture, the mechanical performance of bundles is noticeably decreasing. At RH=70%, the modulus decreased by 31% and strength by 17% compared to NC bundles. Results from loading-unloading tests of RCF bundles with twist are presented in Figure 12. Well defined hysteresis loops were clearly visible, which were the typical phenomena for viscoelastic materials. The overall behavior of specimens was similar to that in simple tensile tests but bundles fail at lower strains of ≈8%, whereas in simple tensile tests bundles failed at >10%. Stress-strain curves for two tested bundles are almost identical which indicates the very good repeatability of experimental results.

Table 7. Mechanical properties for RCF bundles without twist, at different moisture contents.

RH level, %	Elastic modulus, GPa	Max stress, MPa	Strain at max stress, %
Dried	22.7 (0.2)	635.6 (44.0)	8.46 (0.16)
NC	22.6 (0.9)	654.4 (3.7)	8.92 (0.16)
41	21.1 (1.4)	587.5 (2.8)	8.13 (0.21)
70	15.6 (0.1)	541.5 (20.5)	8.28 (0.44)

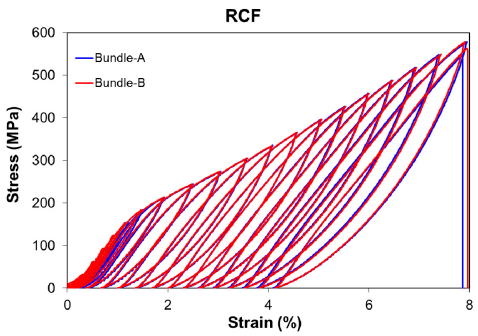

Figure 12. Loading-unloading test for RCF bundles with twist.

Conclusions and future work

A comprehensive characterization of mechanical properties of bio-based resins and RCF fiber with different moisture content was carried out. The analysis of results led to the following conclusions:

- Mechanical properties of bio-based resins were similar to those of reference synthetic resin. Moreover, the bio-based resins (except Tribest) showed even higher elastic modulus than Epoxy;
- In terms of moisture uptake, Envirez and Epoxy resins performed similarly, whereas EpoBioX gained moisture slower than synthetic Epoxy, although the saturation level was the same. Tribest and Palapreg showed much faster and higher moisture uptake;
- The tensile properties of Epoxy and EpoBioX were not affected by moisture but Tribest's strength and stiffness was considerably lower after the increase of RH.

Experiments showed that RCF had reproducible properties. The properties of RCF were drastically affected by moisture, much more significantly than properties of polymers. It is also shown that these fibers exhibit a highly nonlinear behavior. In general, it can be concluded that bio-based resins are good candidates for the development of polymer composites and they perform well even at elevated humidity levels. However, a special measure should be taken to protect cellulosic fibers from moisture and the highly nonlinear behavior should be accounted for. The future work will include the development and characterization of completely bio-based composites: bio-based matrix with cellulose fibers as reinforcement.

Acknowledgments

Runar Långström and Peter Mannberg (Swerea SICOMP, Piteå, SWEDEN) are acknowledged for manufacturing of resin plates. Authors are very thankful to students from University of Rouen (FRANCE) Benjamin Schamme and Quentin Viel visiting LTU within Erasmus exchange program and AMASE student Ingmar Fleps and EEIGM student Fanny Roos, for their help with experiments.

Contract grant sponsors: Interreg IVA Nord project ANACOMPO, funded by EU and Norrbotten, Läansstyrelsen as well as Erasmus Mundus Doc-MASE program funded by EU.

References

[1] J. Lampinen, Trends in bioplastics and biocomposites, VTT Tiedotteita - Valtion Teknillinen Tutkimuskeskus, **1** (2010).

[2] C. Johansson, J. Bras, I. Mondragon, P. Nechita, D. Plackett, P. Šimon, D. G. Svetec, S. Virtanen, M. G. Baschetti, C. Breen, F. Clegg, and S. Aucejo, *BioResources*, **7**, 2506 (2012).
[3] A. Magurno, *Die Angewandte Makromolekulare Chemie*, **272**, 99 (1999).
[4] P. Malnati, *Compos. Technol.*, **15**, 46 (2009).
[5] J. Müssig, M. Schmehl, H. B. von Buttlar, U. Schönfeld, and K. Arndt, *Ind. Crops. Prod.*, **24**, 132, (2006).
[6] G. Marsh, *Mater. Today*, **6**, 36 (2003).
[7] S.K. Ramamoorthy, Q. Di, K. Adekunle, and M. Skrifvars, *J. Reinf. Plast. Comp.*, **31**, 1191 (2012).
[8] L. Rozite, J. Varna, R. Joffe, and A. Pupurs, *Thermoplast. Compos. Mater.* (2011).
[9] B. Siroka, M. Noistering, U.J. Griesser, and T. Bechtold, *Carbohyd. Res.*, **343**, 2194 (2008).
[10] A. Bismarck, I. Aranberri-Askargotta, J. Springer, T. Lampke, B. Wielage, A. Stamboulis, I. Shenderovich, and H.-H. Limbach, *Polym. Composite.*, **23**, 872 (2002).
[11] A. Stamboulis, C.A. Baillie, and T. Peijs, *Compos. Part A-Appl. S.*, **32**, 1105 (2001).
[12] A. Bessadok, S. Marais, S. Roudesli, C. Lixon, and M. Metayer, *Compos. Part A-Appl. S.*, **39**, 29 (2008).
[13] S. Alix, E. Philippe, A. Bessadok, L. Lebrun, C. Morvan, and S. Marais, *Bioresource Technol.*, **100**, 4742 (2009).
[14] K. Santhosh, M. Muniraju, N.D. Shivakumar, and M. Raguraman, *J. Comp. Mater.*, **46**, 1889 (2011).
[15] J. Andersons, E. Sparnins, R. Joffe, and L. Wallström, *Compos. Sci. Technol.*, **65**, 693 (2005).
[16] J. Summerscales, N.P.J. Dissanayke, A.S. Virk, and W. Hall, *Compos. Part A-Appl. S.*, **41**, 1329 (2010).
[17] H.I. Bos, J.A. Van Den Oever, and O.C.J.J. Peters, *J. Mater. Sci.*, **37**, 1683 (2002).
[18] K. Charlet, C. Baley, C. Morvan, J. P. Jernot, M. Gomina, and J. Breard, *Compos. Part A-Appl. S.*, **38**, 1912 (2007).
[19] K. Charlet, J.P. Jernot, M. Gomina, J. Bréard, C. Morvan, and C. Baley, *Compos. Sci. Technol.*, **69**, 1399 (2009).
[20] E. Sparnins, and J. Andersons, *J. Mater. Sci.*, **44**, 5697 (2009).
[21] K. Charlet, J.P. Jernot, S. Eve, M. Gomina, and J. Bréard, *Carbohyd. Res.*, **82**, 54 (2010).
[22] N. Graupner, A.S. Herrmann, and J. Müssig, *Compos. Part A-Appl. S.*, **40**, 810 (2009).
[23] B. Bax, and J. Mussig, *Compos. Sci. Technol.*, **68**, 1601 (2008).
[24] W. Gindl, M. Reifferscheid, R.-B. Adusumalli, H. Weber, T. Röder, H. Sixta, and T. Schöberl, *Polymer*, **49**, 792 (2008).

[25] R. Joffe, J. Andersons, and E. Sparnins, Applicability of Weibull strength distribution for cellulose fibers with highly non-linear behavior, *Proceedings of the 17th International Conference on Composite Materials: ICCM-17* (2009).
[26] V. Fombuena, L. Sánchez-Nácher, M. Samper, D. Juárez, and R. Balart, *J. Am. Oil Chem. Soc.*, **90**, 449-457 (2013).
[27] J.-M. Raquez. M. Deleglise, M.-F. Lacrampe, and P. Krawczak, *Prog. Polym. Sci.*, **35**, 487 (2010).
[28] "CORDENKA® High Tenacity Rayon Filament Yarn", data sheet from CORDENKA GmbH.
[29] ASTM D 638, *Standard test Method for Tensile Properties of plastics* (1995).
[30] ASTM D 790M, *Standard Test Methods for Flexural Properties of Unreinforced and Reinforced Plastics and Electrical Insulating Materials*, (1993).
[31] ISO 179, *Plastics – Determination of Charpy Impact Strength* (1993).
[32] ASTM D 5045, *Standard Test Methods for Plane-Strain Fracture Toughness and Strain Energy Release Rate of Plastic Materials* (1995).
[33] C. Shen, and G. Springer, *J. Compos. Mater.*, **10**, 2 (1976).
[34] ASTM D3379, *Standard Test Method for Tensile Strength and Young's Modulus for High-Modulus Single Filament Materiala* (1989).

Paper B

Moisture uptake and resulting mechanical response of bio-based composites. II. Composites

Newsha Doroudgarian[1], Liva Pupure[1], Roberts Joffe[1,2]

[1]Division of Materials Science, Luleå University of Technology, S-97187 Luleå, SWEDEN
[2]Group of Materials Science, Swerea SICOMP, S-94126 Piteå, SWEDEN

Reformatted paper published in:
POLYMER COMPOSITES, Volume 36, Issue 8

Moisture uptake and resulting mechanical response of bio-based composites. II. Composites

Newsha Doroudgarian[1], Liva Pupure[1], Roberts Joffe[1,2]

[1]Division of Materials Science, Luleå University of Technology, S-97187 Luleå, SWEDEN
[2]Group of Materials Science, Swerea SICOMP, S-94126 Piteå, SWEDEN

Abstract. The durability of entirely bio-based composites with respect to the exposure to elevated humidity was evaluated. Different combinations of bio-based resins (Tribest, EpoBioX, Envirez) and cellulosic fibers (flax and regenerated cellulose fiber rovings and fabrics) were used to manufacture unidirectional and cross-ply composite laminates. Water absorption experiments were performed at various humidity levels (41%, 70%, and 98%) to measure the apparent diffusion coefficient and moisture content at saturation. The effect of chemical treatment (alkali and silane) of fibers as a protection against moisture was also studied. However, fiber treatment did not show any significant improvement and in some cases, the performance of the composites with treated fibers was lower than those with untreated reinforcement. The comparison of results for neat resins and composites showed that moisture uptake in the studied composites was primarily due to cellulosic reinforcement. Tensile properties of the composites, as received (RH=24%) and conditioned (RH=41%, 70%, and 98%), were measured, in order to estimate the influence of humidity on behavior of these materials. The results were compared with data for glass fiber reinforced composites, as a reference material. Previous results from the study of unreinforced polymers showed that resins were resistant to moisture uptake. Knowing that moisture sorption was primarily dominated by natural fibers, the results showed that some of the composites with bio-based resins performed very well and had comparable properties with composites of synthetic epoxy, even at elevated humidity.

Introduction

Over the last two decades, the research on natural fiber reinforced plastics (NFRP) is intensifying and leading to its wider use as construction materials. The governments around the world as well as the society in general are also becoming aware of the potential of these materials. For instance, there were several large projects funded by European Union, such as ANACOMPO (www.interregnord.com), ECOFINA (www.ecofina.org), BIOCOMP (www.biocomp.eu.com), and WOODY (www.woodyproject.eu), which emphasized on eco-efficient technologies and products based on natural fiber composites. Due to their decent mechanical properties and low

density, natural fibers are of great interest for a wide range of industries (e.g. automotive, construction, sports).

However, disadvantages such as variable quality, moisture absorption, low durability, low impact strength, and restricted processing temperatures, are the limiting factors of natural fibers [1–3]. Compared with synthetic fibers, the natural counterparts show much higher variability of properties and a nonlinear stress–strain response. The large scatter in properties of the natural fibers is a result of growing and processing conditions [1]. Further drawbacks, such as poor dimensional stability (swelling) and low microbial resistance (rotting), restrict the natural fibers' use in high performance structural composites [4,5].

Obviously the above mentioned advantages are a good motivation to use natural fiber reinforcements with high cellulosic contents but there are still some shortcomings that should be eliminated. This has been somewhat achieved by the development of textile manmade regenerated cellulose fibers (RCF) initially known as "artificial silk". The introduction of RCF overcomes the problem of inhomogeneity and discontinuity of natural fibers. Contrary to the natural fibers, RCF offer stable and reproducible properties. Since the main constituent of these fibers (cellulose) is the same as in the other plant fibers, these reinforcements have similar issues associated with performance and processing. However, it should be noted that even though, RCF may be anisotropic, if stretched during manufacturing, they do not have a hierarchical structure like natural fibers which might result in a different behavior (e.g., with respect to the moisture uptake).

Despite the fact that limited processing temperature of natural fibers restricts the choice of suitable matrix material, thermoplastics are being used as well as thermosets. There are a number of synthetic thermoplastic resins (e.g., polypropylene, polyethylene) combined with natural fibers such as flax, wood, hemp, etc., being popular candidates for a wide range of applications [6]. Likewise, thermoset polymers such as epoxies, vinylesters, and polyesters are being used. Moreover, there are great attempts to develop structural composites using bio-based resins instead of synthetic polymers. Utilizing bio-based polymers, like polyester amide and natural oils (e.g. soy oil), opens the opportunity to introduce high performance composites which are fully bio-based [7–13].

Because of the high cellulose content, natural fibers are strongly polar, due to hydroxyl groups (OH), acetal, and ether linkages present in cellulose structure. Consequently, cellulosic fibers have a poor interfacial compatibility when it comes to reinforcing non-polar polymers [14]. Presence of OH-groups makes fibers also hydrophilic. Many of common matrix polymers used in composites are highly hydrophobic. This causes a manufacturing issue in NFRP development [1]. Solutions to this problem can be either applying different treatments (improve chemical and mechanical bonding) to the fibers or modifying chemical composition of the matrix

(adding compatibilizers). The surface treatment of fibers not only improves the stress transfer at the fiber matrix interface, resulting in increased mechanical properties of composites [15,16], but it can also reduce the water absorption and consecutive swelling. Examples of typical chemical surface treatments are silane and alkali treatments which have been used in the studied materials. These methods have achieved improved fiber matrix adhesion in NFRPs [17,18]. However, such surface treatments can be costly and damage the fibers [18].

Diffusion in synthetic fiber composites has been studied for years but there is a limited amount of studies on moisture uptake in bio-based composites. There are a few studies showing the swelling phenomenon in natural fibers and natural resins as well as their combinations [19]. Moisture absorption and desorption of different natural fibers and their composites have also been the subject of number of studies [20–22]. What has also been of interest is the moisture effect on mechanical performance of composites reinforced with RCF [21].

The general aim of this work has been development of high performance fully bio-based composites with improved performance in harsh environment (elevated temperature and moisture). Consistent and comprehensive investigation of moisture effect on mechanical properties of bio-based materials was performed. The material compositions were new and the data for such materials in literature was very limited (or even non-existent). Therefore, the information presented in this article should be of interest to large number of researchers involved in developing bio-based composites.

The previous study (Part I) [23] focused on the performance of composite constituents (bio-based resins and RCF) at elevated relative humidity (RH). In this article durability of entirely bio-based composites with respect to the exposure to elevated humidity has been explored. Different combinations of bio-based resins and cellulosic fibers (flax and RCF rovings as well as fabrics) were investigated. Water absorption experiments were performed at various RH levels and effect of chemical treatment (alkali and silane) of fibers as protection against moisture was studied. Tensile properties of composites were measured, in order to estimate the influence of humidity on behavior of these materials. Results were compared with data for glass fiber reinforced composite, as a reference material.

Materials and manufacturing

COMPOSITE CONSTITUENTS

Bio-based resins were derived from recyclable and renewable raw materials. Three thermoset bio-resins were used – Tribest, EpoBioX, Envirez. Tribest is an acrylated and epoxidized soy oil based vinylester resin, from Cognis. EpoBioX Super SAP is a pine oil based epoxy, from Entropy Resins. Envirez G8600 INF-60 is unsaturated soybean

oil based polyester, from Ashland. Tribest has 75 wt% bio-content, EpoBioX 60 wt%, and Envirez 12 wt%. The resins curing cycles are summarized in Table 1.

Table 1. Resin types and curing cycles of laminates.

Resin	Curing agent (mixing ratio)	Curing	Post curing
Tribest	Peroxide Benox 40LV (2.25 wt%)	8h at 70°C	–
EpoBioX	CA35TG (100:27)	RT[a] over night	2h at 80°C
Envirez	Norpol No1 (2 wt%)	RT over night	2h at 70°C

[a]RT=Room temperature (≈23°C)

The fibers used for the reinforcement were RCF, flax fibers (FF) and standard E-glass fibers (GF). RCF was produced by a special variant of the viscose process (700 Super 3) by Cordenka. RCF was implied in two forms of no twist rovings and assembled in non-crimp fabrics (NCF). RCF fabric was stitched unidirectionally by Engtex, with an area weight of 182 gsm. FF and GF were in the form of woven fabrics and no twist rovings, respectively. FF weave was from Composite Evolution Biotex, 4x4 hopsack 510 gsm, and GF roving, R338 1200 TEX, was from Ahlstrom.

TREATED FIBERS AND THEIR COMPOSITES

FF and RCF fabrics were exposed to alkali and silane chemical treatments (Table 2). The treatments were done within ANACOMPO project at Tampere University, Finland. Alkalization (alkali treatment) was made using pellets of sodium hydroxide. Silylation (silane treatment) was done by 3 aminopropyltriethoxy silane, 99% [24].

Table 2. Fiber treatments of composite systems and sample notations.

Matrix	Fiber	Fiber treatment	Sample notation
Envirez	Flax	APS 2%	FF/Envirez-2%
		ALK 4% 30 min	FF/Envirez-4%
		APS 5% Eth/H_2O	FF/Envirez-5%
	Regenerated cellulose	APS 2%	RCF/Envirez-2%
		APS 5%	RCF/Envirez-5%

COMPOSITE MANUFACTURING

Composites were manufactured using fiber rovings and fabrics. Fiber roving was wound on steel plates, using a filament winding machine (Waltritsch & Wachter Sondermachinen). Rovings were wound into two layers to form unidirectional (UD)

laminates, in case of RCF and GF. Non-crimp fabric of RCF was also used, stacked in six layers to achieve UD laminates. Also for FF composite, flax weave was stacked in two layers of woven fabrics, to obtain a symmetric configuration. Afterwards, the reinforcement preforms (stacked fabric layers and filament wound rovings) were impregnated, using vacuum infusion with resin heated to 50°C. The vacuum infusion setup consisted of a stiff bottom and flexible top (vacuum bag with polyamide film). Obtained fiber volume fraction in composites was approximately 40%-50%.

Experiments

SPECIMEN PREPARATION AND CONDITIONING

Composite plates were cut into rectangular shaped specimens and their edges were ground and sanded with sandpapers of different grades (up to 800 grit). The approximate dimensions of composite specimens made from fiber roving were 1mm thick and 10mm wide, whereas samples made of fabrics were 2mm thick and 20mm wide. The specimens had at least 150mm in length, whereas the working zone (gauge length) was 100mm.

Specimens were divided into two groups, conditioned and non-conditioned (NC). NC specimens were tested as received (at room environment RH=24%, RT=23°C). Prior to conditioning, the other group of specimens was placed in the oven at 50°C and their mass was constantly monitored until it was stabilized. Afterwards these specimens were conditioned in desiccators (until the moisture content reached saturation level) at three different RH levels: 41%, 70% and 98%. The fixed level of RH was achieved by using of saturated solutions of different salts. The weight of samples was regularly measured to ensure that moisture content equilibrium was reached and also to observe the kinetics of moisture sorption. Conditioning was done on rectangular slender specimens. The accuracy of scale was 0.1 mg and the mass of samples was ranging from a few grams (single specimen) up to 90 g (specimen batch). All composite systems are listed in Table 3. Laminates made out of weave are referred as cross-ply.

DIFFUSION COEFFICIENTS

Diffusion according to Fick's law is assumed and the apparent diffusion coefficient, D_a, for material in case of one-dimension is given by [25]:

$$\frac{4C_s}{b\sqrt{\pi}}\sqrt{D_a} = \frac{C_2 - C_1}{\sqrt{t_2} - \sqrt{t_1}} \tag{1}$$

where C_s is the mass gain at saturation level, b thickness of the sample and $\frac{C_2 - C_1}{\sqrt{t_2} - \sqrt{t_1}}$ is the slope of initial moisture uptake curve (moisture gain C versus square root of time).

It should be mentioned that the edges of specimens were not sealed. Therefore, it was not actually a "one-dimensional" case. That is why the diffusion coefficient is referred to as "apparent" and used for ranking the material performance in this study rather than a direct comparison with literature data.

It has been shown that most often polymer composites follow a Fickian diffusion process [26-28]. However, for explaining the mechanisms behind non-Fickian behavior, other models can be used [26,29-31]. Different methods of measuring water are investigated on laminates and in order to define the diffusion coefficient, moisture uptake studies in glass fiber/epoxy composites have been carried out. The influence of different factors (thickness, fiber type, edge effect) on moisture absorption has been analyzed, through experimental and finite element methods. It was shown that the saturation limit is only dependent on the relative humidity level in a linear manner [26-28]. Diffusion coefficient showed a linear relation with respect to the applied temperature as well [22,28].

Table 3. Summary of all composite laminates with notations.

Fiber	Matrix	Sample notation	Layup	RH, %
Flax	Envirez	FF/Envirez[a]	Cross-ply	NC/98
Regenerated cellulose	Envirez	RCF/Envirez[b]	UD	NC/98
	Tribest	RCF/Tribest	UD	41/70
	EpoBioX	RCF/EpoBioX	UD	41/70
Glass	Tribest	GF/Tribest	UD	41/70
	EpoBioX	GF/EpoBioX	UD	41/70

[a]Woven fabric

[b]Non-crimp fabric

TENSILE TEST

Quasi-static tensile tests were performed, in a displacement controlled mode at 2mm/min (≈2%/min) on an electromechanical tensile machine Instron 3366, equipped with 10 kN load cell and pneumatic grips. Even though, the ASTM D638-95 standard [40] was used as guidance for the test, sample geometry was slightly different, due to the limited availability of materials. Standard Instron extensometers with 50 mm base were used to measure the axial strain, whereas transverse strain was measured using strain gages (to obtain Poisson's ratio). Small loading-unloading ramp was performed and E-modulus was calculated on both loading and unloading cycles, (E_L, E_U). Elastic modulus (E) and Poisson's ratio (ν) were calculated from the stress-strain and transverse-axial strain curves, respectively, by a linear fit of experimental data points in the axial

strain region of 0.05%-0.2%. Furthermore, from the complete stress-strain curves (loading until the failure of sample) maximum stress (σ_{max}) and strain at maximum stress ($\varepsilon_{\sigma max}$) were measured. It should be noted that strain at max stress corresponds to strain at failure, that is, the stress monotonically increased until the failure of specimens. All mechanical tests were performed at least on three samples.

MICROSCOPY

Optical and scanning electron microscopies (OM and SEM, respectively) were carried out to study the microstructure of the materials. The OLYMPUS, VANOX-T was used for OM, whereas SEM was done on JEOL, JSM-5200.

Results and discussions

MOISTURE UPTAKE

Moisture uptake in composites as a measure of mass gain over square root of time is presented in Figures 1 and 2. The summary of these results (C_s and D_a) at different RH for various composites are presented in Table 4. Due to a very small mass gain, the moisture uptake at RH=41% was not possible to measure.

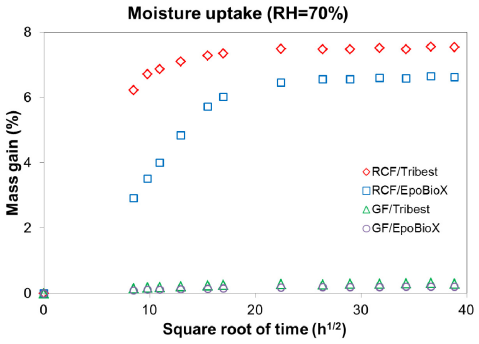

Figure 1. Moisture uptake of GF and RCF composites at 70% RH.

Results in Table 4 indicate that RCF/Tribest had a double diffusion rate in comparison to RCF/EpoBioX and also reached a higher saturation level (by 14%). However, GF/Tribest counterpart showed a lower diffusion rate than GF/EpoBioX (by 28%) but reached a higher saturation level (by 51%). It should also be noted that diffusion rate of GF composites were smaller than RCF composites, by an order of magnitude, and the saturation level of RCF reinforced materials was more than 30 times higher than for GF ones, see Figure 1.

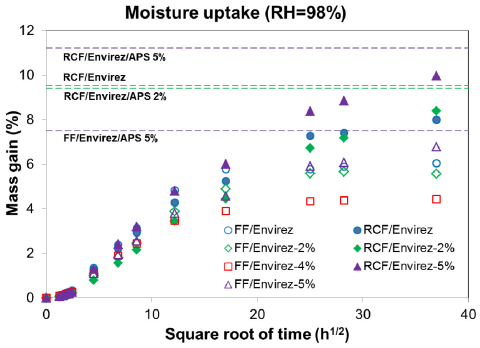

Figure 2. Moisture uptake of treated fiber composites at 98% RH. Saturation level obtained from additional test on different samples is indicated as the dashed lines.

Table 4. Apparent diffusion coefficient and saturation level, GF, and RCF composites at RH=70%, FF, and RCF composites at RH=98%.

Composite	RH, %	D_a, m^2/s	C_s, %
RCF/EpoBioX	70	$1.4 \cdot 10^{-13}$	6.6
RCF/Tribest		$2.8 \cdot 10^{-13}$[a]	7.5
GF/EpoBioX		$5.7 \cdot 10^{-14}$	0.2
GF/Tribest		$4.1 \cdot 10^{-14}$	0.3
FF/Envirez	98	$1.1 \cdot 10^{-12}$	6.1
FF/Envirez-2%		$1.5 \cdot 10^{-12}$	5.6
FF/Envirez-4%		$2.0 \cdot 10^{-12}$	4.4
FF/Envirez-5%		$1.1 \cdot 10^{-12}$	7.5
RCF/Envirez	98	$3.6 \cdot 10^{-13}$	9.5
RCF/Envirez-2%		$5.1 \cdot 10^{-13}$	9.4
RCF/Envirez-5%		$6.9 \cdot 10^{-13}$	11.2

[a]The value cannot be confirmed since limited data points were obtained due to higher absorption rate than other materials.

Analysis of results in Table 4 showed that the treatment of FF by 2%APS and 4%ALK increased the diffusion rate (increase by 36% and 82% respectively) but decreased the saturation level (by 7% and 27%, respectively). However, FF/Envirez 5%APS did not follow the same trend, diffusion rate was unchanged compared to the

untreated fiebrs but saturation level was higher (by 24%). This behavior could probably be related to swelling and opening of the hierarchical structure of the natural fibers.

There was a trend seen in Table 4, showing a raise in rate of water uptake when increasing the treating agent, by 42% and 92% for 2% and 5% APS treatment, respectively. However, the saturation level was kept almost unchanged for 2% APS treatment and increased by 18% for 5% treatment. Furthermore, comparing the results of RCF composites to their FF counterparts indicated that the rate of moisture uptake in FF composites was by an order of magnitude higher than for RCF composites but the saturation level showed the opposite and was lower in FF/Envirez than RCF/Envirez, as seen in Figure 2. This might be related to slight differences in the fiber volume fractions in different composites. In order to study the effect of reinforcement on moisture uptake of composites in more detail, additional experiments on composites with different fiber volume fractions would be required. Moreover, there was a nonlinearity shown in Figure 2 at the initial part of the sorption curve. This nonlinearity is most likely caused by fluctuation of RH due to opening of desiccator during the mass measurement. Therefore, it may be considered as an artifact. The comparison of moisture absorption of composites and unreinforced polymers [23] showed that water uptake in the composites was predominantly defined by the fibers. The higher saturation level in RCF than FF composite might be due to the different form of cellulose in these fibers, considering that the crystallinity in RCF is significantly lower than in FF [17]. It is of importance to mention that FF/Envirez composites showed unstable moisture absorption data and started to degrade and lose mass after about 3 months in high humidity conditions.

The results found in the literature for bio-based and synthetic composites show that the data obtained in this study compare well with those values. The studied materials performed better (lower diffusivity and moisture content at saturation) than wood/starch composites [33] or hemp/cellulose acetate [34]. The performance was similar to (or better than) synthetic composites [35] (e.g. glass fiber reinforced polyester, epoxy and vinylester) as well as to epoxy reinforced with recycled cellulose fibers [36].

MECHANICAL CHARACTERIZATION

RCF and GF composites. Figure 3 shows the representative stress–strain curves of GF and RCF composites. It should also be noted that graphs of transverse–axial strain demonstrated linear curves and the initial slope of these graphs have been subjected to calculate Poisson's ratio values. The summary of tensile properties of GF and RCF reinforced composites at different RH (41% and 70%) is shown in Table 5.

These results indicated that stiffness of GF composites was not affected by moisture whereas stiffness of RCF composites was slightly reduced (≈14% and ≈8% for RCF/EpoBioX and RCF/Tribest, respectively). Strength values (σ_{max}) of all composites (RCF and GF based) were reduced by ≈10% when exposed to high RH

level. Poisson's ratio (ν) of GF composites decreased but increased for RCF composites. The overall mechanical performance of RCF composites showed that RCF acted well in reinforcing polymers, which applied even in the case of weak resins such as Tribest.

Table5. Moisture influence on mechanical properties of RCF and GF composites.

Material	RH	E_L, GPa	E_U, GPa	ν	σ_{max}, MPa	$\varepsilon_{\sigma max}$, %
GF/Tribest	41%	41.7 ± 1.1	41.9 ± 0.9	0.43 ± 0.09	831 ± 77	2.1 ± 1.2
RCF/Tribest		14.5 ± 1.2	14.8 ± 1.2	0.37 ± 0.00	356 ± 82	7.9 ± 0.7
GF/EpoBioX		36.4 ± 3.1	36.4 ± 3.1	0.31 ± 0.00	833 ± 51	2.1 ± 0.2
RCF/EpoBioX		14.3 ± 1.2	14.7 ± 1.1	0.34 ± 0.11	245 ± 23	4.3 ± 0.6
GF/Tribest	70%	41.5 ± 1.5	42.0 ± 1.3	0.31 ± 0.03	722 ± 42	1.8 ± 0.2
RCF/Tribest		12.5 ± 0.5	12.9 ± 0.5	0.42 ± 0.03	320 ± 50	8.0 ± 1.8
GF/EpoBioX		36.6 ± 2.9	36.7 ± 3.0	0.27 ± 0.02	748 ± 84	2.6 ± 0.3
RCF/EpoBioX		13.2 ± 0.3	13.6 ± 0.3	0.50 ± 0.12	229 ± 12	3.6 ± 2.4

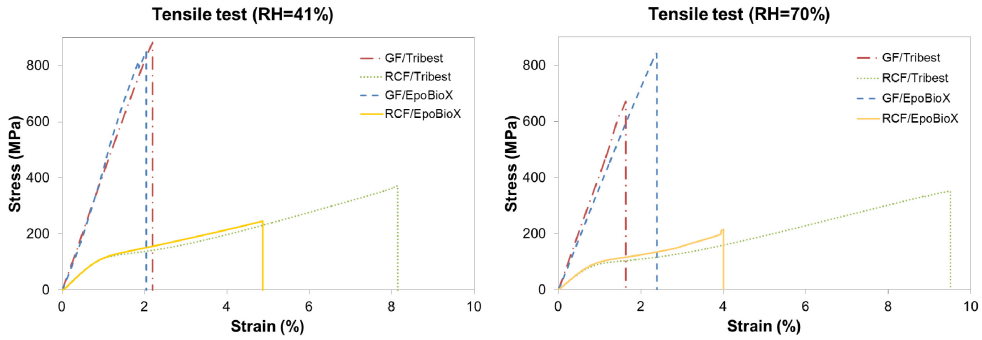

Figure 3. Stress-strain curves of GF and RCF composites.

However, in order to better understand how the diffusion mechanism influences mechanical properties, it is of interest to have a comparison between different types of cellulose fiber composites [33,37,38].

Composites with treated fibers. Table 6 summarizes the tensile properties of composites with treated fibers (results for composites with untreated reinforcement are also presented for comparison). For a more convenient overview, the same results are presented in Figures 4 and 5 in a normalized way (normalized with respect to the values for materials with untreated fibers). Typical stress-strain curves are shown in Figures 6 and 7.

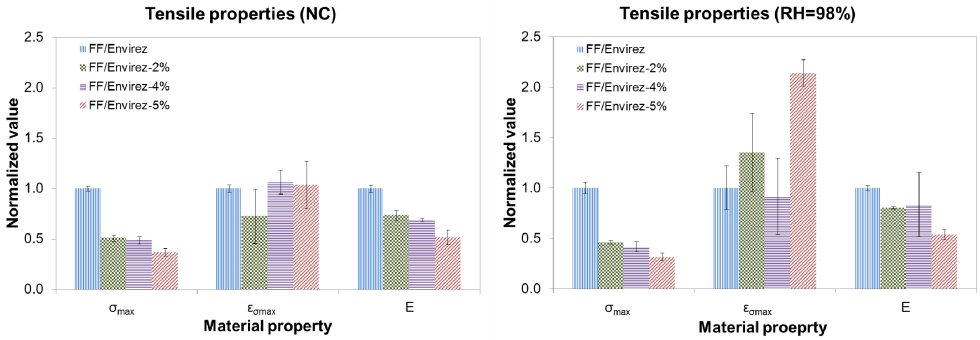

Figure 4. Bar-charts representing FF treatments influencing mechanical properties. Normalization is with respect to materials with untreated FF.

Table 6. Moisture influence on mechanical properties of composites with treated and untreated fibers.

Material	RH	E_L, GPa	E_U, GPa	σ_{max}, MPa	$\varepsilon_{\sigma max}$, %
FF/Envirez	NC	7.5 ± 0.2	8.0 ± 0.3	57 ± 1	1.9 ± 0.1
FF/Envirez-2%		5.6 ± 0.3	5.9 ± 0.4	29 ± 2	1.4 ± 0.5
FF/Envirez-4%		5.3 ± 0.1	5.4 ± 0.2	28 ± 2	2.0 ± 0.2
FF/Envirez-5%		3.9 ± 0.6	4.1 ± 0.7	21 ± 2	1.9 ± 0.4
FF/Envirez	98%	3.9 ± 0.1	4.5 ± 0.2	66 ± 4	3.7 ± 0.8
FF/Envirez-2%		3.1 ± 0.1	4.3 ± 1.2	31 ± 1	5.0 ± 1.4
FF/Envirez-4%		2.7 ± 0.2	3.1 ± 0.3	28 ± 3	3.4 ± 1.4
FF/Envirez-5%		2.1 ± 0.2	2.4 ± 0.2	21 ± 2	7.9 ± 0.5
RCF/Envirez[a]	NC	8.0	8.7	174	7.7
RCF/Envirez-2%[a]		8.3	8.7	146	7.0
RCF/Envirez-5%		7.7 ± 0.7	8.0 ± 0.9	145 ± 15	7.0 ± 1.3
RCF/Envirez	98%	3.5 ± 0.1	3.8 ± 0.2	101 ± 2	10.1 ± 1.6
RCF/Envirez-2%		3.4 ± 0.6	3.7 ± 0.6	101 ± 2	11.0 ± 0.4
RCF/Envirez-5%		3.3 ± 0.3	3.5 ± 0.2	94 ± 3	11.0 ± 0.3

[a]Only one specimen available for testing.

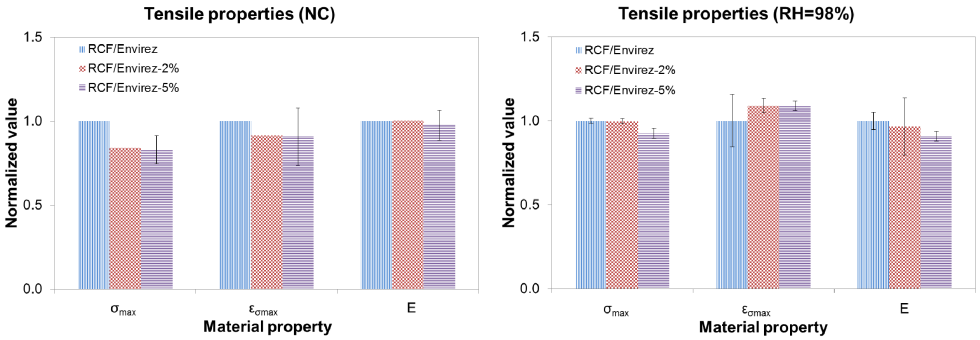

Figure 5. Bar-charts representing RCF treatments influencing mechanical properties. Normalization is with respect to materials with untreated RCF.

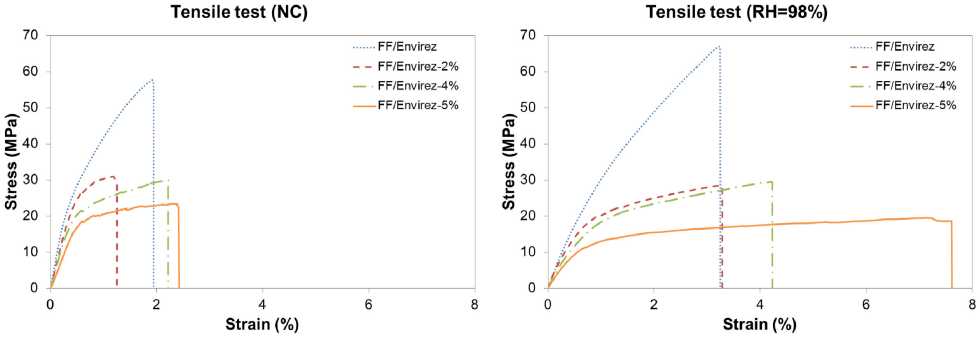

Figure 6. Stress-strain curves of FF/Envirez composites, conditioned and NC, with different fiber treatments.

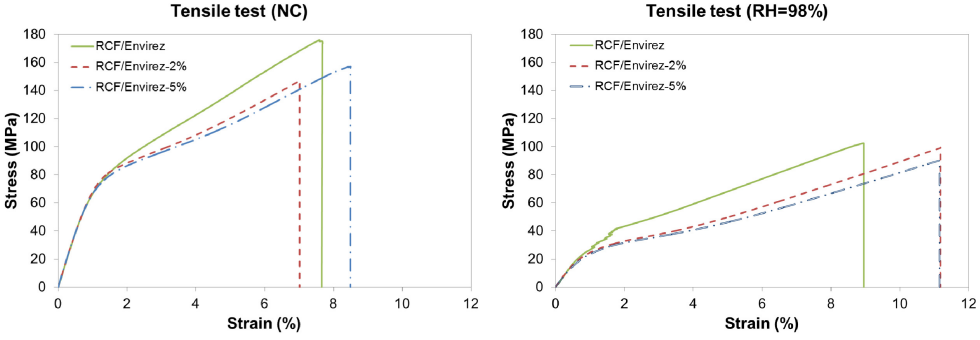

Figure 7. Stress-strain curves of RCF/Envirez composites, conditioned and NC, with different fiber treatments.

Stiffness and strength of both FF and RCF composites were drastically reduced by moisture at RH=98%, whereas the strain at failure was increased. The treatments seemed to be too harsh and resulted in a decrease of stiffness and strength of the composites, which was more significant in the case of FF composites than in RCF. However, the strain values were not affected much by the treatment. Also, moisture almost did not affect FF but RCF was really hit. This could be due to the fact that cellulose in FF has a much higher crystallinity than in RCF. However, the treatment did not seem to help RCF with respect to moisture uptake, whereas it worked for FF, as indicated by strength values. In the following, the impact of chemical surface treatment on the microstructure of materials was further studied. One possible reason that treatment did not improve moisture resistance could be that it was limited to the surface of fibers without significant penetration. If the chemical treatment would be able to affect larger volume (throughout the fiber) a greater protection against moisture could be achieved. For instance, the work done by Almgren et al. indicates a fiber treatment which results in cross-linking of the wood fiber cell wall, and hence reduces moisture sorption [37].

MICROSTRUCTURE

The overall microstructure of RCF/Envirez and FF/Envirez composites are shown in Figure 8. There were no large defects and voids detected in the composites. Fibers in composites were well consolidated and a rather high volume fraction of fibers (≈50%) was obtained. Further microscopy was run on fracture surfaces of composites with treated fibers, to detect the treatment's influence on the fracture properties (see Figures 9 and 10). The selected images of single fibers are representative of the overall fiber morphologies of materials.

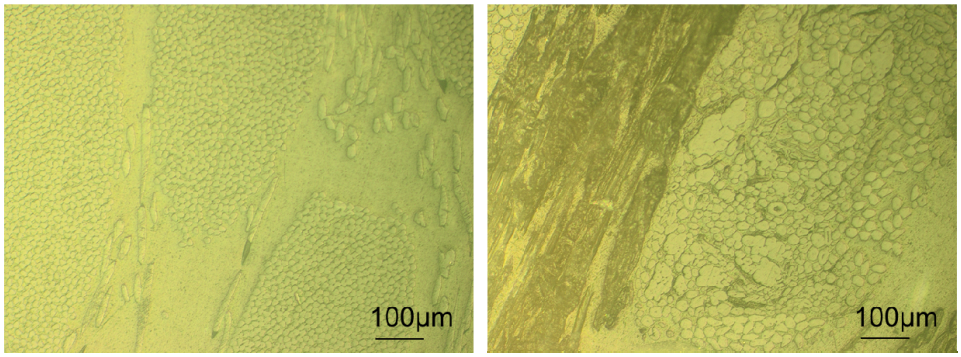

Figure 8. Optical microscopy images of RCF/Envirez (left) and FF/Envirez (right) composites.

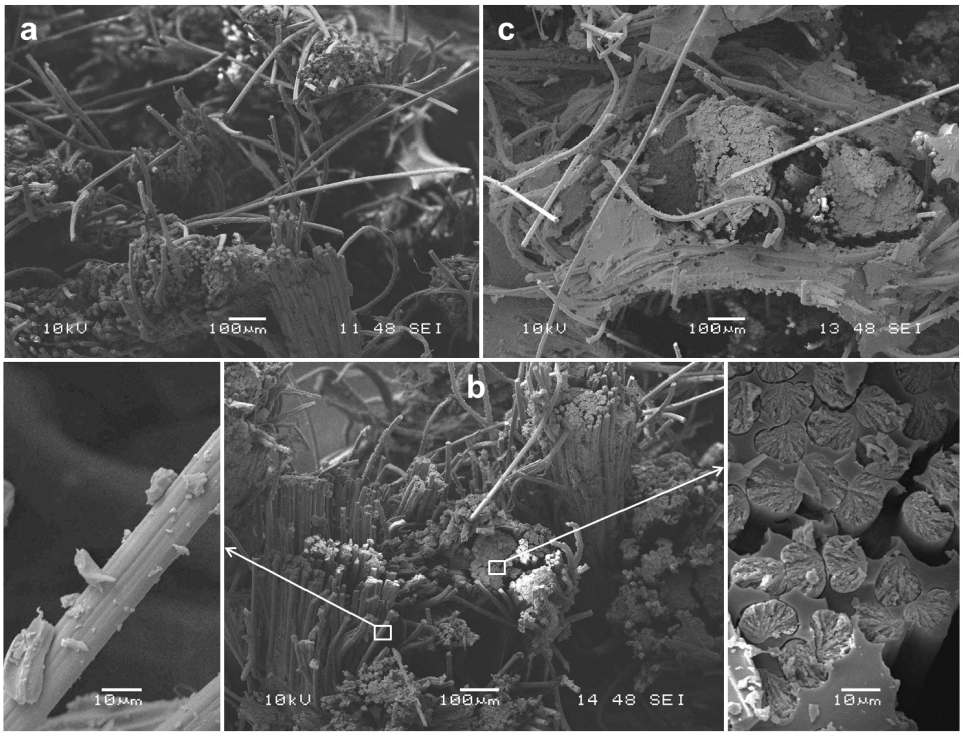

Figure 9. SEM images of fracture surfaces, RCF/Envirez-0% (a), RCF/Envirez-2% (b) and RCF/Envirez-5% (c).

Figure 9 represents how the treatment caused disturbances in the microstructure; see the magnified single fiber of RCF/Envirez with 2% APS treatment. However, the treatment's impact was more significant in the case of FF composites which might explain the drastic drop of mechanical properties, see Figure 10.

Conclusions

Comprehensive characterization of mechanical properties of fully bio-based composites with treated and untreated cellulosic fibers (FF and RCF) with different moisture content was carried out. The analysis of results led to the following conclusions:

- Moisture uptake in presented natural fiber composites was predominantly due to the water transport and accumulation by the reinforcement. This might have influenced some of the comparisons between different composites since fiber volume fraction in different materials slightly varied.
- Composites with cellulosic fibers absorbed much more moisture than GF composites. The diffusivity coefficient of RCF composites was by an order of

magnitude higher than for GF composites with the same bio-based resins. The moisture saturation level was up to 30 times higher in RCF than in GF composites.

- The diffusivity coefficient of FF reinforced composites was 2-3 times higher than that of RCF materials. However, the saturation level for RCF composites was higher than that for FF reinforced materials. This might have been related to the form and degree of crystallinity in FF and RCF.
- Mechanical performance of RCF composites with Tribest and EpoBioX was not severely affected by the raise in moisture from 41% to 70% RH. The decrease of stiffness and strength due to moisture uptake was within 15%. The mechanical properties of RCF composites with Envirez resin was significantly affected by moisture (~50%-70% reduction of strength and more than 100% reduction of stiffness). However, it should be noted that the moisture content in Envirez composites was approximately 1.5 times higher than that in Tribest and EpoBioX based materials. Envirez based composites were conditioned at higher RH than Tribest and EpoBioX (98% vs. 41% and 70%) and were compared with their as received NC counterparts.
- The fiber treatment did not improve the resistance of cellulosic fibers to moisture. Moreover, FF seemed to be considerably damaged by the treatment which resulted in much lower properties of FF composites with treated fibers, in comparison with composites based on untreated reinforcement. This could be the result of microfibrillation or fiber damage by the treatment but also of an inferior interfacial adhesion.

The results of this study showed that the moisture absorption by cellulosic fiber composite was critical, in terms of the degradation of mechanical properties. The most common methods of fiber treatment did not seem to protect the fibers from moisture. The future work should focus on designing and tailoring the fiber treatment to have a more efficient protection against moisture. The development of protection of composites and their structures against moisture on a larger scale (e.g. gel coats, protective paints etc.) should also be investigated.

Acknowledgments

The support from ANACOMPO project partners in Swerea SICOMP, Birgitha Nyström, Peter Mannberg and Runar Långström, is appreciated. The assistance received from Johnny Grahn and Andrejs Pupurs is greatly acknowledged for performing SEM studies.

Contract grant sponsors: Interreg IVA Nord project ANACOMPO, funded by EU and Norrbotten, Länsstyrelsen as well as Erasmus Mundus DocMASE program funded by EU.

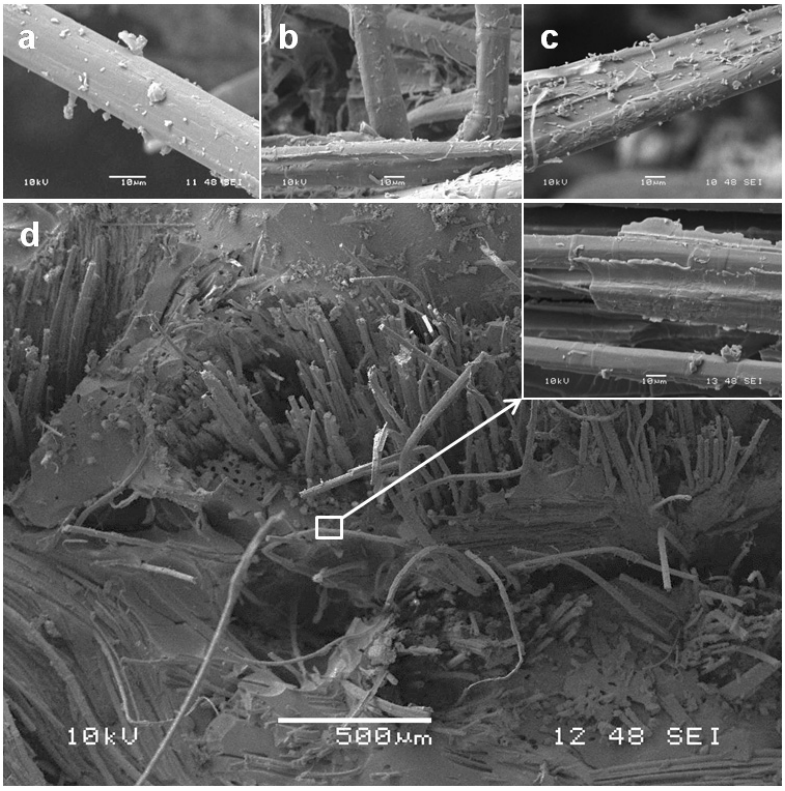

Figure 10. SEM images of fracture surfaces, FF/Envirez-0% (a), FF/Envirez-2% (b), FF/Envirez-4% (c) and FF/Envirez-5% (d).

References

[1] H. Lilholt, and J.M. Lawther, "Natural organic fibers," in Comprehensive Composite Materials, Vol. 1, T.W. Chou, Ed., *Elsevier Science, Amsterdam*, **303** (2000).
[2] J.C.M. De Bruijn, Appl. *Compos. Mater.*, **7**, 415 (2000).
[3] S. Chapple, and R. Anandjiwala R., *Thermoplast. Compos. Mater.*, **23**, 871 (2010).
[4] A. Bismarck, I. Aranberri-Askargorta, J. Springer, T. Lampke, B. Wielage, A. Stamboulis, I. Shenderovich, and H.H. Limbach, *Polym. Compos.* **23**, 872 (2002).
[5] C.A.S. Hill, and H.P.S.A. Khalil, *Appl. Polym. Sci.*, **77**, 1322 (2000).
[6] K. Van de Velde and P. Kiekens, *Polym. Test.*, **20**, 885 (2001).
[7] L. Jiang and G. Hinrichsen, Angew. *Makromol. Chem.*, **268**, 13 (1999).
[8] L. Jiang and G. Hinrichsen, Angew. *Makromol. Chem.*, **268**, 18 (1999).
[9] G.I. Williams and R.P. Wool, *Appl. Compos. Mater.*, **7**, 421 (2000).
[10] T. Nishino, K. Hirao, M. Kotera, K. Nakamae, and H. Inagaki, *Compos. Sci. Technol.*, **63**, 1281 (2003).

[11] K. Oksman, M. Skrifvars, and J.F. Selin, *Compos. Sci. Technol.*, **63**, 1317 (2003).
[12] A. Keller, *Compos. Sci. Technol.*, **63**, 1307 (2003).
[13] D. Plackett, T.L. Andersen, W.B. Pedersen, and L. Nielsen, *Compos. Sci. Technol.*, **63**, 1287 (2003).
[14] M.N. Belgacem, P. Bataille, and S. Sapieha, *Appl. Polym. Sci.*, **53**, 379 (1994).
[15] I.K. Varma, and V.B. Gupta, "Thermosetting resin," in Comprehensive Composite Materials, Vol. 2, A. Kelly and C. Zweben, Eds., *Elsevier Science, Amsterdam*, **1** (2000).
[16] S. Zhandarov and E. Mader, *Compos. Sci. Technol.*, **65**, 149 (2005).
[17] P.J. Herrera Franco, and A. Valadez-Gonzalez, "Fiber-matrix adhesion in natural fiber composites," in Natural Fibers, Biopolymers, and Biocomposites, Editors: A.K. Mohanty, M. Misra, and L.T. Drzal, *CRC Press, Boca Raton*, **180** (2005).
[18] S. Kalia, B.S. Kaith, and I. Kaur, *Polym. Eng. Sci.*, **49**, 1253 (2009).
[19] R. Masoodi, and K.M. Pillai, *Reinf. Plast. Compos.*, **31**, 285 (2012).
[20] A. Celino, S. Freour, F. Jacquemin, and P. Casari, *Appl. Polym. Sci.*, **130**, 297 (2013).
[21] S.K. Ramamoorthy, Q. Di, K. Adekunle, and M. Skrifvars, *Reinf. Plast. Compos.*, **31**, 1191 (2012).
[22] S.J. Christian, and S.L. Billington, *Composites: Part B*, **43**, 2303 (2012).
[23] L. Pupure, N. Doroudgarian, and R. Joffe, *Polym. Compos.*, **35**, 1150-9 (2014).
[24] K. Ilomäki, Adhesion between natural fibers and thermosets, Master thesis, *Tampereen teknikinnen yliopisto* (2011).
[25] C. Shen ,and G. Springer, *Compos. Mater.*, **10**, 2 (1976).
[26] L. Kumosa, B. Benedikt, D. Armentrout, and M. Kumosa, *Composites: Part A*, **35**, 1049 (2004).
[27] C.A. Smith, *Circuit World*, **14**, 22 (1988).
[28] M. Cotinaud, P. Bonniau, and A.R. Bunsell, *Mater. Sci.*, **17**, 867 (1982).
[29] S. Popineau, C. Rondeau-Mouro, C. Sulpice-Gaillet, and M.E.R. Shanahan, *Polymer*, **46**, 10733 (2005).
[30] W.K. Loh, A.D. Crocombe, M.M. Abdel Wahab, and I.A. Ashcroft, *Adhes. Adhes.*, **25**, 1 (2005).
[31] L.R. Grace, and M.C. Altan, *Polym. Compos.*, **34**, 1144 (2013).
[32] ASTM D638, *Standard test method for tensile properties of plastics* (1995).
[33] J. Duanmu, E.K. Gamstedt, and A. Rosling, *Compos. Sci. Technol.*, **67**, 3090 (2007).
[34] S.J. Christian and S.L. Billington, *Composites: Part B*, **43**, 2303 (2012).
[35] L. Kumosa, B. Benedikt, D. Armentrout, and M. Kumosa, *Composites: Part A*, **35**, 1049 (2004).
[36] H. Alamri, and I.M. Low, *Polym. Test.*, **31**, 620 (2012).

[37] K.M. Almgren, E.K. Gamstedt, F. Berthold, and M. Lindström, *Polym. Compos.*, **30**, 1809 (2009).
[38] A. Espert, F. Vilaplana, and S. Karlsson, *Composites: Part A*, **35**, 1267 (2004).

Paper C

Bio-based composites under fatigue loading: review on characterization and performance

Newsha Doroudgarian[1], Marc Anglada[2], Roberts Joffe[1]

[1]Composite Centre Sweden, Luleå University of Technology, S-97187 Luleå, SWEDEN
[2]CIEFMA, Technical University of Catalonia, Avda. Diagonal 647, 08028 Barcelona, SPAIN

Manuscript to be submitted to:
COMPOSITES SCIENCE AND TECHNOLOGY

Bio-based composites under fatigue loading: review on characterization and performance

Newsha Doroudgarian[1], Marc Anglada[2], Roberts Joffe[1]

[1]Composite Centre Sweden, Luleå University of Technology, S-97187 Luleå, SWEDEN
[2]CIEFMA, Technical University of Catalonia, Avda. Diagonal 647, 08028 Barcelona, SPAIN

Abstract. The current paper was intended to present a short introduction and overview of the mechanical performance of natural fiber composites, including durability studies. Although the mechanical properties of natural fiber composites are frequently discussed in the literature, the durability data are not easy to come across. Therefore, a comprehensive review of this topic is challenging but at the same time it is a necessary mission. The information presented here was meant to discuss and identify the tasks that need to be addressed in future investigations, to understand the factors affecting the mechanical durability of natural fiber composites. The information collected in this study indicated that the conventional approach to analyze fatigue data of natural fiber composites might not be optimal, due to their complex structure and variability of properties. It was suggested that the hierarchical structure of natural fibers might lead to a nonlinear behavior of the reinforcement and composite which would result in different performance of these materials in fatigue compared to synthetic fibers. Questions related to the accelerated test methods for characterization of long term performance (creep and fatigue) of natural fiber composites are briefly discussed. A concise list of modeling methods to predict long term behavior of the natural fiber composites is presented, with the suggestion of using it as a tool for the design of bio-based materials for structural applications.

Introduction

Potential problems associated with the growing consumption of oil and its products (including materials) in the recent years, such as increasing pollution as well as apparent changes of climate, have raised environmental concerns and public awareness for a sustainable, environmentally friendlier economy and society. This prompted the scientists to turn towards research on sustainable products and technology, which also comprises the development of environmentally friendlier materials from renewable resources [1,2] (e.g. bio-based composites). Luckily, the industry follows this suit [1,3-7] and the use of natural materials as well as renewable resources are starting to play a major role in the economy of developed industrialized countries (e.g. USA, EU [8-10], Japan, etc.). Likely, in the world of composites, there have been great efforts on

introducing naturally grown raw materials, to synthesize polymers and produce reinforcement [6]. Among fiber reinforced plastics, natural fibers with a high cellulosic content derived from wood and plants have shown a promising potential as reinforcement [11–14], due to their high stiffness, reasonable strength and low weight. Some of the best performing natural fibers are flax and hemp with cellulose content of over 60%. People have realized good properties of cellulose and already more than 150 years ago the first regenerated (manmade) cellulose fibers (RCF), so-called artificial silk [15], were produced. However, until recently, these fibers were used only in the textile industry or in other applications (e.g. tires) where they did not fully utilize the high mechanical properties of RCF. Lately, researchers have been focused on the use of RCF in more demanding applications, like in polymer composites for load bearing structures. RCF not only show very decent mechanical properties (although somewhat lower than that of natural fibers) but also have overcome the issues with variability in properties, instability of geometry and length limitation. Continuous fibers with very stable cross section and diameter can be produced and assembled in various types of fabrics for using in the composites as reinforcement.

Apart from the benefits of using natural fiber reinforced composites, there are some characteristic downsides which restrict their use and leave some space for improvement. The highly nonlinear nature of natural fibers and specially RCF, contrary to the conventional fiber reinforcement (e.g. carbon and glass) is one of the factors which complicates the designing of structures from these materials. Furthermore, the natural fibers are extremely sensitive to environmental changes (namely temperature and moisture) which also significantly increase the nonlinearity of these materials.

Developing bio-based composites accounts for structural applications where the material has to hold under loading for long time intervals. However, during the recent decades, the research on bio-based composites has mostly been limited to the static properties. The amount of data on long term performance of these materials, such as in creep and fatigue, is scarce. Understanding how these materials behave and the ability to model their long term performance are vital in the designing of new products as well as in demonstrating their potential for a wider use in high performance demanding and load carrying applications. Most of the available results concerning the durability of bio-based composites are related to the environmental endurance (e.g. the effects of moisture and temperature), whereas the results on long term mechanical performance (e.g. creep and fatigue) are not that widely presented. Specially, the data in literature about the behavior of these materials in fatigue are very limited.

The current paper gives a brief overview of natural fibers and their composites with the main focus on the review of the published data on the behavior of cellulosic fiber (natural fiber and RCF) reinforced composites under dynamic loading, in comparison with synthetic fiber composites. Differences and similarities of approaches used for conventional and bio-based composites are discussed. One of the main interests in this

context is to understand the mechanisms governing the material's behavior, in particular the sources of damage initiation and failure mechanisms that have been identified. A brief summary of modeling technics to predict the lifetime of materials and structures is presented. Recommendations for the future research topics that are crucial for the development of bio-based materials are offered.

Why natural fibers?

Our planet Earth is overpopulated and therefore rapidly losing its resources. This motivates us as materials engineers to look for environmentally friendly and sustainable products to save the resources for future generations. One should consider that the production methods which create intensive pollution and CO_2 emission lead to greenhouse gases. This is believed to be the cause of global warming and must be eliminated or at least significantly reduced. Furthermore, the use of sustainable resources should be promoted to replace petroleum based materials. However, careful engineering is required in order to develop competitive renewable materials which are cost effective and offer similar performance to materials that are currently in use.

The polymer composite materials are nowadays the dominating materials in industries like aerospace, automotive, light weight construction and sports [16]. Aramid, carbon and glass fiber are commonly used as reinforcements in these composites. Among conventional fiber reinforcements, glass fibers are the most widely used [17] due to their low cost and fairly good mechanical properties.

However, contrary to their benefits, glass fibers have drawbacks which promote the use of natural counterparts as green alternatives (see Table 1). Natural fibers generally offer low production costs, friendly processing (low tool wear and little skin irritation) and good thermal and acoustic insulation properties [18]. Furthermore, as compared to glass fibers, low specific weight of natural fibers provides them a higher specific strength and stiffness [19].

Table 1. Qualitative comparison between natural and glass fibers, adapted from [18].

	Natural fibers	**Glass fibers**
Density	Low	Twice that of natural fibers
Cost	Low	Low but higher than natural fibers
Renewability	Yes	No
Recyclability	Yes	No
Energy consumption	Low	High
CO_2 neutral	Yes	No
Abrasion to machines	No	Yes
Health risk when inhaled	No	Yes
Disposal	Biodegradable	Not biodegradable

Considering their renewable and biodegradable nature, natural fibers are growingly being used in composite materials [20]. Today the European Union is encouraging the development and usage of such materials. There are several European directives on recycling and the reuse of the industrial waste, for instance in the automotive sector [8-10]. Furthermore, there were a number of related projects funded by the European Union, for instance ECOFINA, BIOCOMP, WOODY or ANACOMPO (INTERREG IV-A North), which emphasize eco-efficient technologies and products based on natural fiber composites.

NATURAL FIBERS

A direct use of natural fibers is in one-dimensional products, such as lines and ropes. Moreover, in the early times, natural fibers were applied for footbridges, suspended across rivers, or for rigging of naval ships. During the 1990s, a renaissance began in the use of natural fibers as reinforcements in technical applications [21].

However, disadvantages such as variable quality, moisture absorption, low durability, low impact strength, and restricted processing temperatures, are the limiting factors of natural fibers' usage [3]. The advantages and disadvantages of using natural lignocellulosic fibers in the design of high performance composite products are listed in Table 2.

Table 2. Main advantages and disadvantages of lignocellulosic fibers, adapted from [22,23].

Advantages	**Disadvantages**
Low cost	High moisture absorption
Renewable	Poor microbial resistance
Low density	Low thermal resistance
Nonabrasive	Local and seasonal quality variations
Low energy consumption	Demand and supply cycles
High specific properties	Nonlinear stress-strain response
High strength and elasticity modulus	Non-continuous fibers
No skin irritations	
No residues when incinerated	
Fast absorption/desorption of water[a]	
Biodegradability[a]	
Good thermal conductivity[a]	

[a]Considered advantageous depending on the application.

Typically, the natural fiber based composites are compared with glass fiber reinforced polymers, considering the same matrix, manufacturing method, fiber volume fraction as well as fiber dimensions (e.g. length), shape and configuration. The comparison results

in that natural fiber composites can have very good specific stiffness and reasonable specific tensile strength, competing glass fiber composites (see Table 3) [18,24]. Unfortunately, the impact strength of natural fiber reinforced composites does not compare well with glass fiber composites [25-27] but it can be increased by improving the adhesion between the matrix and fibers [28]. Flexural strength is also somewhat lower in natural fiber composites than in glass fiber counterparts [29].

Table 3. Typical properties of flax, hemp, jute, and E-glass fibers, adapted from [30].

Fibers	Modulus, GPa	Strength, MPa	Density, g/cm^3	Specific modulus	Specific strength
E-glass	72	3530	2.54	28.2	1390
Flax	50-70	500-900	1.4-1.5	~ 41	~ 480
Hemp	30-60	300-800	1.48	~ 30	~ 370
Jute	20-55	200-500	1.3-1.5	~ 27	~ 250

Flax and hemp compared to other natural counterparts contain a high amount of straw and fibers which make them favorable alternatives as reinforcing natural fibers. Cellulose is the main element of plant fibers and fibers such as hemp and flax contain considerably high amount of cellulose. The presence of cellulose makes the fibers strongly polar due to the hydroxyl groups, acetal and ether linkages in the cellulose structure (Figure 1). Consequently, cellulosic fibers have poor interfacial compatibility when it comes to reinforcing non-polar polymers like polypropylene [30]. Moreover, the cross sectional shape of the natural fibers is usually rather irregular and the fiber itself has a highly hierarchical structure consisting of cellulose fibrils arranged in layers with different fibril orientations (see Figure 2).

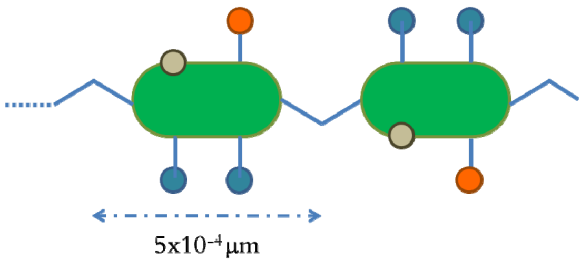

Figure 1. Cellulose molecule. Rings contain five carbon atoms and one oxygen. Bridges are single oxygen atoms, paired projections are OH groups and single projections CH_2OH and other valences are occupied by hydrogen atoms.

Typical composition and geometrical characteristics of hemp and flax are listed in Table 4. In general, it can be stated that agro-based fibers acquiring appropriate aspect

ratios have the potential to offer outstanding reinforcements to polymers [31]. However, as it can be seen in Table 4, physical characteristics of natural fibers are highly variable depending on the agricultural parameters.

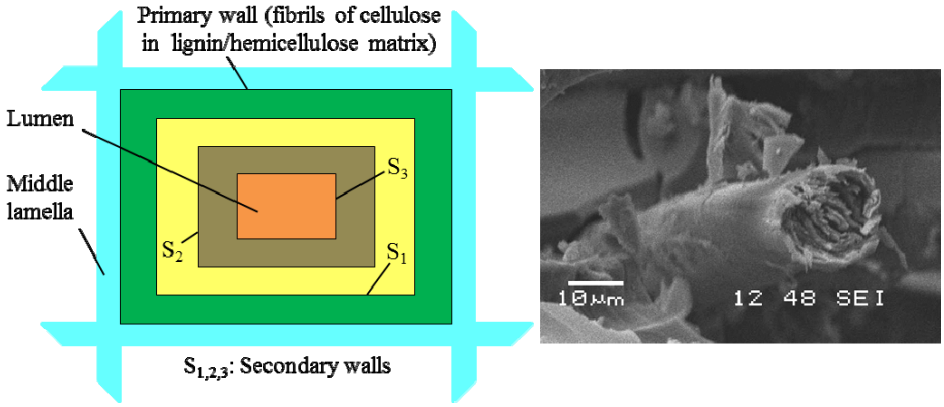

Figure 2. Simplified representation of plant fiber cross section (left), scanning electron microscopy image of a flax fiber (right). Lumen is the hollow space in the middle and S_2 is the secondary wall containing microfibrils aligned in 10° angles.

Table 4. Physical characteristics of hemp and flax, adapted from [19,20,32].

Characteristic		**Hemp**	**Flax**
Component (wt%)	Cellulose	70-78	60-81
	Hemicellulose	17-22	14-21
	Pectin	1-2	1-3
	Lignin	3-5	2-5
Dimension[a] (mm)	Length	5-55	9-70
	Diameter	0.01-0.05	0.005-0.038

[a]The values correspond to single fibers.

REGENERATED CELLULOSE FIBERS

Apart from the naturally occurring fibers, there are other types of cellulosic fibers which are manmade, known as regenerated cellulose fibers (RCF). In the early 1850s, a substance from plant cellulose was accidentally discovered and then introduced to the manufacturing of textile fibers. Almost a century later, strong RCF rayon yarns were successfully produced and massively used in automobile tires [15].

RCF, contrary to the natural fibers, have a controlled geometry which allows creating composites with compact and well-defined microstructure, like in the synthetic composites (see Figure 3).

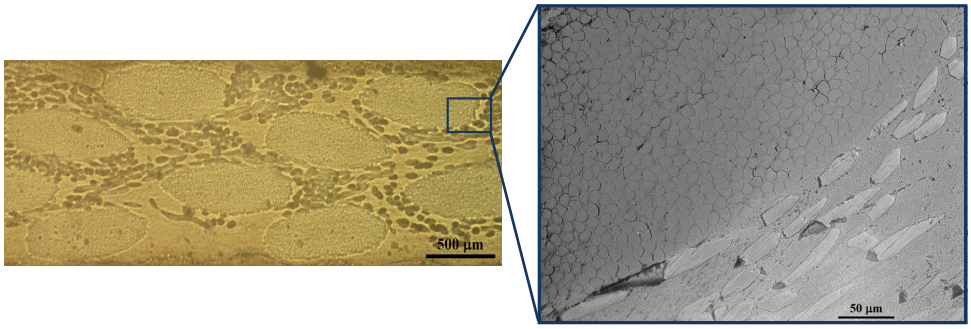

Figure 3. Transversal cross section of RCF based unidirectional composite laminate with distinct bundle structure (left) and RCF bundles with high packing density of fibers (right).

However, even manmade cellulose fibers have a wide variation of properties depending on the manufacturer and type of the process [33]. The plot in Figure 4 illustrates the stress-strain curves of different regenerated cellulose fibers. These results clearly demonstrate that compared to the typical viscose rayon RCF (which are the commonly used fibers), there are better performing types of RCF available. For instance, tensile performance of high tenacity fibers (e.g. Cordenka^{TM}), which are made by modifications of viscose process, is significantly better compared to the regular viscose [33].

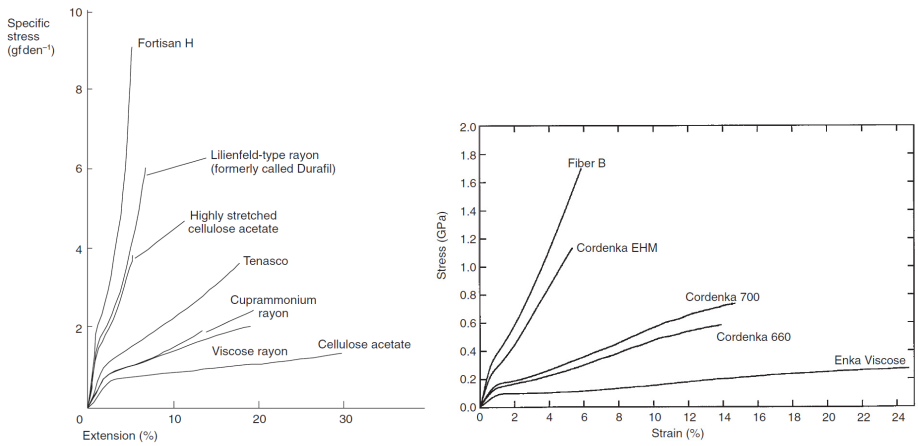

Figure 4. Stress-strain curves of: variants of regenerated cellulose fibers with different spin conditions and chemical solutions (left), 10gfden^{-1} = 0.88Ntex^{-1} (gf = grams force) and of: fiber B, RCF spun from phosphoric acid solution, and RCF viscose fibers (right) [33,34].

High performance bio-based composites

Natural fiber reinforcements have been already introduced in non-structural applications, for example in the interior of cars. There are already several car manufacturers which use flax or hemp fibers reinforced polymers in parts like car roofs and door panels [3,4]. There are several reasons to introduce natural fibers and their composites into the wide range of load carrying applications rather than only for non-structural usage. It is already accepted that natural materials offer ecological and commercial benefits compared to the petroleum based alternatives. One of the very first natural fiber reinforced composites, developed for structural purposes, refers to the mid-1930s. The composite (Gordon Aerolite) was combined of flax fiber and phenol formaldehyde matrix, fabricated by Aero Research Limited for aircraft construction. However, in the 1940s research on natural fiber composites lost its attraction since Owens-Corning introduced the highly competitive glass fiber reinforcement for plastic laminates. This ended up in a massive use of synthetic composites in airplanes and boats. Nevertheless, over the last two decades, the research on natural composites is intensifying again and leading to its wider use as construction materials [1,19]. This has been a result of the improvements of natural composites, regarding the fiber matrix compatibility, impact strength, etc. [35]. Natural fiber reinforced composites have even been considered as alternatives for aerospace applications [36,37].

The major motivation of natural fiber applications in polymer composites is their low density which is of interest, for instance in the automotive industry. But weight is not the only factor that defines the use of natural fiber composites in cars. For instance, flax fibers are used in car disk brakes instead of asbestos fibers [38,39].

In general, for fiber reinforced plastics, higher critical loads for damage initiation, higher failure loads and lower damage propagation rates can be engineered by [40]:

- Higher fiber strength and modulus;
- Stronger fiber matrix adhesion;
- Higher fiber fractions.

However, early fiber matrix debonding as a result of ageing has been the limiting natural composites to short term applications [40]. It is also the sensitivity to humidity, temperature and UV radiation that restricts the use of natural fibers [41]. Therefore, there is a need of systematic and detailed analysis of properties, durability and failure mechanisms to be undertaken on fiber composites [40]. The structural applications of polymer matrix composites demand lifetimes of about 15 to 50 years and have to be hardly affected by ageing. Moreover, the mechanical properties of these composites, e.g. strength and stiffness, are time dependent due to their viscoelastic nature. Hence, in order to make these composites predictable alternatives and to consequently extend their use, lifetime models should be introduced which account for viscoelastic materials [42].

NONLINEARITY

Natural fiber composites exhibit an inherently nonlinear (viscoelastic) behavior, such as time dependent stress-strain response, hysteresis loops and sensitivity of mechanical properties to variations of loading rate [43]. Figure 5 shows stress-strain response of RCF bundles [44]. As it is seen the stress-strain curve of RCF demonstrates a biphasic pattern with two linear portions of distinctly different slopes. Furthermore, the repeated cycles of loading and unloading display the evolving hysteresis loops as a result of viscoelastic effects. This nonlinearity in the reinforcing fibers is then reflected in the behavior of the composites [45].

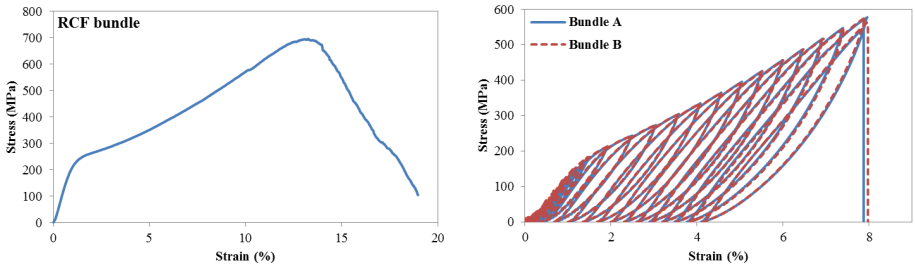

Figure 5. Typical stress-strain curves of RCF bundle, under monotonic tensile (left) and cyclic loading unloading (right).

STATIC VS. DYNAMIC

The research on natural fiber composites for structural applications is rather young. Manufacturing of such composites is challenging due to the variability of the fibers in geometry and properties. Therefore, the major mechanical characterization tests are focused on the static properties. Tensile, flexural and impact are the most frequent mechanical tests to characterize these materials.

Additionally, the mechanical properties of natural fiber composites, due to their organic nature and high moisture absorption, have higher rate of degradation than synthetic fiber composites. However, to increase the potential of these eco-friendly, inexpensive natural fibers to be involved in polymers, the degradation mechanisms under the lifetime of natural fiber reinforced composites have to be understood [41].

STATIC FATIGUE, CREEP

One of the measures of the long term behavior of materials is the evolution of deformation under a constant load - creep (also known as the static fatigue). Creep is observed in most of the materials but it is strongly present in polymers and their composites (including natural fibers). Its development is defined under three stages (decreasing, constant and accelerating creep rates) leading to the failure of material [46].

However, the second stage is the most responsible in determination of the creep resistance. Creep behavior under a constant stress in natural fiber composites is a complex phenomenon. Properties of the matrix as well as fibers, e.g. molecular orientation, crystallinity, volume fraction, aspect ratio, configuration and mechanical properties, influence the creep in natural composites. Furthermore, external factors such as the applied stress and environmental loads have an impact on creep [47–49].

In the creep test, a stress is suddenly applied to the material and is then kept constant during the test. What is measured is the strain as a function of time. In viscoelastic materials, such as polymers, stress and strain are functions of time. Thus, the deformation as a result of a constant applied load is initially elastic (independent of time) followed by a creep deformation (viscous flow) which is time dependent [41].

There are several mathematical expressions and models proposed to describe the creep behavior in conventional polymer composites which can be applied for natural composites as well [47]. The models used in analyzing the creep behavior are generally based on two theories of viscoelasticity. One is represented by simple rheological models using viscous elements (dashpots) and elastic elements (springs). This model is appropriate for materials tested in the linear viscoelastic creep, e.g. Bürgers model. The other is for the nonlinear viscoelastic range using a power law model known as Schapery's model [47].

It is very time consuming to obtain reliable creep data since it requires a large number of long experiments. However, it is possible to perform a number of short term creep experiments and obtain parameters that can be used in modeling of long term behavior of the materials. The Schapery's model was modified and successfully used to predict the behavior of RCF composites [50]. It was also shown [51,52] that it is possible to predict the nonlinear behavior of composites, by using the description of nonlinear fiber and matrix (RCF and EpoBioX) in combination with micromechanics.

Another way to obtain creep results in a reasonably short time is to employ time temperature superposition. In this case, tests are performed at elevated temperature which translates into longer times of experiment. This approach was used by performing dynamic mechanical thermal analysis at different temperatures to construct creep master curves for bio-based resins [48] and cellulosic fiber composites [49].

Dynamic fatigue

The failure in structural composites occurs often due to mechanical fatigue. In design engineering, the fatigue phenomenon is a serious cause of design failures. Because of that, there are strong concerns when it comes to materials durability and long term performance [41]. Therefore, the mechanical durability in composites, in terms of fatigue life prediction, has been an interesting subject during the last four decades [53]. Despite the fact that there have been several articles published on fatigue of different composite materials and a significant amount of experimental data is available, there is

not a definite conclusion on specific predictive algorithms [54,55]. Fatigue mechanisms in composite materials are numerous complex phenomena interacting with each other throughout the whole structure [56]. All these discussions agree on that the difficulty in defining and modeling the damage mechanisms during fatigue results from anisotropy of composites [53]. The mechanical properties of composites, including fatigue, depend on the composite's constituents (matrix and reinforcement) as well as on the interfacial strength between them. Thus, even after small changes in the fiber, matrix, interface or the processing procedure, the composite has to be recharacterized [57]. Furthermore, every composite laminate with a different layup constitutes a new material with new mechanical properties. Therefore, the characterization of fatigue life of composites becomes a very time and resource consuming procedure.

FATIGUE IN CONVENTIONAL COMPOSITES, 1970s–PRESENT

Conventionally, in materials science, fatigue data are used to construct Wöhler (S–N) diagrams where the stress value is plotted over the number of cycles to failure [56]. However, for composite materials, Talreja [58] introduced the fatigue life diagrams (plot of the initial peak strain against the number of cycles to failure) which provided the analysis of fatigue mechanisms (see Figure 6). Fatigue life diagrams represent three basic regions throughout the lifetime of the composite until failure and the underlying damage mechanisms. Region I indicates the non-progressive (chaotic) mechanism of fiber failure. Region II consists of the progressive damage with matrix cracking and fiber matrix debonding. In the region III, below the fatigue limit, matrix cracks are arrested and slowed down. The failure below the fatigue limit occurs following a high number of cycles, 107 or more [59]. Talreja [59] has argued that the trends in region II and the fatigue limit in region III are influenced by the fiber stiffness, see Figure 7.

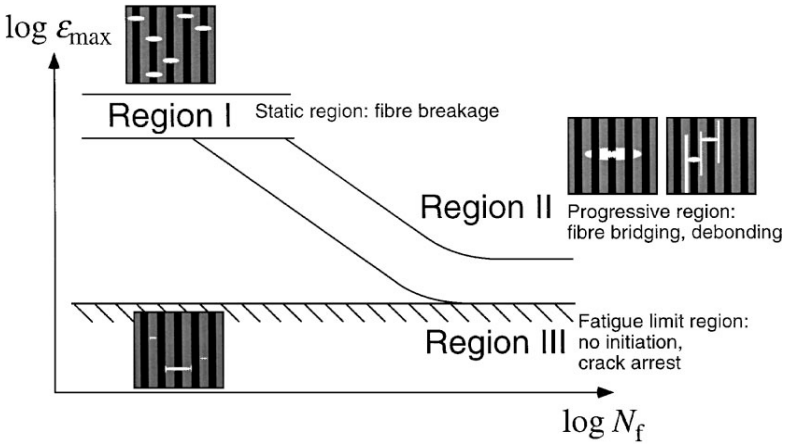

Figure 6. Fatigue life diagram of longitudinal composites in tension–tension fatigue [56].

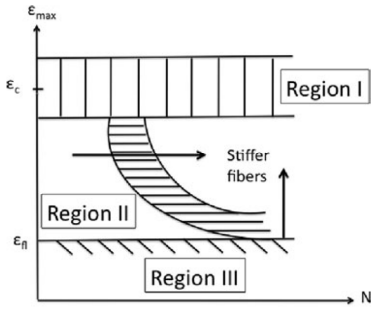

Figure 7. The effect of fiber stiffness on regions II and III of fatigue life diagram for unidirectional composite under cycle tensile loading in fiber direction [59].

There are further studies carried out beyond this basic case scenario of unidirectional composites, in order to adapt the fatigue life diagram to multidirectional laminates undergoing biaxial cyclic loading. Figure 8 illustrates the fatigue damage mechanisms of a multidirectional composite laminate, consisting of two stages prior to the "characteristic damage state" (CDS) and post-CDS [60]. CDS is where all the inclined plies ($\theta \neq 0°$) reach a saturation state of cracking. Subsequently, an extensive interface cracking, namely delamination, begins. Then the 0° plies are responsible for carrying most of the fatigue load and continue to hold until a sufficient number of fibers break [60].

FATIGUE IN NATURAL FIBER COMPOSITES

It is examined that natural composites perform fairly well in static loading but there is a need to determine their long term performance as well. Some published results in the literature show that the performance of natural fiber composites is comparable with that of glass fiber composite materials. For instance, the graphs in Figure 9 demonstrate that not only the static properties of hemp composites are better than that of glass fiber based materials but also the fatigue performance is comparable or even better [61]. However, it should be noted that in the case of glass fiber composite, the layup of the laminate was [±45°]. Whereas, the hemp fiber composite was made out of a randomly oriented mat. Moreover, the weight fraction of fibers was the same in both of these composites which means that the volume fraction of fibers was significantly higher in hemp laminates than in glass.

The S-N diagrams presented in Figure 9 are examples of the case where these diagrams cannot provide a complete understanding of the behavior of the material. Even though, the stress-strain curves indicated that the natural fiber composite is much more brittle than the glass fiber counterpart, there was no visible damage found in the hemp composite. Whereas, multiple matrix cracks were present in the glass fiber composite. This was also supported by measurement of the residual elastic modulus of

the materials. Glass fiber composite's stiffness was gradually decreasing during the fatigue tests while the stiffness of hemp composite stayed on the same level until failure. The authors of the paper [61] attributed this behavior to the different fiber type and shape as well as to the differences of material's morphology (random hemp fiber mat vs. [±45°] glass fiber laminate). However, the reason of such behavior may also be the viscoelastic nature of the material which does not reveal itself during the fairly short quasi-static tensile tests but is observed under loading over a long time interval (fatigue). A similar behavior has been detected for RCF when stiffness was measured from loading and unloading parts of the stress-strain curve [62] in stepwise loaded fiber bundles. In the unloading ramp (after loading of the fiber bundle to a high strain level) the decrease of stiffness was observed whereas the next loading ramp did not show any changes in the modulus.

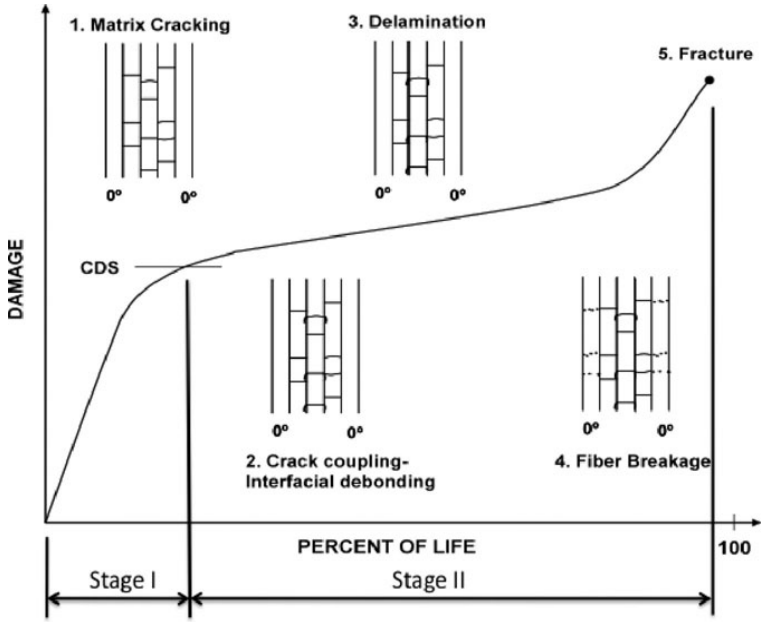

Figure 8. Damage mechanisms in fatigue of multidirectional laminates proposed by Jamison et al [60]. Laminate schematics represent the edge views with outer plies in 0° to loading direction and matrix cracks in off-axis plies.

Another study compared flax fiber composites with glass fiber based materials [63]. It was concluded that the fatigue resistance of [±45°] oriented flax fiber laminate is superior to that of glass reinforced epoxy while the glass fiber cross-ply laminates had a better performance than the flax counterparts. This was attributed to the combination of low density of flax fibers and the matrix controlled behavior in [±45°] laminates. However, in this study it was also shown that the glass fiber composite experienced a

much higher loss of modulus than the flax fiber material. As a matter of fact, the flax fiber cross-ply laminate showed an increase of stiffness by 2%. This was explained by the self-straightening effect of flax fibers in association with the realignment of microfibrils, causing a stiffening effect which is by now a well-established phenomenon in natural fibers [64-66]. These results show that the behavior of natural fiber composite materials under mechanical loads is defined by the complex microstructure of the fibers and the resulting nonlinear response.

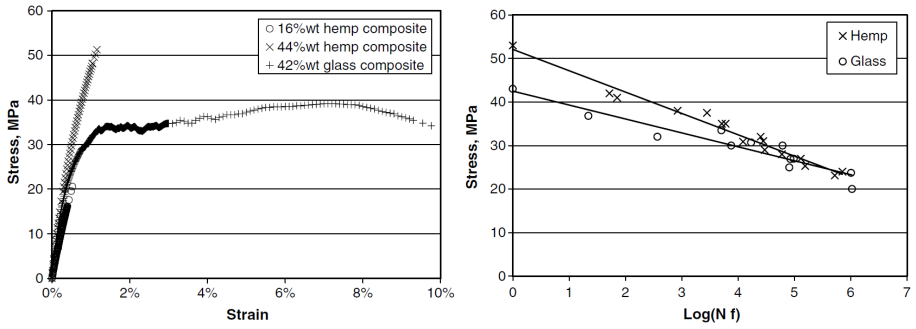

Figure 9. Stress-strain curves (left) and S-N diagrams (right), for hemp and glass fiber composites [61].

The strong influence of fibers microstructure is also evident from the fatigue tests performed on sisal fibers [67]. These results show the dependence of dissipated energy on the load level as well as on the number of cycles (reflected in the area and width of hysteresis loops). This is a typical behavior for solids with cellular characteristics. In this respect, sisal fibers have a high degree of porosity and are visually very similar to foams. The data on sisal fiber composites, by Towo et al., also demonstrated the evolution of hysteresis loops during fatigue [68]. But in this case, the area of hysteresis loops was gradually decreasing with the number of cycles, i.e. the composites dissipated the most energy within the initial stage of fatigue. The reason to this, argued by the authors, was the stiffening of composites in the fiber direction, indicated by the slight increase in the loading side of the hysteresis loop. However, this was also attributed to "conditioning" of the samples during the time under load [68]. Such conditioning is well known in the case of creep experiments where specimens are subjected to a constant load for a long period of time prior to the actual testing, in order to eliminate the plasticity. The testing on sisal fibers was performed on non-treated as well as on alkali treated fibers [68]. It was concluded that tension-tension fatigue was not significantly affected by fiber treatment. It actually increases the rate of degradation during fatigue loading while tension-compression fatigue behavior is greatly influenced by the fiber surface treatment. This is due to the interfacial damage, developing more rapidly in compression [69,70].

The data on jute/PLA composites [71] also indicate that the creep of material during fatigue is evident. It was reported that the stiffness of composite remained unchanged during fatigue, whereas the average strain continued to increase.

In the fatigue study of Gassan [40] on flax and jute reinforced polymer composites, it is stated that one factor affecting the fatigue behavior is the natural fiber's structure. Fiber structure is the factor which directly influences the stress-strain behavior. In the case of natural fibers, the energy is just partially used up during structural and cumulative fiber degradation and a large percentage is gone as heat due to internal frictions during viscoelastic deformation of fibers. There is a mechanism proposed by Hamad [72] to relate the viscoelastic behavior of the natural fibers to their structural elements. The reinforcing cellulose microfibrils in each fiber's layer moderate the load bearing role of hemicellulose and lignin matrix. Cellulose microfibrils transfer stresses to adjacent layers and thus decrease the energy loss [72]. Further damage phenomena of fatigued fibers are a result of cumulative micromechanical degradation, followed by structural breakdown of microfibrils [72]. The interactions between cellulose microfibrils and the matrix influence the delamination crack growth. Likewise, microfibrilar alignment/placement to the crack plane plays a key role in interlaminar delamination in the natural fiber [40].

Due to the complex hierarchical structure of natural fibers, the approach based on S-N curves may not be an optimal method for the composites of this type. Therefore, despite the fact that S-N curves are the common approach to study fatigue behavior in synthetic composites, the approach for natural fibers should likely include more detailed information about the fiber structure, geometry, nonlinearity as well as the impact of environment. All of these factors are reflected in the failure mechanisms observed in these materials as well as in the resulting fatigue life. If these aspects are not taken into account, the only reliable way to characterize these materials will be experimenting and semi-empirical methods, such as by constant life diagrams, dynamic mechanical thermal analysis (DMTA) or statistical analysis of fatigue data (probabilistic S-N curves) [73–75]. Unfortunately, the fatigue tests are very time consuming and costly. This will hinder the development of products made out of natural composites since reliable tools are required to design durable structural materials.

One of the ways to save time, energy, resources is modeling, which shortens the development and validation time of designing the structural bio-based composites. However, these models must include detailed information about the behavior of materials in fatigue (such as failure mechanisms, damage accumulation and nonlinearity) [41].

CLASSIFICATION OF MODELING TECHNICS

To classify fatigue modeling efforts, empirical, phenomenological and mechanistic models may be considered. An empirical model introduces a damage parameter

regarding the final failure, without considering the other physical interpretations as accumulating of the fatigue damage. For metallic materials, mostly empirical approaches have been introduced [53].

Unlike empirical models, phenomenological formulations are correlating fatigue damage with a physically measurable quantity such as the residual stiffness or strength. These models treat the fatigue life prediction from macro to meso or even down to microscale. Since there are various interactions between fatigue damage mechanisms, phenomenological modeling can provide an appropriate solution to the problem. Still, several parameters have to be measured in each laminate [53].

Mechanistic models are the third class of composites life prediction. Such models provide the missing link between fatigue damage mechanisms and macromechanical properties of laminates under arbitrary stress conditions. These models solve the problem from micro to meso or to macroscale. The advantage of these models is a small amount of experimental input which is required from the fiber, matrix and their interface mechanical properties [53].

An intermediate class of fatigue modeling is the so-called laminate-to-lamina approach. In which, phenomenological models reflect fatigue damage mechanisms directly in the mesoscale of laminates. All the models mentioned above require knowledge of some basic fatigue parameters which could be considered as modules. The modules establish the building blocks for a general life prediction under arbitrary fatigue loads. These modules are as following [53]:

1. S-N curve definition: To obtain life prediction, the fatigue behavior of the material is considered under constant amplitude fatigue. Subsequently, a model is assumed to extrapolate or interpolate fatigue lives at any stress level. S-N curve is the simplest of all life prediction models, owing to a uniaxial stress field, constant amplitude and constant R ratio.

2. Generalizing to various R ratios: Hereby, it is required that a wide variety of fatigue cycles are performed, at different maximum and minimum stress.

3. Damage accumulation metric: This is mainly an assumption of the point at which fatigue failure occurs.

4. Fatigue failure criterion: In the case of multiaxial stress fatigue, some kind of failure function must be used to contribute each component of the stress tensor to the failure of composite. The variety of failure criteria for multiaxial static loading is a result of anisotropy in composites, caused by their layup and the loading characteristics.

5. An additional module: This is the algorithm for analyzing irregular load time runs, using a series of constant amplitude cycles, rather than sinusoidal load cycles.

FAILURE MECHANISMS

In general, fatigue in composites is characterized by the initiation of cracks. Cracks initiation in composites depends on the ductility of matrix and the fiber modulus

[40,44]. Due to the complexity of damage mechanisms in fiber reinforced polymer composites, the majority of fatigue models have been empirical, relying on curve fitting of the test data. By identifying the active micromechanisms and the influence of constituents and interface properties in the fatigue damage, prediction of the macroscopic fatigue behavior will be possible. The goal is to establish a link between the microscopic scale to the mesoscopic and further to the macroscopic fatigue behavior of the composites. Therefore, studies of microscopic properties and morphology of the matrix, fibers, interface and the fracture surfaces, over to the mechanisms governing the mesoscale of a few fibers diameter, as well as the macroscopic fatigue behavior (e.g. fatigue lives and residual stiffness) are necessary [57]. If the natural composites behave the same way as the synthetic ones then the following step is adapting and applying the models developed for synthetic composites into natural composites.

Since the early 2000s, the research on fatigue behavior in natural fiber composites is intensifying, exploring potential experimental methods to understand the fatigue mechanisms [76–80]. There are several types of wood and plant fiber composites being investigated in fatigue. However, the data on manmade cellulose fibers are still scarce.

Conclusions

The current paper offers a brief introduction on the mechanical behavior of natural fiber composites. There is a fairly large number of publications dealing with the mechanical properties of these composites obtained from static tests but a very little reliable information about the durability. Most often, the durability studies are related to the environmental factors (e.g. moisture and temperature) affecting the natural fiber composites while the performance of these materials in mechanical fatigue is not readily available. Moreover, the natural fibers have a very large variability of properties which not only depends on the fiber type and processing technics but also on the region and the weather conditions where the plants were harvested. Therefore, a comprehensive, complete and reliable review of this topic is a very challenging task. However, the presented information is intended to define the principal directions on which investigations should be focused.

It has been shown that using the conventional method of generating S-N diagram to characterize the fatigue performance of synthetic materials is not necessarily suited for natural fiber composites. Due to their complex structure and variability, natural fiber composites exhibit a different behavior than synthetic fibers and these differences are crucial for identification of the failure mechanisms present in these materials. It can be stated that the hierarchical structure of natural fibers may lead to a nonlinear behavior of the reinforcement and accordingly the composite which will result in a very different performance of these materials in fatigue compared to the synthetic fibers.

In order to avoid the large number of time consuming tests to characterize long term performance (e.g. creep and fatigue) of natural fiber composites, accelerated test methods should be employed. Another essential tool for the designing of natural composites for structural applications is modeling which, if carried out properly (e.g. accounting for the failure mechanisms, damage accumulation, nonlinearity, etc.), can save time, energy and resources.

Acknowledgment

The financial support from DocMASE (EU Erasmus Mundus program) project is acknowledged.

References

[1] D.B. Dittenber, and H.V.S. GangaRao, *Composites Part A: Applied Science and Manufacturing,* **43**, 1419-1429 (2012).
[2] O. Faruk, A.K. Bledzki, H. Fink, and M. Sain, *Progress in Polymer Science,* **37**, 1552-1596 (2012).
[3] G. Marsh, *Materials Today,* **6**, 36-43 (2003).
[4] J. Müssig, M. Schmehl, H. von Buttlar, U. Schönfeld, and K. Arndt, *Industrial Crops and Products,* **24**, 132-145 (2006).
[5] A.N. Netravali, and S. Chabba, *Materials Today,* **6**, 22-29 (2003).
[6] O. Faruk, A.K. Bledzki, H. Fink, and M. Sain, *Macromolecular Materials and Engineering,* **299**, 9-26 (2014).
[7] M.P. Dicker, P.F. Duckworth, A.B. Baker, G. Francois, M.K. Hazzard, and P.M. Weaver, *Composites part A: Applied Science and Manufacturing,* **56**, 280-289 (2014).
[8] EC–European Commission, *White Paper, Communication,* **144** (2011).
[9] E. Roadmap, *2050, Brussels, 15.12.2011 COM,* **885** (2011).
[10] E. Directive, *Official Journal of the European Union, L Series,* 34-42 (2000).
[11] H. Lilholt and J. Lawther, *Comprehensive Composite Materials,* **1**, 303-325 (2000).
[12] R. Joffe, J. Andersons, and L. Wallström, *Composites Part A: Applied Science and Manufacturing,* **34**, 603-612 (2003).
[13] J. Andersons, E. Spārniņš, R. Joffe, and L. Wallström, *Composites Sci. Technol.,* **65**, 693-702 (2005).
[14] J. Summerscales, N.P. Dissanayake, A.S. Virk, and W. Hall, *Composites Part A: Applied Science and Manufacturing,* **41**, 1329-1335 (2010).
[15] C. Woodings, A brief history of regenerated cellulosic fibers, Editor: C. Woodings, Regenerated cellulose fibers, *Woodhead Publishing Limited*, **1**, 1-21 (2001).
[16] A. Kelly, and C.H. Zweben, *Comprehensive Composite Materials,* Elsevier (2000).
[17] M.G. Bader, *Comprehensive Composite Materials. Amsterdam: Elsevier,* **6** (2000).

[18] P. Wambua, J. Ivens, and I. Verpoest, *Composites Sci. Technol.,* **63**, 1259-1264 (2003).
[19] S. Chapple and R. Anandjiwala, *J. Thermoplast. Compos. Mater.,* **23**, 871-893 (2010).
[20] J. Biagiotti, D. Puglia, and J.M. Kenny, *Journal of Natural Fibers,* **1**, 37-68 (2004).
[21] E. Sparnins, Mechanical properties of flax fibers and their composites, *Luleå tekniska universitet* (2009).
[22] A. Bismarck, I. Aranberri-Askargorta, J. Springer, T. Lampke, B. Wielage, A. Stamboulis, I. Shenderovich, and H. Limbach, *Polymer Composites,* **23**, 872-894 (2002).
[23] C. Hill, and H. Abdul, *J Appl Polym Sci,* **77**, 1322-1330 (2000).
[24] K. Oksman, *Applied Composite Materials,* **7**, 403-414 (2000).
[25] T. Lampke, Beitrag zur Charakterisierung naturfaserverstärkter Verbundwerkstoffe mit hochpolymerer Matrix, *Chemnitz University of Technology* (2001).
[26] S. Garkhail, R. Heijenrath, and T. Peijs, *Applied Composite Materials,* **7**, 351-372 (2000).
[27] M. Van den Oever, H. Bos, and K. Molenveld, *Die Angewandte Makromolekulare Chemie*, **272**, 71-76 (1999).
[28] J. Gassan, and A. Bledzki, *Applied Composite Materials,* **7**, 373-385 (2000).
[29] M. Van den Oever, H. Bos, and M. Van Kemenade, *Applied Composite Materials,* **7**, 387-402 (2000).
[30] M. Belgacem, P. Bataille, and S. Sapieha, *J Appl Polym Sci,* **53**, 379-385 (1994).
[31] J. d'Almeida, *Polym. Plast. Technol. Eng.,* **40**, 205-215 (2001).
[32] R.R. Franck, Overview, Editor: R.R. Franck, Bast and other plant fibres, *Woodhead Publishing Limited,* **1**, 1-23 (2005).
[33] J.W.S. Hearle, Physical structure and fibre properties, Editor: C. Woodings, Regenerated cellulose fibers, *Woodhead Publishing Limited*, **8**, 37-61 (2001).
[34] M.G. Northolt, H. Boerstoel, H. Maatman, R. Huisman, J. Veurink, and H. Elzerman, *Polymer,* **42**, 8249-8264 (2001).
[35] J. Biagiotti, D. Puglia, and J.M. Kenny, *Journal of Natural Fibers,* **1**, 37-68 (2004).
[36] M. John, R. Anandjiwala, P. Wambua, S. Chapple, T. Klems, M. Doecker, M. Goulain, and L. Erasmus, *2nd SAIAS symposium* (2008).
[37] J. Giancaspro, C. Papakonstantinou, and P. Balaguru, *Compos. Sci. Technol.,* **68**, 1895-1902 (2008).
[38] R.S. Coutts, *Cement and Concrete Composites,* **27**, 518-526 (2005).
[39] D. Bloyer, R. Ritchie, and K.V. Rao, *Metallurgical and Materials Transactions A,* **30**, 633-642 (1999).
[40] J. Gassan, *Compos Part A: Appl Sci Manuf,* **33**, 369-374 (2002).
[41] M. Misra, S.S. Ahankari, and A.K. Mohanty, Creep and fatigue of natural fibre composites, Editor: N.E. Zafeiropoulos, Interface engineering of natural fibre composites for maximum performance, *Woodhead publishing limited,* **11**, 289-340 (2011).

[42] R. Guedes, *Composites Sci. Technol.,* **67**, 2574-2583 (2007).
[43] L. Pupure, J. Varna, R. Joffe, and A. Pupurs, *Mechanics of Composite Materials,* **49**, 139-154 (2013).
[44] N. Doroudgarian, M. Anglada, and R. Joffe, Fatigue on regenerated cellulose fiber bundles and composites, *Submitted to Industrial Crops and Products* (2016).
[45] L. Köhler, and H. Spatz, *Planta,* **215**, 33-40 (2002).
[46] W.D. Callister, and D.G. Rethwisch, Materials science and engineering: an introduction, *Wiley New York* (2007).
[47] S. Mishra, and M. Sain, Long-term performance of natural-fiber composites, Editor: K.L. Pickering, Properties and performance of natural-fibre composites, *Woodhead Publishing Limited,* **14**, 460-502 (2008).
[48] P. Mannberg, B. Nyström, and R. Joffe, *J. Mater. Sci.,* **49**, 3687-3693 (2014).
[49] P. Mannberg, B. Nyström, L. Wallström, and R. Joffe, *J. Mater. Sci.,* **49**, 5265-5270 (2014).
[50] L. Pupure, J. Varna, and R. Joffe, *Advanced Composites Letters,* **24**, 125-129 (2015).
[51] L. Pupure, J. Varna, and R. Joffe, Micromechanics based modeling of time-dependent longitudinal response of UD composites, *Submitted to Composite Science and Technology* (2015).
[52] L. Pupure, Non-linear model applied on composites exhibiting inelastic behavior: development and validation, *Luleå tekniska universitet* (2015).
[53] V.A. Passipoularidis, and P. Brøndsted, Fatigue evaluation algorithms: Review, *Risø National Laboratory of Sustainable Energy,* **1740**, (2009).
[54] J. Degrieck, and W. Van Paepegem, *Appl. Mech. Rev.,* **54**, 279-299 (2001).
[55] B. Harris, A historical review of the fatigue behaviour of fibre-reinforced plastics, Editor: B. Harris, Fatigue in composites, Science and technology of the fatigue response of fibre-reinforced plastics, *Woodhead Publishing Limited,* **1**, 3-35 (2003).
[56] E. Gamstedt, and R. Talreja, *J. Mater. Sci.,* **34**, 2535-2546 (1999).
[57] E.K. Gamstedt, L.A. Berglund, and T. Peijs, *Composites Sci. Technol.,* **59**, 759-768 (1999).
[58] R. Talreja, Fatigue of composite materials: damage mechanisms and fatigue-life diagrams, *Proc. R. Soc. Lond. A.*, **378**, 461-475 (1981).
[59] R. Talreja, *ZAMM-Journal of Applied Mathematics and Mechanics/Zeitschrift für Angewandte Mathematik und Mechanik,* **95**, 1058-1066 (2015).
[60] R.D. Jamison, K. Schulte, K.L. Reifsnider, and W.W. Stinchcomb, "Characterization and analysis of damage mechanisms in tension-tension fatigue of graphite/epoxy laminates" Effects of defects in composite materials, *ASTM International*, (1984).
[61] T. Yuanjian, and D. Isaac, *Composites Sci. Technol.,* **67**, 3300-3307 (2007).
[62] A. Hajlane, H. Kaddami, R. Joffe, and L. Wallström, *Cellulose,* **20**, 2765-2778 (2013).

[63] S. Liang, P.B. Gning, and L. Guillaumat, *Composites Sci. Technol.,* **72**, 535-543 (2012).
[64] H. Spatz, L. Köhler, and K.J. Niklas, *J. Exp. Biol.,* **202**, 3269-3272 (1999).
[65] C. Baley, *Composites Part A: Applied Science and Manufacturing,* **33**, 939-948 (2002).
[66] F. Bensadoun, K.A.M. Vallons, L.B. Lessard, I. Verpoest, and A.W. Van Vuure, *Composites Part A: Applied Science and Manufacturing,* **82**, 253-266 (2016).
[67] A. Belaadi, A. Bezazi, M. Bourchak, and F. Scarpa, *Mater Des,* **46**, 76-83 (2013).
[68] A.N. Towo, and M.P. Ansell, *Composites Sci. Technol.,* **68**, 915-924 (2008).
[69] E. Correa, V. Mantič, and F. París, *Eng. Fract. Mech.,* **75**, 4085-4103 (2008).
[70] E. Gamstedt, and B. Sjögren, *Composites Sci. Technol.,* **59**, 167-178 (1999).
[71] H. Katogi, Y. Shimamura, K. Tohgo, and T. Fujii, *Advanced Composite Materials,* **21**, 1-10 (2012).
[72] W.Y. Hamad, *J. Mater. Sci. Lett.,* **17**, 433-436 (1998).
[73] S. Liang, P. Gning, and L. Guillaumat, *Int. J. Fatigue,* **63**, 36-45 (2014).
[74] D.U. Shah, P.J. Schubel, M.J. Clifford, and P. Licence, *Compos. Sci. Technol.,* **74**, 139-149 (2013).
[75] A.N. Towo, and M.P. Ansell, *Composites Sci. Technol.,* **68**, 925-932 (2008).
[76] F. Bensadoun, J. Baets, A.W. Van Vuure, and I. Verpoest, *Eur. Conf. Composit. Mater., ECCM* (2014).
[77] F.d.A. Silva, N. Chawla, and R.D. de Toledo Filho, *Materials Science and Engineering: A,* **516**, 90-95 (2009).
[78] Y. Ueki, H. Lilholt, and B. Madsen, Fatigue behaviour of uni-directional flax fibre/epoxy composites, *20th International Conference on Composite Materials* (2015).
[79] I. El Sawi, Z. Fawaz, R. Zitoune, and H. Bougherara, *J. Mater. Sci.,* **49**, 2338-2346 (2014).
[80] C.L. Hacker and M.P. Ansell, *J. Mater. Sci.,* **36**, 609-621 (2001).

Paper D

Fatigue on regenerated cellulose fiber bundles and composites

Newsha Doroudgarian[1], Marc Anglada[2], Roberts Joffe[1,3]

[1]Composite Centre Sweden, Luleå University of Technology, S-97187 Luleå, SWEDEN
[2]CIEFMA, Technical University of Catalonia, Avda. Diagonal 647, 08028 Barcelona, SPAIN
[3]Group of Materials Science, Swerea SICOMP, S-94126 Piteå, SWEDEN

Manuscript submitted to:
INDUSTRIAL CROPS AND PRODUCTS

Fatigue on regenerated cellulose fiber bundles and composites

Newsha Doroudgarian[1], Marc Anglada[2], Roberts Joffe[1,3]

[1]Composite Centre Sweden, Luleå University of Technology, S-97187 Luleå, SWEDEN
[2]CIEFMA, Technical University of Catalonia, Avda. Diagonal 647, 08028 Barcelona, SPAIN
[3]Group of Materials Science, Swerea SICOMP, S-94126 Piteå, SWEDEN

Abstract. This work was aimed at developing natural fiber composites for long term structural applications. Regenerated (manmade) cellulose fibers (RCF) and their composites have been studied under fatigue loading conditions. Regenerated cellulose fibers exhibited highly nonlinear behavior which also strongly influenced the performance of their composites. Therefore, the main focus in this study was directed towards failure mechanisms and evolution of mechanical properties of these materials under fatigue, rather than establishing lifetime (S-N) diagrams. Fatigue studies on RCF bundles indicated stiffening of the material at large numbers of cycles. This behavior was mirrored in the composites reinforced by RCF. The results were confirmed by extensive studies on the strain evolution during fatigue as well as by the strain recovery after fatigue.

Introduction

The environmental concerns due to the enormous use of petroleum based plastics and their composites in recent decades have attracted the focus of research on the use of natural fiber reinforced polymers. This study is towards the development of structural bio-based composites. In previous studies, it was shown that properties of these materials were rather promising [1-3]. These properties are however concerning the short term performance (quasi-static) of materials but the failure of structures usually (or most often) occurs in fatigue [4,5] and that is why this study is focused on the performance of natural fiber composites under fatigue. The global aim was to understand how these materials behaved and to identify the most critical issues under long term loading. The fatigue behavior and mechanisms causing the failure in bio-based composites must be identified. In general, fatigue properties in polymer composites are their weakness when it comes to the structural applications and long term performance [6,7]. There are a limited number of studies on fatigue in natural fiber reinforced polymers [8-11]. Usually, the investigation is done with respect to the lifetime diagrams (S-N curves) [12-15] and the developing failure mechanisms are not well understood.

Regenerated cellulose fiber (RCF) reinforced composites among other types of natural composites, are in particular likely to exhibit different fatigue behavior and failure mechanisms, compared to the conventional composites [6,11,16,17]. Normally, polymer composites consist of brittle fibers reinforcing a more ductile matrix, for this case failure mechanisms are fairly well studied and recognized (see Figure 1). Since the fibers are more brittle they fail first and then either the fibers are debonded along theirs lengths or cracks are propagating in the matrix, depending on the fiber matrix interface strength. In both cases these fiber cracks are causing an overload on the other neighboring fibers. Ultimately, the fiber breaks coalesce, causing the failure of specimen/structure [18,19]. However, RCF exhibit highly nonlinear behavior with very high strain at failure (≈10%), in comparison with the more brittle polymers that are typically used in composites, as seen in the previous studies [20]. Moreover, composites containing these constituents also exhibit nonlinearity with a strain at failure higher than their pristine matrix [21].This is an uncommon phenomenon for polymer matrix composites where the matrix is usually more ductile than the fibers. This implies that the mechanisms governing crack development in these composites differ from the conventional polymer composites, due to the high strain at failure of RCF. Thus, it is logical to assume that RCF based composites behave similarly to the brittle ceramic matrix reinforced with ductile fibers [22-26]. Accordingly, an alternative damage sequence is proposed where the first failure event in these composites is expected to be the matrix cracking, see Figure 2. However, the direct experimental evidence is not presented in the current paper to confirm this hypothesis and the work is still in progress.

This work presents preliminary findings on fatigue in RCF based composites and it is aimed at identification of failure mechanisms and their sequence in material with complex nonlinear behavior exhibiting significant viscoelasticity and viscoplasticity [27].

Materials and manufacturing

The fibers used as reinforcement were RCF produced by a special variant of viscose process (Cordenka 700 Super 3) at Cordenka GmbH & Co. KG. The choice of the resin was Envirez, a thermoset bio-based resin with 12 wt% bio-content. Envirez G8600 INF-60 is unsaturated polyester based on soybean oil from Ashland Inc. Neat resin plates were produced and characterized in the previous study [20]. RCF were used in forms of no twist rovings as well as non-crimp fabrics (NCF), produced by Engtex (custom made for Interreg IVA Nord ANACOMPO project). The unidirectional (UD) stitched NCF had an area weight of 182 gsm. In order to assemble fabrics, the fiber bundles were slightly twisted. Mechanical properties of the resin and nontwisted fiber bundles are listed in Table 1.

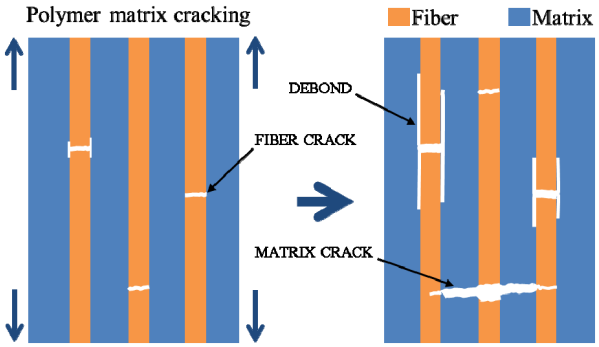

Figure 1. Typical crack development in polymer composites, fiber failure, debonding at poor interfaces, or fiber bridging at strong interfaces, leading to composite failure [18].

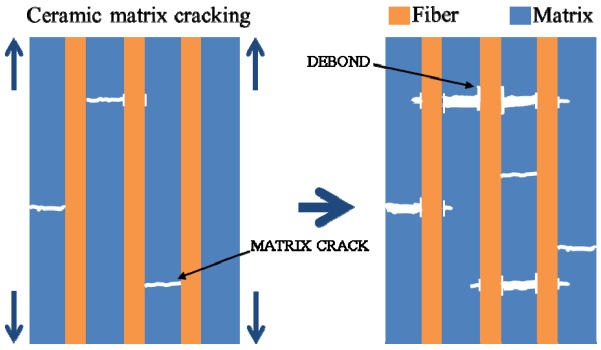

Figure 2. Matrix cracking expected in RCF reinforced composites by analogy to ceramic matrix composites.

Table 1. Mechanical properties of composites constituents [20].

Material	E, GPa	σ_U, MPa	ε_U, %	Density, g/cm^3
Envirez	3.4	39.4	1.20	1.2
Cordenka	22.6±0.9	654.4±3.7	9.25±0.54	1.5

UD laminates were manufactured by the use of both types of reinforcement. Fiber roving was wound on steel plates with dimensions of 26 cm x 26 cm, using a filament winding machine (Waltritsch & Wachter Sondermachinen). RCF rovings were wound into 6 layers and fabrics stacked into 8 layers in order to form UD laminates with approximately the same thickness (≈1.6 mm). Afterwards, heated resin at 50°C was introduced through the preformed reinforcement, using vacuum infusion. The vacuum

infusion setup consisted of a stiff bottom and a flexible top (a vacuum bag of polyamide film). The composite plates with filament wound (FW) rovings and stacked NCF layers (plate size 35 cm x 45 cm) were cured at 80°C for 7 hours. The obtained fiber volume fraction in FW and NCF composites were measured as 54% and 21%, respectively. Even though, the overall fiber volume fraction in NCF composites was somewhat low, it was as high as 59% inside the individual bundles. This was because fabric was rather loose with large distances in between the bundles (see Figure 3). It should also be mentioned that this fabric contained large amounts of stitches, up to 13% by volume. However, the stitches were placed transversally to the load direction and hence they had no major effect on the longitudinal E-modulus. Optical microscopy (OM) images of cross section in FW and NCF composites are presented in Figure 4.

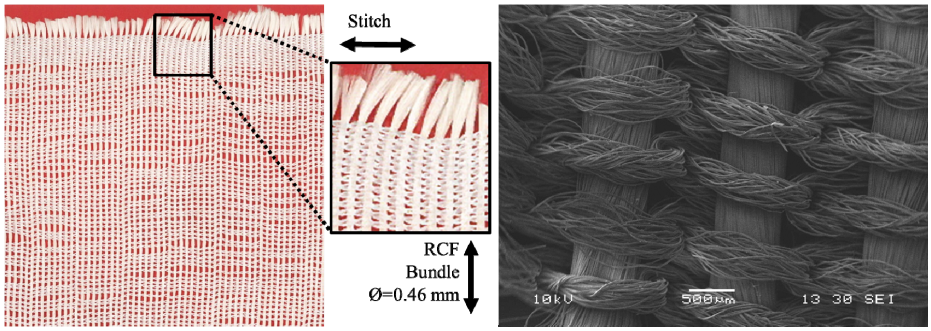

Figure 3. RCF bundles stitched together in NCF.

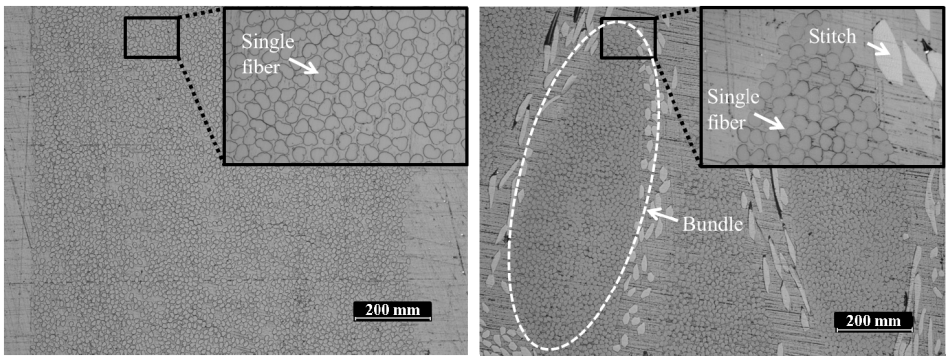

Figure 4. Optical microscopy images of FW (left) and NCF (right) composites cross section.

Experiments

RCF bundles as well as FW and NCF composites were subjected to three types of mechanical testing, 1) simple tensile test until failure; 2) quasi-static tensile test, loading-

unloading sequence with increasing maximum strain level in each consecutive step; 3) tension–tension fatigue. All tests were performed at ambient conditions in the lab.

RCF bundles. Each end of the bundle was fitted with wooden tabs using a two component epoxy adhesive Araldit 2011. The distance between tabs (gauge length) was chosen as 50 mm for loading–unloading and 100 mm for simple tension and fatigue tests, respectively. Strain in bundles was calculated, translating the crosshead's displacement and accounting for the machine's compliance, similarly described in the standard for single fiber tensile test (ASTM C1557-03). Fiber bundle tensile tests were performed on an Instron 4411 electro-mechanical material tester in a displacement controlled mode with 10%/min loading rate. The machine was equipped with mechanical grips and 500N load cell. Similarly, loading–unloading was carried out at 10%/min loading rate with stepwise increasing load levels. The, applied load at every step was 5N higher than in the previous loading and the test was carried on until failure of the specimen. Fatigue testing was done in a load controlled mode on an Instron E3000 equipped with pneumatic grips and load cell of 250 N. Tension–tension fatigue with 0.1 R ratio ($R=\sigma_{min}/\sigma_{max}$) and 1 Hz frequency was carried out. Fatigue stress level (σ_{max}) was set at 30% and 40% of the material's tensile strength (σ_U). Tests were stopped after 250k and 500k cycles. The fatigue experimental matrix is summarized in Table 2. It should be noted that the frequency values for fatigue loading were strictly limited, due to practical considerations and the nature of the material. The values were chosen in a way that the materials stay in the linear elastic region during testing. Therefore, the stress levels were fairly low since they were selected within the linear elastic as well as the elastic–plastic regions. The initial (elastic) and nonlinear regions can be easily distinguished on the graphs of static loading, see Figure 5. In order to evaluate the stiffness degradation, there have been quasi-static loading ramps (loading to certain stress level and unloading) performed in between fatigue cycles. The applied strain rate in these ramps was 2%/min and the measurements were performed at first, last, and cycles with 10 orders of magnitude (10, 100, 1000, etc). The ramp was introduced by Wavematrix, the Instron's software, as shown in Figure 6. Stiffness was measured on both loading and unloading parts of the ramp. The measurement interval was chosen as 60–100 MPa for RCF bundles so that it approximately corresponded to the interval in static testing, 0.3–0.7%. The interval was within the linear regions of stress–strain curves presented in Figure 7. After fatigue test was stopped samples were left in the "recovery mode" for at least 2 hours during which the load was kept constant at a very low value (almost zero) and strains were monitored. At least one sample from each batch was in the recovery mode for a longer time to verify the time for a complete recovery.

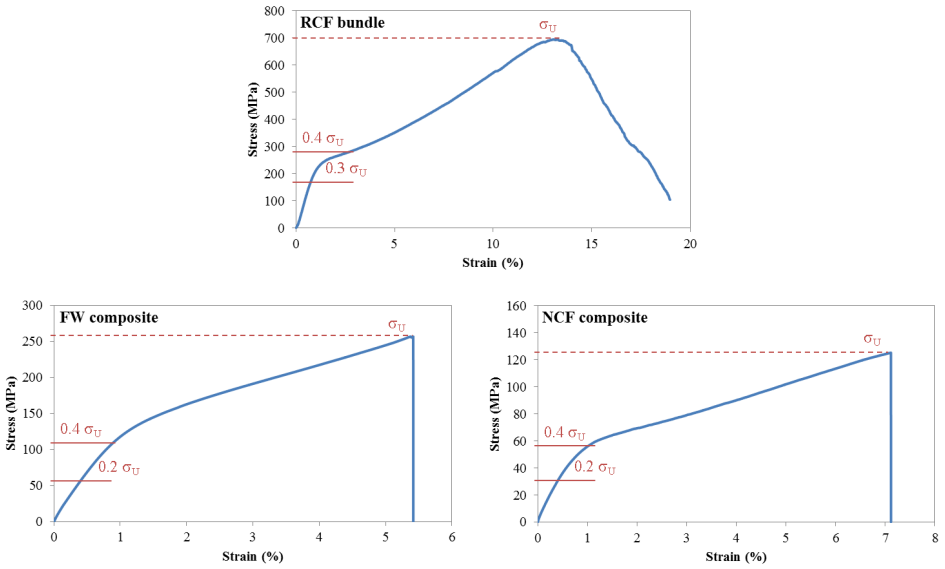

Figure 5. Typical stress-strain curves of RCF bundle, FW and NCF composites.

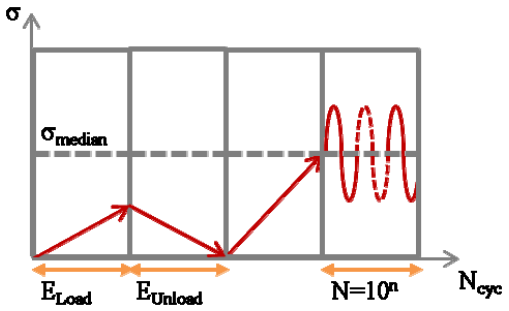

Figure 6. Fatigue test cycle.

Table 2. Fatigue experimental matrix (number of specimens in parentheses.

Material	Max stress, $\%\sigma_U$	N_{cyc}, 10^3x	Recovery, min	Total # of samples
RCF	30 (3) & 40 (2)	250 (4) & 500 (1)	120-1080	5
FW	20 (3) & 40 (3)	100 (3) & 1000 (3)	120-1560	6
NCF	20 (2) & 40 (3)	100 (2) & 1000 (3)	120-720	5

Composites. Composite plates were cut into rectangular specimens and their edges were ground by sandpapers up to 800 grit, to obtain the required geometry and to

eliminate the defects induced by cutting. The approximate thickness and width of specimens were 1.7 and 14 mm, respectively, with length of at least 180 mm. Static tensile tests were performed in a displacement controlled mode at 2%/min on an Instron 3366 equipped with 10 kN load cell and pneumatic grips. The complete procedure for tensile test can be found in the previous study on the same composites [21]. Composites were also subjected to quasi-static loading-unloading tests. Cycles were controlled by stepwise increasing displacement levels at 2%/min loading rate. Applied displacement was increased initially by steps of 0.2% until 1% was reached, then 0.5% until 4%, and finally by 1% until failure of the material. Fatigue testing was done in a load controlled mode on an Instron E10000 equipped with pneumatic grips and load cell of 10 kN. Tension-tension fatigue with R=0.1 and 5 Hz frequency was carried out. Fatigue stress level (σ_{max}) was set at 20% and 40% of the material's tensile strength. Tests were stopped after 100k and 1M cycles. Standard Instron extensometer was used to measure longitudinal strain. See the fatigue experimental matrix in Table 2. As for RCF bundles, the frequency values for fatigue loading of composites were chosen in the linear elastic region during testing. The stress levels were only selected within the linear elastic region, see Figure 5. Stiffness degradation was evaluated in the same manner as for RCF bundles. The measurement intervals were 7-25 MPa, and 3-13 MPa for FW composites and NCF composites, respectively, as shown in Figure 7. The intervals were approximately corresponding to the interval in static testing, 0.05-0.2%. Strain recovery was also monitored in the same way as for bundles.

Results and discussions

STIFFNESS EVOLUTION

Figure 8 shows the change of stiffness during quasi-static loading-unloading test on FW and NCF composites. As seen from those graphs, the stiffness of the composite changed only marginally, even after applying about 7% strain, which was far higher than the resin's strain of failure (1.2%). Moreover, the increase of stiffness with applied strain was observed in some cases. This was observed previously for other types of matrices and has been attributed to the nonlinear behavior of the reinforcement (viscoelastic and viscoplastic phenomena) as well as to the changes of microstructure of RCF due to the applied strain [28]. The quasi-static tensile tests confirm the previous statement that the behavior of these materials are determined by properties of reinforcement and that this behavior may be different from what normally expected from polymer composites (see Figure 2). On the other hand, due to the lack of stiffness reduction, it can be assumed that there is no significant damage developed in the composites or this damage is on a very small scale and cannot be detected by conventional technics (extensive optical microscopy did not reveal any fiber or matrix

cracks). Therefore, the mechanism of failure proposed in Figure 2 at this stage remains to be a working hypothesis which still has to be verified.

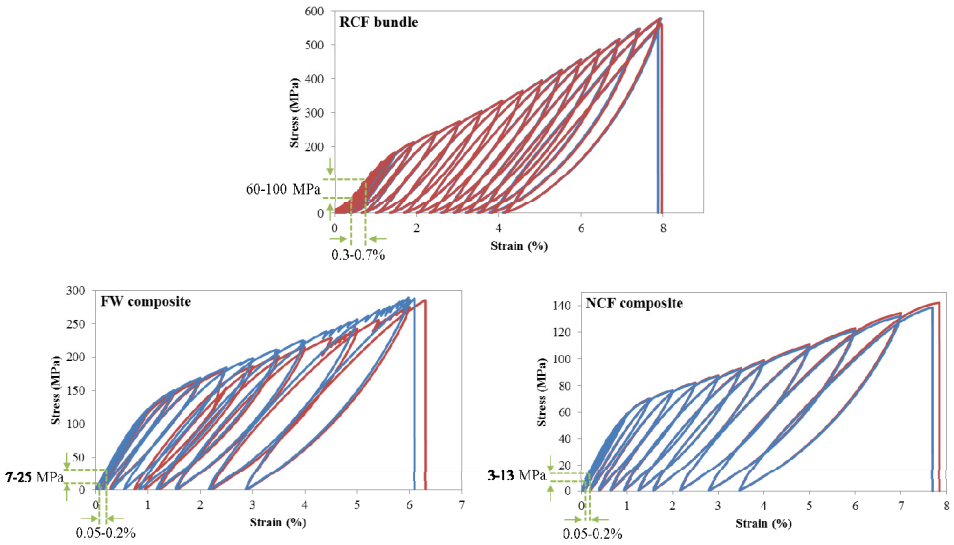

Figure 7. Loading-unloading cycles and intervals chosen for modulus measurements for RCF, FW and NCF.

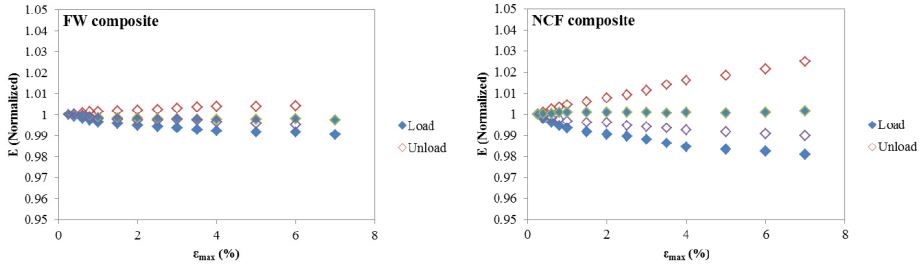

Figure 8. Changes of normalized stiffness values under loading-unloading test.

Stiffness change in RCF bundles has been also investigated under loading-unloading by Hajlane et al [28]. Moreover, the initial stiffness and the stiffness after 100k number of cycles for RCF bundles, FW and NCF composites are summarized in Tables 3,4 and 5, respectively. Fatigue results demonstrated a good repeatability. There was an increasing trend in modulus of bundles by the number of cycles. However, at large numbers of cycles there seemed to be a drop in stiffness. In both NCF and FW samples at high stress levels the stiffness seemed to grow when the number of cycles went over 100'000. Mechanical properties of NCF composites were inferior to FW due to a

lower volume fraction of fibers. Normalized values of stiffness over number of cycles are presented in Figure 9.

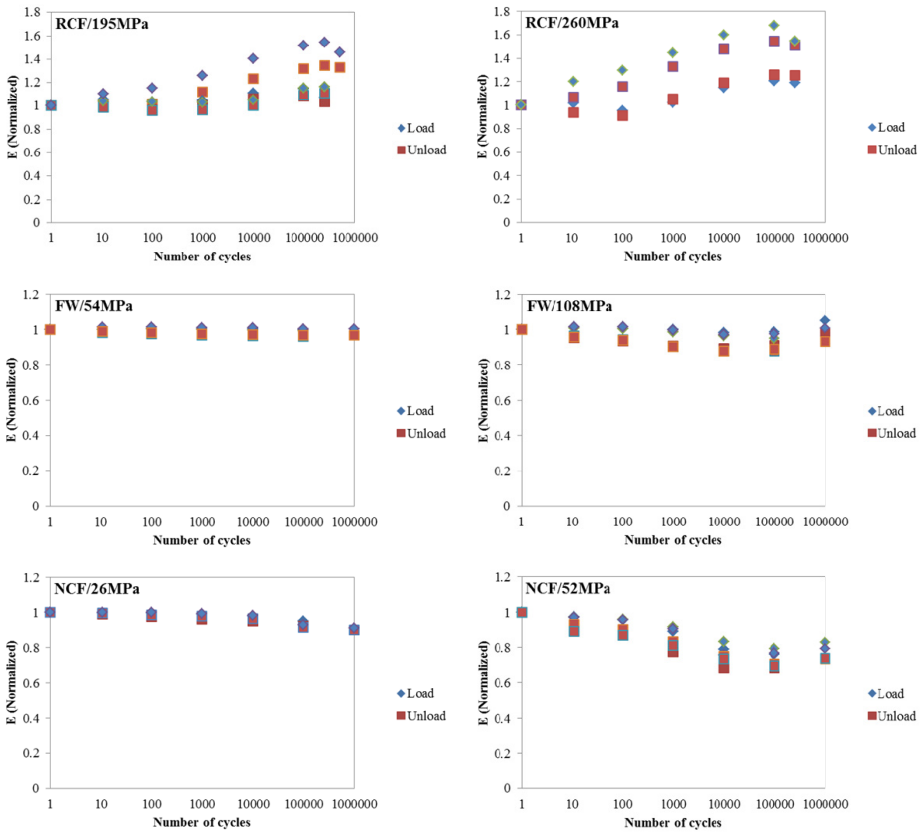

Figure 9. Stiffness degradation in RCF, FW and NCF, at lower (left) and higher (right) stress level.

The increasing trend in RCF stiffness values happened after about 10k cycles. However, the increasing trend in composites was only seen at high fatigue stress levels ($0.4\sigma_U$) and starting at higher number of cycles, namely about 100k. By a simple calculation, rule of mixture, it can be shown that the stress experienced in bundle specimens is much higher than the stress that bundles hold within the composites. A rough estimation for the stress held by bundles in FW and NCF composites results in $\sigma f_{FW} \approx 2\sigma_{FW}$-34 MPa and $\sigma f_{NCF} \approx 5\sigma_{NCF}$-148 MPa, respectively. Viscoelasticity and viscoplasticity are time-dependent behaviors as well as stress-dependent [27]. This means that at higher stress levels higher strain is developed, which would define the nonlinear behavior in composites. Therefore, it seems that elevating the stress level in composites can result in similar increasing trend of stiffness in composites as well.

Table 3. Stiffness degradation in RCF bundles. E0 and E100k represent the initial stiffness and the stiffness after $100x10^3$ cycles, respectively (L for loading and U for unloading ramps).

σ_{max}	Sample	E0-L, GPa	E0-U, GPa	E100k-L, GPa	E100k-U, GPa
195MPa	RCF10-4	22.4	25.8	25.7	27.9
	RCF10-5	23.7	26.3	27.3	28.8
	RCF10-7	21.0	25.2	31.8	33.3
	Ave±StDev	22.4 ± 1.4	25.7 ± 0.5	28.3 ± 3.2	30.0 ± 2.9
260MPa	RCF10-3	21.0	20.2	25.4	25.4
	RCF10-6	17.4	18.8	29.3	29.1

Table 4. Stiffness degradation in FW composites. E0 and E100k represent the initial stiffness and the stiffness after $100x10^3$ cycles, respectively (L for loading and U for unloading ramps).

σ_{max}	Sample	E0-L, GPa	E0-U, GPa	E100k-L, GPa	E100k-U, GPa
54MPa	FW9-4	14.3	14.6	14.4	14.2
	FW9-5	15.0	15.4	14.9	14.8
	FW9-9	15.4	15.8	15.5	15.3
	Ave±StDev	14.9 ± 0.5	15.2 ± 0.6	14.9 ± 0.5	14.7 ± 0.6
108MPa	FW9-6	15.1	15.5	14.9	14.1
	FW9-7	14.4	14.7	13.7	13.0
	FW9-8	14.9	15.3	14.5	13.7
	Ave±StDev	14.8 ± 0.4	15.2 ± 0.4	14.4 ± 0.6	13.6 ± 0.6

Table 5. Stiffness degradation in NCF composites. E0 and E100k represent the initial stiffness and the stiffness after $100x10^3$ cycles, respectively (L for loading and U for unloading ramps).

σ_{max}	Sample	E0-L, GPa	E0-U, GPa	E100k-L, GPa	E100k-U, GPa
26MPa	NCF4-3	7.8	7.8	7.4	7.2
	NCF4-4	6.4	6.4	5.9	5.9
52MPa	NCF4-2	6.9	7.0	5.3	4.8
	NCF4-5	7.3	7.3	5.8	5.1
	NCF4-6	7.3	7.3	5.6	5.2
	Ave±StDev	7.2 ± 0.2	7.2 ± 0.2	5.6 ± 0.3	5.0 ± 0.2

STRAIN EVOLUTION

The evolution of total strain, consisting of elastic, viscose and plastic strains, was monitored. Strain evolution in the material was measured from the collected strain data. The changes of strain amplitude $\Delta\varepsilon$ (ε_{max}-ε_{min}) were calculated for each sample during the fatigue (see Figure 10). The results for bundles and composites are summarized in Tables A-1 and A-2 in appendix A, respectively.

The trend of strain evolution over number of cycles per material and per stress level is presented in Figure 11. The following trends with respect to the evolution of strain amplitude were identified:

RCF bundles. $\Delta\varepsilon$ was decreasing during the test (by 13-33%, depending on the number of cycles and the stress level).

FW composites. No significant changes occurred. $\Delta\varepsilon$ was fairly stable during the test (changes are within 10% with no consistent trend).

NCF composites. $\Delta\varepsilon$ was increasing during the test (by 15-36%, depending on the number of cycles and the stress level).

The fact that the curves of ε_{max} and ε_{min} were converging together for RCF bundles, at large numbers of cycles, indicated the disappearance of plasticity (samples were somewhat conditioned by introduction of an irreversible strain). This might explain the increase of modulus values by the number of cycles. As if the plastic deformation was saturated and so, according the Hooke's law, the increase of stress directly resulted in the increase of stiffness. However, there was no increase in the modulus of composites. This might be explained by a lower stress experienced by bundles within the composites, compared with the standalone bundles. Furthermore, the stress level in fatigue appeared to have a significant effect on the trends in strain evolution, see Figure 11. It was confirmed by the values presented in Tables A-1 and A-2 that lower stress levels caused lower plasticity. Strain evolution of representative samples per each batch are also presented over time (Figure 12).

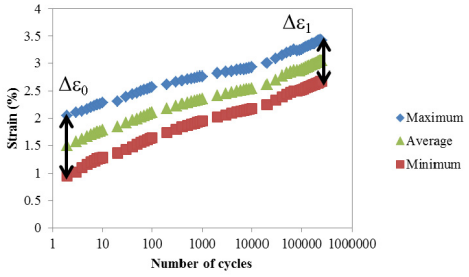

Figure 10. Calculating $\Delta\varepsilon$ (ε_{max}-ε_{min}) from the graph of strain evolution over Ncyc.

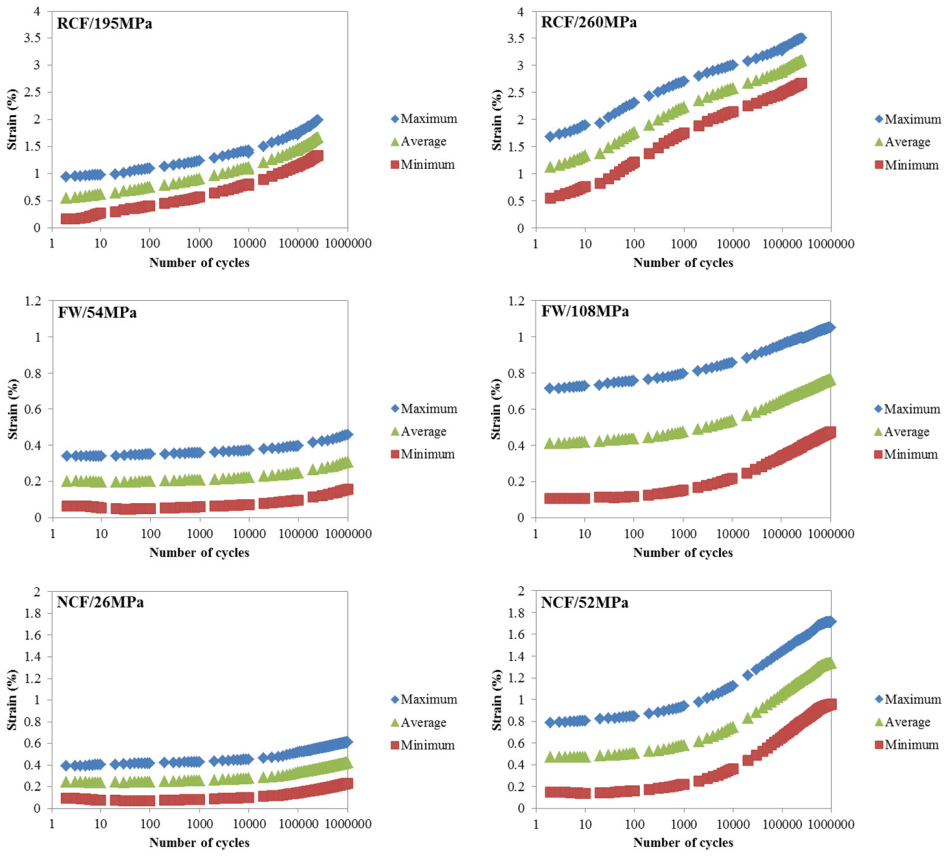

Figure 11. Strain evolution over Ncyc, for RCF, FW and NCF.

STRAIN RECOVERY

The strain was measured at the end of the experiment (ε_{EOE}), after 2 hours rest (ε_{2H}) and at the end of recovery time (ε_{REC}). Graphs of strain recovery over time are summarized in Figure 13. Tables A-3 and A-4 in appendix show the strain recovery for RCF bundles as well as in FW and NCF composites. The recovery time should be scaled up according to the time the specimen has been loaded. For instance, the recovery time of 2 hours for 100k cycles corresponds to 20 hours for 1M cycles. It is likely that the time of recovery even for 100k number of cycles is not enough. It is suggested to have a recovery time at least 5 times greater than loading duration [27]. In order to compare the recovery after different numbers of cycles, the time of recovery should be proportional to the time that specimen has gone under loading. However, the purpose of these tests were not to obtain a full recovery but to get a rough

estimation of residual strain's magnitude and an indication in what manner the strain recovery took place.

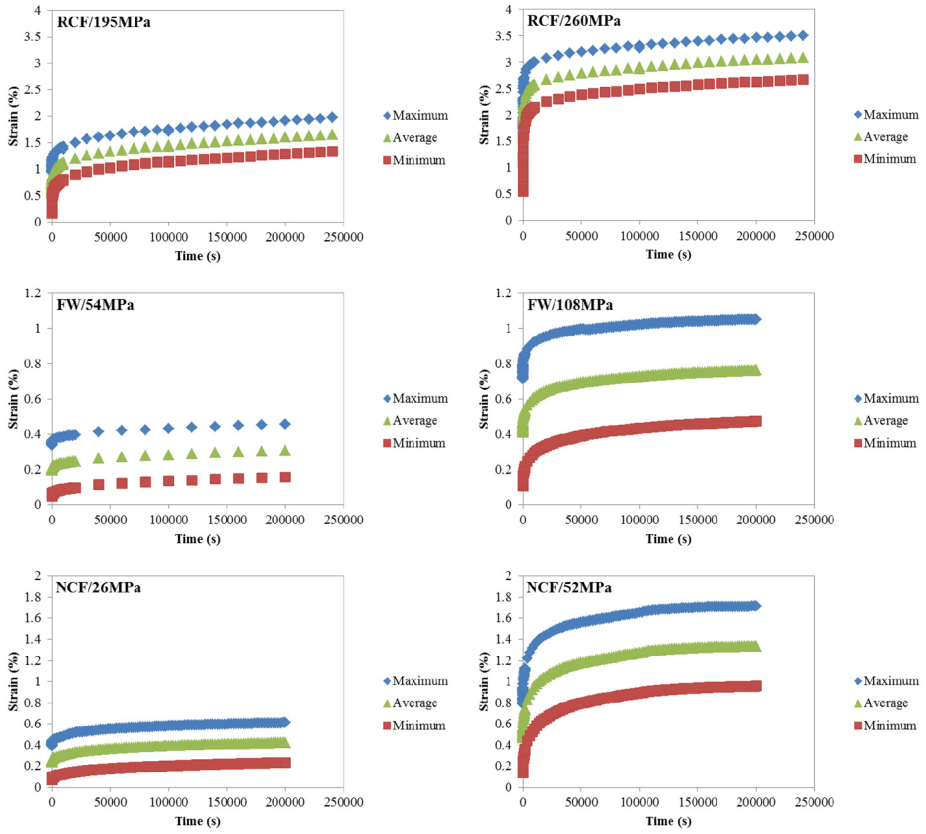

Figure 12. Strain evolution over cycle start time, for RCF, FW and NCF.

Conclusions

The composites based on the highly nonlinear fibers were studied, under quasi-static and fatigue loading. The fatigue experiments were performed in order to identify the failure mechanisms developing in these materials. Previous studies as well as results of quasi-static tests obtained in this work indicated that, due to the combination of a very ductile reinforcement with a much more brittle matrix, the failure sequence in these materials should differ from the typical behavior of polymer composites. However, the proposed hypothesis about failure mechanisms/sequence was not verified, probably due to the small scale of distributed damage throughout the whole volume of material that could not be detected by conventional methods. The analysis of the results was also hindered by nonlinearity of RCF which resulted in the presence of very significant

viscoelastic and viscoplastic strains in the fibers and in composite. Based on the results obtained from fatigue testing, the following statements could be made:

- The reinforcement governed the properties of composite which resulted in the nonlinear behavior of FW and NCF composites with very high strain at failure.
- RCF bundles exhibited stiffening under fatigue at large numbers of cycles, which was attributed to the fact that the effect of plasticity ceased with time under loading. This can be seen as a kind of conditioning of the material, typically used in creep tests, to eliminate plasticity and to obtain purely viscoelastic behavior.
- The latter behavior in RCF was mirrored in the composites reinforced with RCF.
- A strong similarity was detected between the behavior in fatigue and in creep tests on RCF composites. The fatigue stress level and the time under loading influenced the amount of strain accumulation in the materials as well as the trend how it accumulates. Even though, avdirect comparison between fatigue and creep was not possible in this case, the strain evolution during the fatigue was similar to that observed in creep experiments. This comparison/correlation might be used in the future for accelerated testing of these materials.
- There were substantial residual strains detected right after fatigue tests and some of that strain was recovered within a couple of hours. However, in order to achieve a complete strain recovery, much longer recovery times are required, especially for the higher numbers of fatigue cycles and higher stress levels.

The results of this study provided an interesting initial insight on the behavior of bio-based composites reinforced with highly nonlinear cellulosic fibers under fatigue loading. More comprehensive studies, including creep tests, SEM, microtomography on the composites as well as additional tests on the fibers (e.g. DSC, XRD), are needed to validate these results and to provide correlation between changes of internal structure of materials (fibers and composites) with their performance in fatigue.

Acknowledgements

The manufacturing of specimens done by Mostafa Ismail, student within the project course at Luleå University of Technology, is acknowledged. Mostafa Ismail did additional optical microscopy in order to identify the structure of composites and to measure their constituents' volume fraction. Moreover, the authors would like to acknowledge SWEREA Sicomp for providing the access to filament winding machine and ERASMUS MUNDUS DocMASE program for financing.

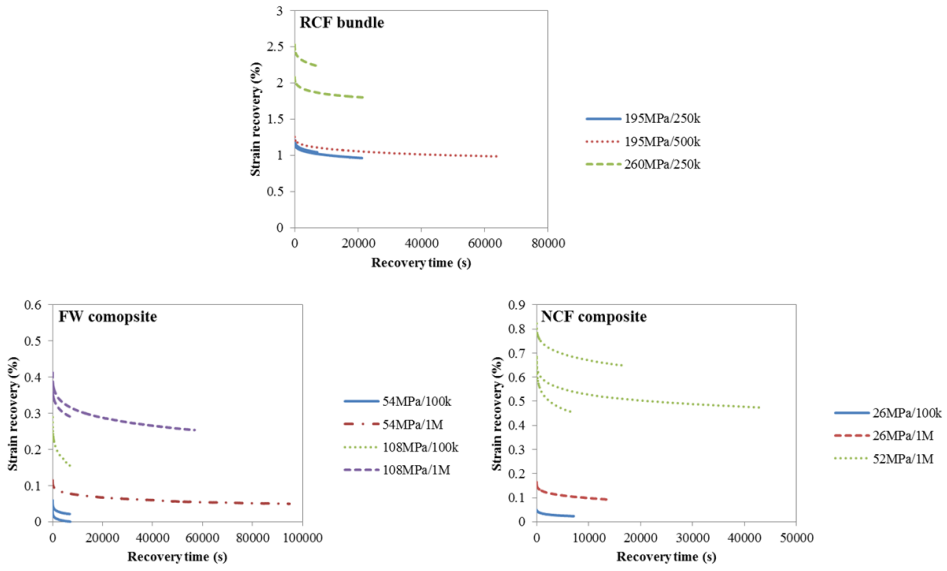

Figure 13. Strain recovery over time.

References

[1] P. Wambua, J. Ivens, and I. Verpoest, *Composites Sci. Technol.,* **63**, 1259-1264 (2003).

[2] J. Biagiotti, D. Puglia, and J.M. Kenny, *Journal of Natural Fibers,* **1**, 37-68 (2004).

[3] D. Puglia, J. Biagiotti, and J.M. Kenny, *Journal of Natural Fibers,* **1**, 23-65 (2004).

[4] A.P. Vassilopoulos, *Fatigue Life Predict. of Compos. and Compos. Struct.,* 1-44 (2010).

5. I. El Sawi, Z. Fawaz, R. Zitoune, and H. Bougherara, *J. Mater. Sci.,* **49**, 2338-2346 (2014).

[6] J. Gassan, *Compos Part A: Appl Sci Manuf,* **33**, 369-374 (2002).

[7] F. Bensadoun, J. Baets, A.W. Van Vuure, and I. Verpoest, *Eur. Conf. Composit. Mater. , ECCM* (2014).

[8] D.U. Shah, P.J. Schubel, M.J. Clifford, and P. Licence, *Composites Sci. Technol.,* **74**, 139-149 (2013).

[9] D.B. Dittenber and H.V.S. Gangarao, *Compos Part A: Appl Sci Manuf,* **43**, 1419-1429 (2012).

[10] T. Yuanjian and D.H. Isaac, *Composites Sci. Technol.,* **67**, 3300-3307 (2007).

[11] S. Liang, P.B. Gning, and L. Guillaumat, *Composites Sci. Technol.,* **72**, 535-543 (2012).

[12] C.L. Hacker and M.P. Ansell, *J. Mater. Sci.,* **36**, 609-621 (2001).

[13] A.N. Towo and M.P. Ansell, *Composites Sci. Technol.,* **68**, 915-924 (2008).

[14] A. Belaadi, A. Bezazi, M. Bourchak, and F. Scarpa, *Mater Des,* **46**, 76-83 (2013).

[15] S. Liang, P. Gning, and L. Guillaumat, *Int. J. Fatigue,* **63**, 36-45 (2014).
[16] S. Giancane, F.W. Panella, and V. Dattoma, *Int. J. Fatigue,* **32**, 46-53 (2010).
[17] F.d.A. Silva, N. Chawla, and R.D. de Toledo Filho, *Materials Science and Engineering: A,* **516**, 90-95 (2009).
[18] I.M. Daniel and A. Charewicz, *Eng. Fract. Mech.,* **25**, 793-808 (1986).
[19] E. Gamstedt and R. Talreja, *J. Mater. Sci.,* **34**, 2535-2546 (1999).
[20] L. Pupure, N. Doroudgarian, and R. Joffe, *Polymer Composites,* **35**, 1150-1159 (2014).
[21] N. Doroudgarian, L. Pupure, and R. Joffe, *Polymer Composites,* **36**, 1510-1519 (2015).
[22] D. Bloyer, R. Ritchie, and K.V. Rao, *Metallurgical and Materials Transactions A,* **30**, 633-642 (1999).
[23] D. Bloyer, R. Ritchie, and K.V. Rao, *Metallurgical and Materials Transactions A,* **29**, 2483-2496 (1998).
[24] K. Vallons, S.V. Lomov, and I. Verpoest, *Composites Part A: Applied Science and Manufacturing,* **40**, 251-259 (2009).
[25] V. Ramakrishnan, and N. Jayaraman, *Journal of Materials Science,* **28**, 5592-5602 (1993).
[26] H. Savastano Jr., S.F. Santos, M. Radonjic, and W.O. Soboyejo, *Cem. Concr. Compos.,* **31**, 232-243 (2009).
[27] L. Pupure, J. Varna, and R. Joffe, *J. Composite Mater.,* 0021998315579435 (2015).
[28] A. Hajlane, H. Kaddami, R. Joffe, and L. Wallström, *Cellulose*, **20**, 2765-2778 (2013).

Appendix A

Table A-1. Strain evolution at RCF bundles. Double results presented on same sample indicate intermediate data resulted from a single test.

Material	Ncyc	σ_{max}, MPa	$\Delta\varepsilon_0$	$\Delta\varepsilon_1$	%Difference
RCF10-3	250k	260	1.14	0.83	-27
RCF10-4	250k	195	0.77	0.65	-16
RCF10-5	250k	195	0.67	0.58	-13
RCF10-6	250k	260	1.10	0.74	-33
RCF10-7	250k	195	0.75	0.50	-33
RCF10-7	500k	195	0.75	0.51	-32

Table A-2. Strain evolution at FW and NCF composites. Double results presented on same sample indicate intermediate data resulted from a single test.

Material	Ncyc	σ_{max}, MPa	$\Delta\varepsilon_0$	$\Delta\varepsilon_1$	%Difference
FW9-4	100k	54	0.31	0.32	3
FW9-5	100k	54	0.27	0.27	0
FW9-6	100k	108	0.61	0.62	2
FW9-6	1M	108	0.61	0.57	-7
FW9-7	100k	108	0.59	0.65	10
FW9-8	100k	108	0.61	0.64	4
FW9-8	1M	108	0.61	0.61	0
FW9-9	100k	54	0.27	0.30	11
FW9-9	1M	54	0.27	0.29	7
NCF4-2	100k	52	0.64	0.87	36
NCF4-3	100k	26	0.26	0.30	15
NCF4-4	100k	26	0.30	0.37	24
NCF4-4	1M	26	0.30	0.37	23
NCF4-5	100k	52	0.63	0.79	25
NCF4-5	1M	52	0.63	0.75	19
NCF4-6	100k	52	0.64	0.79	23
NCF4-6	1M	52	0.64	0.76	19

Table A-3. Strain recovery of RCF bundles. t_{EOE} and t_{REC} correspond to ε_{EOE} and ε_{REC}, respectively.

Material	ε_{EOE}, %	ε_{2H}, %	ε_{REC}, %	t_{REC}, s	Ratio (t_{REC}/ t_{EOE})
RCF10-3	2.53	2.24	ε_{2H}	7200	0.03
RCF10-4	1.22	1.04	ε_{2H}	7200	0.03
RCF10-5	1.17	1.02	0.96	21589	0.09
RCF10-6	2.08	1.87	1.80	21600	0.09
RCF10-7	1.26	1.11	0.99	64800	0.13

Paper E

Interlaminar fracture toughness of composites with nonlinear cellulose reinforcement

Newsha Doroudgarian[1], Abdelghani Hajlane[1], Marc Anglada[2], Roberts Joffe[1,3]

[1]Composite Centre Sweden, Luleå University of Technology, S-97187 Luleå, SWEDEN
[2]CIEFMA, Technical University of Catalonia, Avda. Diagonal 647, 08028 Barcelona, SPAIN
[3]Group of Materials Science, Swerea SICOMP, S-94126 Piteå, SWEDEN

Manuscript submitted to:
COMPOSITES PART A

PAPER E

Interlaminar fracture toughness of composites with nonlinear cellulose reinforcement

Newsha Doroudgarian[1], Abdelghani Hajlane[1], Marc Anglada[2], Roberts Joffe[1,3]

[1]Composite Centre Sweden, Luleå University of Technology, S-97187 Luleå, SWEDEN
[2]CIEFMA, Technical University of Catalonia, Avda. Diagonal 647, 08028 Barcelona, SPAIN
[3]Group of Materials Science, Swerea SICOMP, S-94126 Piteå, SWEDEN

Abstract. This work is an initial study on the interlaminar properties of composites reinforced with regenerated cellulose fibers (RCF). The surface of RCF fabrics was chemically modified and the results were compared to non-treated samples. Double cantilevered beam (DCB) test was used to characterize fracture toughness, under static and fatigue loading. Regenerated cellulose fibers exhibit highly nonlinear behavior and strongly influence the performance of their composites. The obtained fracture toughness values were significantly higher compared to those of synthetic fiber reinforced composites. However, due to the high nonlinearity, a concrete conclusion was not easy to make on the effect of fiber treatment on the materials performance. Thus, scanning electron microscopy studies were carried out on fracture surfaces which confirmed the treatment effect, qualitatively, on the improvement of interfacial adhesion.

Introduction

In the designing of structural polymer composites, various modes of crack growth, intralaminar (transply) as well as interlaminar (delamination), are accounted for [1]. Typical failure modes in laminated composites are fiber matrix deboning, matrix crack and delamination. In order to achieve a good performance in composites, the initiation of damage and growth of delamination should be delayed and suppressed, as much as possible. To be able to predict the initiation and propagation of delamination in composite structures, the fracture toughness of the material should be measured. Fracture toughness, G_C, is a material property, representing the required energy to create new surfaces (further propagation of an existing crack). One of the most common methods to measure the critical energy release rate (or fracture toughness), G_C, is by using the double cantilevered beam (DCB) test. In the designing of advanced laminated composites, fatigue loads must be taken into consideration and the material's resistance to interlaminar fracture needs to be evaluated. Hence, a similar DCB test method is designed to determine G_C based on the number of fatigue cycles required for the onset of delamination growth [2,3,4,5]. The opening Mode I (tensile mode) is

practiced in the fracture toughness tests (static and fatigue). Therefore, G_{IC} is the corresponding term for the critical energy release rate.

However, DCB method is based on linear elastic fracture mechanics (LEFM) theory, whereas the composites of this study exhibit a highly nonlinear behavior [6]. Therefore, alternative methods based on nonlinear elastic (elastic-plastic) fracture mechanics, such as evaluation of J-integral, have been the subject of research studies [7,8,9,10]. Ilcewicz et al [1] have compared different approaches in mode I experiments and reported that the linear *G* approach, which did not account for the nonlinear material behavior, gave the highest fracture toughness values, contrary to the nonlinear *J*-integral approach, giving the lowest values. Therefore, values obtained in the current study may be somewhat overestimated and reflect the behavior attributed not only to the interfacial properties of composites but also to the viscoelastic and viscoplastic phenomena in the material.

Materials and manufacturing

The fibers used as reinforcement were regenerated cellulose fibers (RCF), produced by a special variant of viscose process (Cordenka 700 Super 3 [11]) by Cordenka GmbH & Co. KG. The resin was epoxy Araldite LY 556, by Huntsman International LLC. Fibers were assembled in form of non-crimp fabrics (NCF), more details can be found in the previous study [12]. Furthermore, the fabric was treated chemically, by coupling agents, in order to enhance the interface properties. Notations for composites were assigned according to the type of fabric they were made from, "Treated" and "Non-treated".

In order to perform interlaminar fracture toughness tests DCB specimens were produced. To do so, unidirectional (UD) composite laminates were manufactured, using treated as well as reference non-treated fabrics. The fabric was cut into rectangular pieces of 20 cm x 20 cm and 8 layers of it were stacked to obtain the UD laminate with a final thickness of approximately 3 mm. The manufacturing of DCB specimens was done following the guidelines of ASTM D5528 standard [3]. To introduce the initial crack in DCB samples, a separation Teflon film was placed in between the layers of fabric, in order for the pre-crack to be located in the UD laminate's midplane. The width of insert film was 30 mm (to produce a 30 mm long initial crack), with a thickness below 15 μm. Composite manufacturing was performed using vacuum infusion [12]. After curing, at 80°C for 8 hours, the composite laminates were demolded.

Experiments

CHEMICAL TREATMENT

The chemical treatment of NCF by Methacryloxypropyl trimethoxysilane (MPS) was performed in a reactor of 2 liters where 1.6 liter was filled by a solvent, consisting of 50/50 (vol%) mixture of ethanol and deionized water ($EtOH/H_2O$). The pH was adjusted to 7.0, using a 0.1M Nitric acid (HNO_3) aqueous solution and stirred until it got stabilized at 65°C. Thereafter, NCF pieces of 200 mm x 200 mm were wound on a holder and then placed into the solution and 4 grams of Cerium Ammonium Nitrate (CAN) initiator was dissolved in deionized water and introduced into the reaction. After stirring for 30 minutes, 4 ml of MPS was dropwise added, under an inert atmosphere of N_2. The reaction was stirred at 65°C for 5 hours, as previously described in details [13]. When the reaction time elapsed, the treated NFC was washed twice by ethanol and once by deionized water, to remove the unreacted products trapped in the fabric and finally dried at 50°C then stored in desiccators at 23°C.

MECHANICAL TESTING

Static and fatigue experiments were carried out, to measure the critical energy release rate of the composites in opening Mode I (G_{IC}). Initially, DCB specimens were cut according to the dimensions specified by the ASTM D5528-01 standard. However, due to the limited amount of available treated fabrics, specimen dimensions were downscaled to save material. To validate that the smaller specimen size did not affect the results, both the standard and downscaled specimens of reference composite were tested and the results were compared. It should be noted however, the deviation from the standard dimensions would not influence the conclusions of this study which were comparative in nature. Nevertheless, it was important to confirm the results obtained from these tests were valid, if compared with the data from literature. See the test specimen in Figure 1. The letter "S" at the end of the notations determines the specimens with dimensions according to the standard.

The dimensions of standard and downscaled specimens are listed in Table 1. The experimental matrix is presented in Table 2. The number of test specimens was limited, due to the restricted availability of material. Moreover, some of the samples did not produce reliable results and in other cases tests had to be interrupted due to premature failures of the specimen (e.g. the delamination of stiffener). Thus, the numbers presented in Table 2 indicate only the number of successful tests rather than the total number of tested specimens.

In order to avoid excessive bending of the DCB beams, stiffening tabs made out of woven glass fiber epoxy composites were glued on both sides of the specimens along the whole length. The stiffeners were chosen slightly longer than the composite beam, in order to provide a space to mount the loading hinges (see Figure 1 and Table 1).

Before testing, the delamination induced by the insert film prior to the crack tip was carefully opened by means of a sharp cutter, to enhance the control over crack propagation.

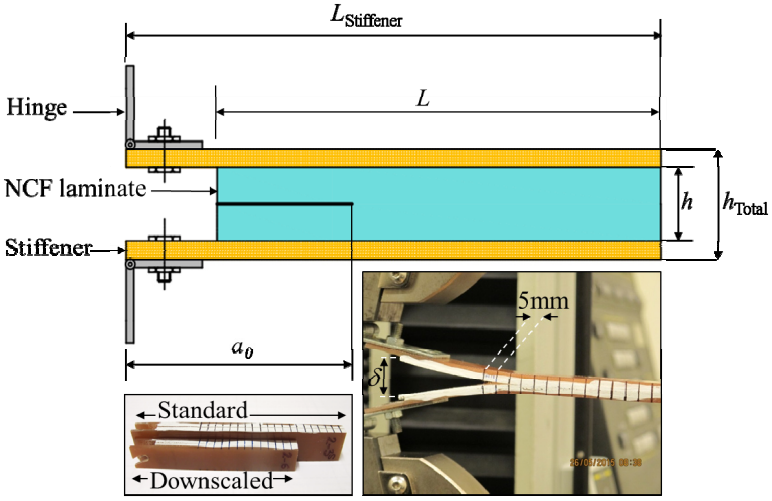

Figure 1. Schematic representation of sample (top), with comparison of standard and downscaled specimens (bottom left) as well as mounted DCB specimen (bottom right).

Table 1. DCB specimen dimensions.

Dimension[a], mm	L	$L_{Stiffener}$	a_0	b	h	h_{Total}
Standard	130	145	30	22	4	8
Downscaled	95	110	30	15	4	8-9

[a]Parameters are clarified in Figure 1.

Table 2. DCB experimental matrix. Number of test specimens is presented in parentheses.

Static			**Fatigue**	
Non-treated-S (2)	Non-treated (2)	Treated (2)	Non-treated (4)	Treated (4)

Edges of sample were grinded by 240 grid sandpapers for a better visibility and painted white to be able to clearly detect and trace the propagation of the crack tip along specimen. The static DCB tests were performed on an Instron 4411 mechanical testing machine in displacement controlled mode with crosshead separation speed of 2 mm/min. The machine was equipped with mechanical grips and 500 N load cell. Two

simple hinges were fastened to the specimen by bolts and nuts. The hinges were then clamped in the machine's grips, through which the load was applied to the sample, as seen in Figure 1.

All tests were performed at ambient conditions (≈25°C and 21-47%RH). Although the ambient humidity was varying significantly, it should be noted that the exposure time was limited to the test duration. Therefore, it was too short for any substantial moisture absorption (i.e. specimens were exposed to the environment for a couple of days, whereas the time for moisture saturation is approximately 3 months) [14]. Static tests were carried out in a stepwise manner. The specimen was loaded until a crack propagation of approximately 5 mm was achieved and then it was unloaded to the initial state (crack completely closed). These steps were repeated until the complete separation of the specimen. The load and the displacement were recorded during each loading-unloading cycle. The position of the crack tip was marked after each loading step. Thus, the crack extensions as well as the load-displacement curves were obtained in each step of the test. Displacement was the distance in between delamination planes which was the displacement corresponding to the movement of the machine grips while loading (see Figure 1) [15].

THEORY AND DATA REDUCTION

When the load is applied on the beams of DCB specimen through hinges the pre-crack opens first (a_0) and then once the critical load (energy) is reached it starts to propagate, from a_0 to a_i. The work to create new surfaces equals the energy released as a result of crack growth. It is assumed that linear elastic fracture mechanics applies and that all the energy is spent for crack propagation. The typical experimental curve obtained from DCB tests is load-displacement (P-δ). These results are then used to construct the plot of compliance-crack length (C-a) and the energy release rate is calculated using the compliance calibration method and plotted over the crack length (G_I-a) [3]. Schematic drawings of P-δ, C-a, and G_I-a graphs are presented in Figure 2. The graph of energy release rate vs. crack length sometimes represents three regions: 1) low values of G_I, corresponding to the initial crack length or small crack propagation (brittle behavior is observed due to a resin rich region in front of the crack tip); 2) plateau corresponding to a stable crack propagation (the values to obtain G_{IC}); 3) increase of GI for longer delamination if fiber bridging occurs. Examples of such data are presented for carbon fiber composites [16].

G_{IC} value, indicating the interfacial properties between the laminate plies, was calculated by Equation 1 [3]:

$$G_{IC} = \frac{P_{\max}^2}{2b}\frac{\partial C}{\partial a} \tag{1}$$

where b is the width of specimen and the best fitting curve to calculate $\frac{\partial C}{\partial a}$ was obtained by an exponential function:

$$C(a) = Ae^{Ba} \tag{2}$$

FATIGUE METHODOLOGY

Fatigue testing was done in a displacement controlled mode on an Instron E3000 equipped with pneumatic grips and 250 N load cell. Tension-tension fatigue with 0.1 R ratio ($R=\delta_{min}/\delta_{max}$) and 5 Hz frequency was carried out. Fatigue displacement level (δ_{max}) was set according to the average value of critical displacement $[\delta_{cr}]_{ave}$ obtained from the static DCB tests, as described in the ASTM D6115 standard [4]:

$$\frac{\delta_{max}^2}{[\delta_{cr}]_{ave}^2} = 0.5 \tag{3}$$

where δ_{cr} is the displacement necessary for delamination growth beyond the insert film [4].

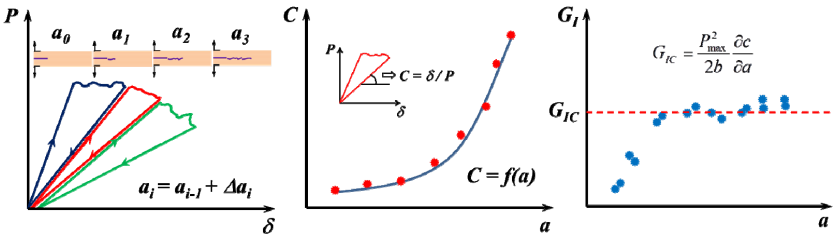

Figure 2. Simple representation of compliance calibration method for calculating G_{IC}.

The value of $[\delta_{cr}]_{ave}$ for the reference composite was 19 mm, whereas for the composite with treated fibers was 14.5 mm. It should be mentioned that the second delamination length was used to calculate the critical δ value, assuming the first delamination right in front of the insert film was not representative and corresponded to the initiation rather than propagation of the crack. This is due to a typical resin rich region formed in front of the crack [1]. Fatigue tests were aimed for a total number of 1M cycles. However, only a few samples reached this target value, for the rest the test had to be interrupted due to various technical issues. Load and displacement data were monitored during fatigue, in order to analyze changes of compliance with number of cycles. These results were used to compare the compliance changes in percentage for different samples. However, using the compliance method for calculating G_{IC} in fatigue was not possible since the crack did not show any significant propagation. The likely

reason for this is the highly viscoelastic and viscoplastic nature of RCF composites where energy dissipation is the dominating mechanism rather than crack propagation. Nevertheless, the obtained results were still quantified by applying the beam theory [3], to calculate the apparent G_{IC}:

$$G_{IC} = \frac{3P_{\max}\delta_{\max}}{2ba} \tag{4}$$

FRACTOGRAPHY

The delamination surfaces of DCB specimens, undergone static as well as fatigue loading, were studied by electron scanning microscopy (SEM) in order to detect qualitative differences between the treated and non-treated laminates. This was performed using a JEOL JSM 5200 scanning electron microscope, operating in high vacuum pressure ($5 \cdot 10^{-2}$ mbar) at accelerating voltage of 15 kV. The samples were previously sputtered with gold using a BLAZER SCD 050 sputter coater under argon atmosphere to obtain high quality images.

Results and discussions

CHEMICAL TREATMENT

SEM images of non-treated and treated RCF fabrics are shown in Figure 3. Comparison of the surface topography of fibers in the treated fabric against non-treated showed that the surface treatment was successfully achieved (non-treated filaments, contrary to the treated ones, exhibited smooth surfaces) [13].

STATIC DCB

Typical load-displacement graphs of non-treated and treated samples are shown in Figure 4, where each curve represents about 5 mm of crack propagation length. These graphs displayed higher loads required for introducing delamination in treated samples compared to non-treated counterparts. Moreover, treated samples experienced more steps until total detachment of laminate surfaces.

In order to fit a function to the compliance curves, different fitting functions, such as exponential, polynomial 2nd and 3rd degree, were examined. Although, the 3rd degree polynomial function gave the closest fit (correlation R^2 value closest to 1), it was too sensitive to small changes of the compliance. Hence, the exponential fit, showing the least scatter among samples, was used for calculations of energy release rate. The accuracy of the fitting function to the experimental data is demonstrated in Figure 5. The comparison of compliance as a function of crack length (functions fitted to the experimental data) for different specimens is shown in Figure 6. The resulting energy release over the crack length obtained by Equation 1 is plotted in Figure 7.

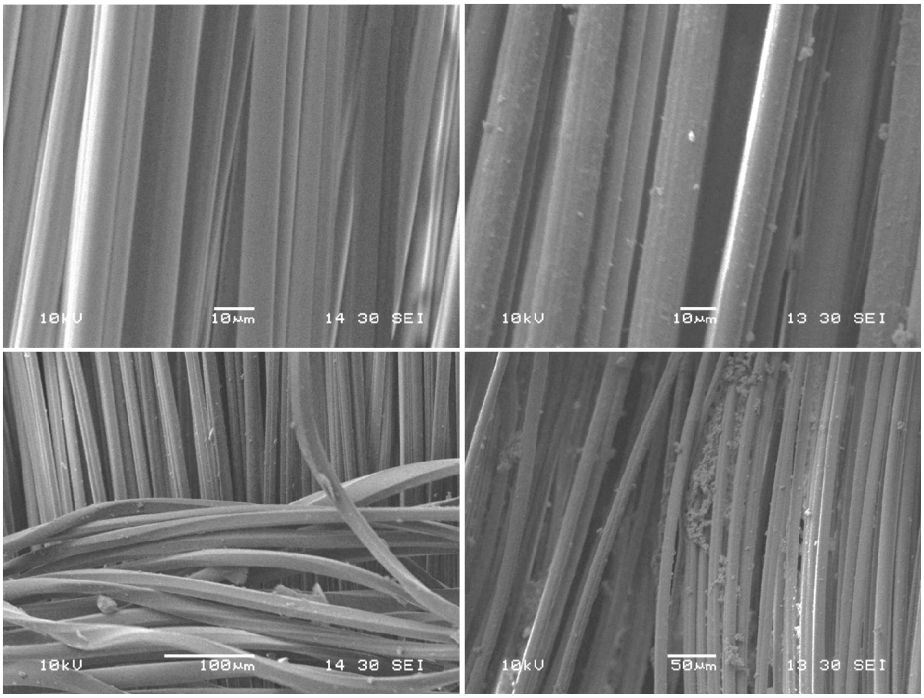

Figure 3. Non-treated (left) and treated (right) RCF fabric.

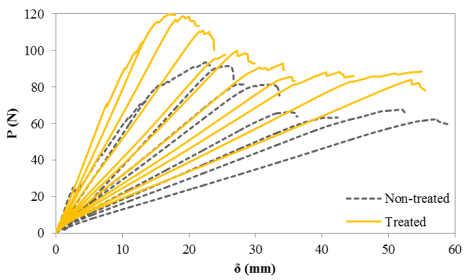

Figure 4. Typical load-displacement curves of non-treated and treated DCB samples.

From the plateau value on the curves in Figure 7, in the interval of $35<a<70$, the average G values for non-treated and treated samples were calculated. The results are summarized in Table 3. It could be noted that the standard and downscaled non-treated specimens produced very close results. Thus, downscaling of sample dimensions did not affect the measurements. G_{IC} values were significantly higher than in conventional high performance composites [15,16]. This could be related to the RCF viscoelasticity and viscoplasticity which resulted in large amounts of energy dissipation. Furthermore, a slightly higher energy release rate in the treated samples compared to non-treated

counterparts might be attributed to an improvement in interface adhesion of composites with treated fibers as well as to enhanced wettability of fibers. Although, G_{IC} values for treated and non-treated specimens were very close and within the experimental scatter. This made it difficult to make concrete conclusions about the improvement of interlaminar fracture toughness due to fiber treatment.

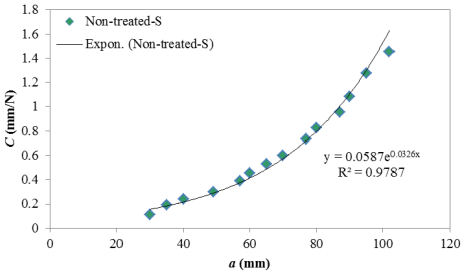

Figure 5. Example of exponential fitting function on standard sized non-treated sample.

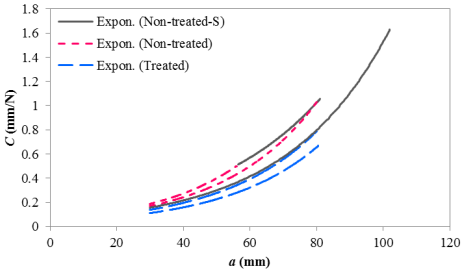

Figure 6. Plot of compliance values over crack lengths, for standard non-treated samples as well as for downscaled samples treated and non-treated.

Table 3. Critical energy release rate, G_{IC}, in non-treated and treated samples.

Material	**Non-treated-S**	**Non-treated**	**Treated**
G_{IC} (kJ/m^2)	2.4 ± 0.6	2.5 ± 0.5	2.6 ± 0.6

In order to make a more comprehensive quantitative analysis of the results, one should use numerical simulations (e.g. FEM) with a nonlinear material model. This type of analysis is out of the scope of this article. Nevertheless, a qualitative discussion is presented by analyzing the stress-strain curves of studied materials.

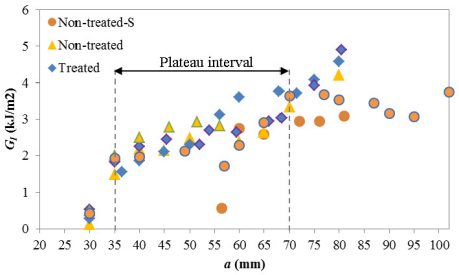

Figure 7. Energy release rate over crack length, non-treated (standard and downscaled) and treated samples (two replicas per sample).

The following graph in Figure 8 shows the typical stress-strain curves of RCF bundles. These fibers could sustain very high strains and exhibited a significant nonlinearity [6]. Since these curves did undergo a drastic change of slope, two clear regions could be distinguished on them, before and after yielding. This yielding point for non-treated fibers was at 1.5% strain and at 2% strain for the treated counterparts. Assuming that the fibers within composites were not subjected to very high strains during DCB tests, only the first region on the stress-strain curve could be considered for obtaining the strain energy in the material. The energies were calculated by the area below the curve in that region (see Table 4). These results showed that the energy dissipation by treated fibers was significantly higher than non-treated ones. Thus, the effect of the fiber surface treatment was shadowed by the differences in performance of RCF which defined the behavior of composites.

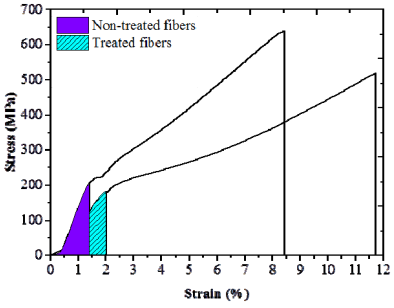

Figure 8. Typical stress-strain curves for non-treated and treated RCF bundles.

Table 4. Energy dissipated in tensile test of RCF bundles (average of 3 samples).

Fiber	Mean energy (kJ/m^2)
Non-treated	2.73 ± 0.35
Treated	3.46 ± 0.07

DCB IN FATIGUE

In Figure 9, the graph of compliance growth is plotted under the fatigue cycles for non-treated and treated samples. Fatigue results showed a good repeatability.

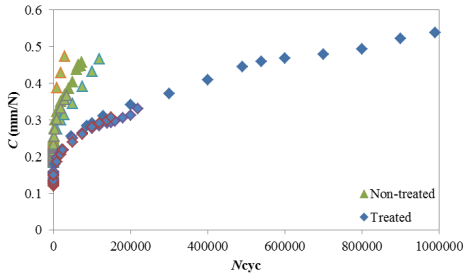

Figure 9. Compliance growth under fatigue, non-treated and treated samples.

In Table 5, G_{IC} values are reported (calculated using the beam theory). As it is seen, the values are contradicting the static test results. The fracture toughness in treated samples was inferior to the non-treated ones. It is possible that due to the higher strain rates under fatigue, as compared with the static loading, the behavior of RCF has changed and has consequently altered the trend in mechanical performance of non-treated and treated materials.

Table 5. Critical energy release rate measured in fatigue (according to beam theory).

Material[a]	Non-treated	Treated
G_{IC} (kJ/m^2)	2.4 ± 0.1	2.0 ± 0.1

[a]Specimens were all downscaled.

SEM FRACTOGRAPHY

SEM images of fracture surfaces for samples tested in static and fatigue loading are presented in Figure 10 and Figure 11, respectively. SEM images confirmed the conclusions based on the comparison of fracture toughness data obtained from the static tests. The fracture surface in treated samples was rough, exhibiting fiber pullouts, whereas in non-treated samples smooth spots free of fibers were found (Figure 11). Fiber wetting in treated samples is the indication for improvement of compatibility between resin and fibers when the surface of reinforcement is treated.

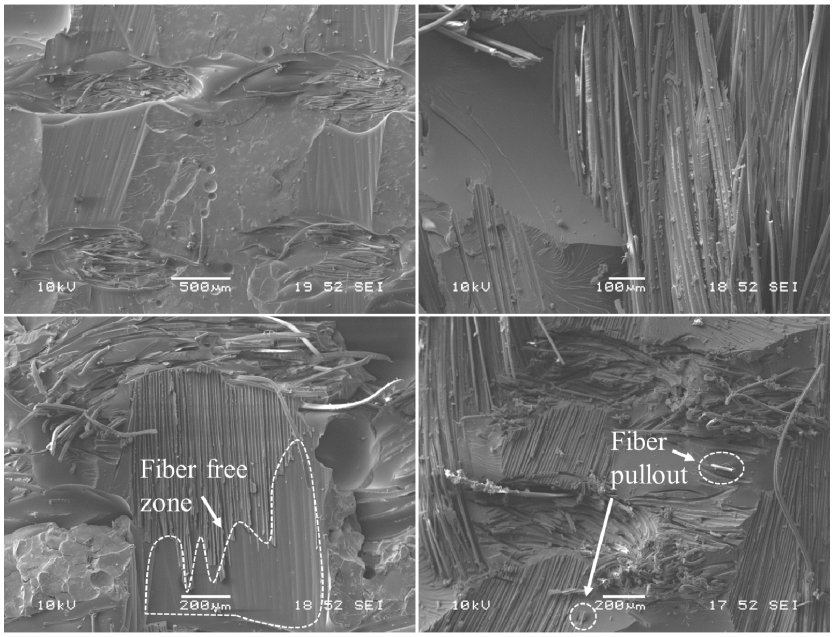

Figure 10. SEM fractography of DCB static samples, non-treated (left) vs. treated (right).

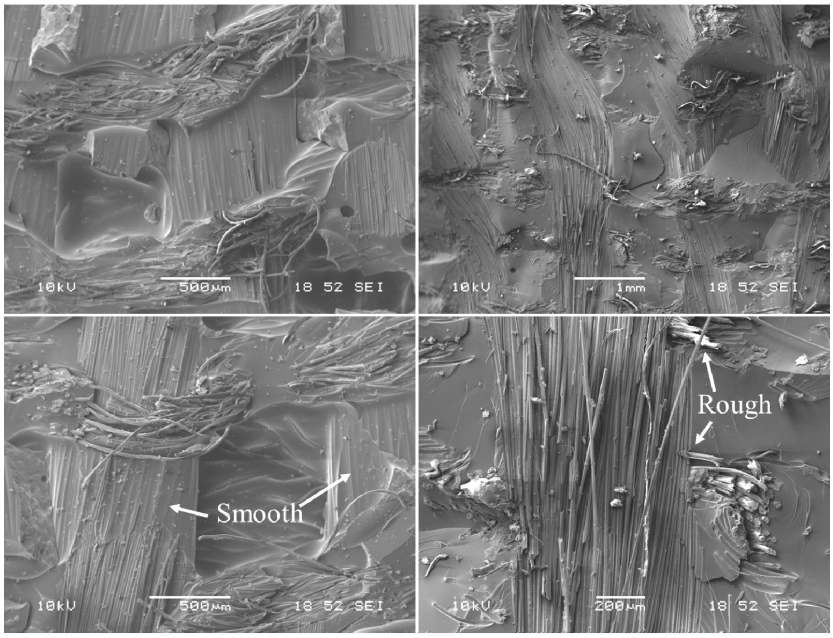

Figure 11. SEM fractography of DCB fatigue samples, non-treated (left) vs. treated (right).

Conclusions

The objective to characterize the fracture toughness of RCF composites was met. This characterization was performed through static and fatigue DCB tests, in order to compare G_{IC} values and to analyze the fracture surface of tested specimens. The performance of studied materials was defined by the fibers which were highly nonlinear. Due to the presence of the fibers' viscoelastic and viscoplastic effects, the composite exhibited a highly nonlinear behavior as well. This complicated the analysis of DCB test results as well as the evaluation of fiber treatment effect on interlaminar fracture toughness of RCF based composites. However, the following statements could be issued based on the obtained results and observations:

- Extremely high G_{IC} values found for both non-treated and treated samples indicated a high energy dissipation due to the nonlinear nature of reinforcing fibers, which could not be found in conventional (glass fiber , carbon fiber) composites. This, however, raised the question about the validity of results obtained by using of LEFM and also about the efficiency of fiber treatment in terms of increasing the fiber matrix adhesion. In order to obtain more reliable data for fracture toughness of these composites, one needs to implement advanced data processing method to separate energy dissipation by crack propagation and by viscoelasticity and viscoplasticity of the material.
- Even though, the obtained values of G_{IC} were inconclusive, SEM fractography showed significant differences between the composites with treated and non-treated fibers. Nevertheless, it cannot be directly related to the experimental data since it is not only the crack propagation which is responsible for energy dissipation.
- According to the DCB data under fatigue, change of compliance was very rapid by the number of cycles. However, the crack did not propagate. It can be concluded that energy dissipates by other mechanisms (most likely through the internal energy of material).

Acknowledgments

The financial support from DocMASE (EU Erasmus Mundus program) and EXCEL (Norrbotten, Länsstyrelsen) projects is acknowledged.

References

[1] L. Ilcewicz, P. Keary, and J. Trostle, *Polymer Engineering & Science,* **28**, 592-604 (1988).

[2] G.B. Murri, *ASC 27th Technical Conference/15th US-Japan Conference on Composites/ASTM D30*, 1-3 (2012).

[3] ASTM D5528-01, *Standard Test Method for Mode I Interlaminar Fracture Toughness of Unidirectional Fiber-Reinforced Polymer Matrix Composites* (2014).
[4] ASTM D 6115-97, *Standard Test Method for Mode I Fatigue Delamination Growth Onset of Unidirectional Fiber-Reinforced Polymer Matrix Composites* (2011).
[5] K. Shivakumar, H. Chen, F. Abali, D. Le, and C. Davis, *Int. J. Fatigue,* **28**, 33-42 (2006).
[6] L. Pupure, N. Doroudgarian, and R. Joffe, *Polymer Composites,* **35**, 1150-1159 (2014).
[7] A. Biel and U. Stigh, *Archives of Mechanics,* **59**, 311-327 (2007).
[8] B.F. Sørensen, and S. Goutianos, *20th International Conference on Composite Materials* (2015).
[9] J.D. Gunderson, J.F. Brueck, and A.J. Paris, *International Journal of Fracture,* **143,** 273-276 (2007).
[10] V. Pavelko, *Key Engineering Materials*, **665**, 273-276 (2015).
[11] Cordenka™ 700 super 3, High-tenacity rayon filament yarn, *CORDENKA GmbH* (2009).
[12] N. Doroudgarian, M. Anglada, and R. Joffe, Fatigue on regenerated cellulose fiber bundles and composites, *Submitted to Industrial Crops and Products* (2016).
[13] A. Hajlane, H. Kaddami, and R. Joffe, A green route for modification of regenerated cellulose fibres by cellulose nano-crystals, *Submitted to Cellulose* (2016).
[14] N. Doroudgarian, L. Pupure, and R. Joffe, *Polymer Composites*, **36**, 1510–1519 (2014).
[15] P.R. Thakre, D.C. Lagoudas, J.C. Riddick, T.S. Gates, S.J.V. Frankland, J.G. Ratcliffe, J. Zhu, and E.V. Barrera, *Journal of Composite Materials*, **45,** 1091-1107 (2011).
[16] K.L. Kepple, G.P. Sanborn, P.A. Lacasse, K.M. Gruenberg, and W.J. Ready, *Carbon,* **46**, 2026-2033 (2008).